A MODEL BASED APPROACH FOR AIRCRAFT SENSOR FAULT DETECTION

A THESIS SUBMITTED TO
THE GRADUATE SCHOOL OF NATURAL AND APPLIED SCIENCES
OF
MIDDLE EAST TECHNICAL UNIVERSITY

BY

ÖMÜR SERÇEKMAN

IN PARTIAL FULFILLMENT OF THE REQUIREMENTS
FOR
THE DEGREE OF MASTER OF SCIENCE IN
AEROSPACE ENGINEERING

SEPTEMBER 2018

Approval of the thesis:

A MODEL BASED APPROACH FOR SENSOR FAULT DETECTION IN CIVIL AIRCRAFT CONTROL SURFACE

submitted by **ÖMÜR SERÇEKMAN** in partial fulfillment of the requirements for the degree of **Master of Science in Aerospace Engineering Department, Middle East Technical University** by,

Prof. Dr. Halil Kalıpçılar
Dean, Graduate School of **Natural and Applied Sciences** _____

Prof. Dr. Ozan Tekinalp
Head of Department, **Aerospace Engineering** _____

Asst. Prof. Dr. Ali Türker Kutay
Supervisor, **Aerospace Engineering Dept., METU** _____

Examining Committee Members:

Prof. Dr. Ozan Tekinalp
Aerospace Engineering Dept., METU _____

Asst. Prof. Dr. Ali Turker Kutay
Aerospace Engineering Dept., METU _____

Prof. Dr. Nafiz Alemdaroğlu
School of Civil Aviation, Atilim University _____

Prof. Dr. Coşku Kasnakoğlu
Electrical and Electronics Engineering Dept., TOBB ETU _____

Assoc. Prof. Dr. İlkay Yavrucuk
Aerospace Engineering Dept., METU _____

Date: _____

I hereby declare that all information in this document has been obtained and presented in accordance with academic rules and ethical conduct. I also declare that, as required by these rules and conduct, I have fully cited and referenced all material and results that are not original to this work.

Name, Last name : ÖMÜR SERÇEKMAN

Signature :

ABSTRACT

A MODEL BASED APPROACH FOR AIRCRAFT SENSOR FAULT DETECTION

Serçekman, Ömür

M.S., Department of Aerospace Engineering

Supervisor: Prof. Dr. Ali Turker Kutay

September 2018, 111 Pages

This thesis presents a reformative approach to a model-based fault detection and diagnosis (FDD) method that improves the capability of aircraft flight control systems and acquires low complexity and computational requirements. The main objective of the FDD techniques that are extensively applied in industrial systems is to increase the sensitivity of fault detection scheme with respect to additional noise, uncertainty or disturbances.

The designed fault detection model is integrated to a civil aircraft model of Boeing 747. The developed system mainly consists of a nonlinear closed-loop aircraft model to verify the effectiveness of sensor fault detection technique, an observer to estimate states of the aircraft during steady state flight, a fault indicator to propagate faulty responses to the system and a reconfigurator to identify flight condition if it is faulty or fault-free by comparing the states which are achieved from sensors in real-time. Fault detection is accomplished by using mainly a Kalman filter as a linear observer design.

The scheme presented based on Kalman filter decreases the effect of model uncertainty extensions, constitutes a residual sensitive to stuck faults and maintains a reliable fault detection approach incorporating the rejection of false alarm that is required for system reliability. The monitoring progression of the state estimation permits to observe any off-nominal system attitude and detects faults. The developed method is a viable solution for earlier detection of sensor stuck to lower threshold amplitude under multi-simulation tests performed in MATLAB Simulink.

Keywords: electronic flight control systems, sensor fault detection, state estimation, kalman filter, state-space models

ÖZ

UÇAK SENSOR HATA TESPİTLERİNE YÖNELİK MODEL TABANLI YAKLAŞIM

Serçekman, Ömür
Yüksek Lisans, Havacılık ve Uzay Mühendisliği Bölümü
Tez Yöneticisi: Asst. Prof. Dr. Ali Türker Kutay

Eylül 2018, 111 Sayfa

Bu tez, uçağın uçuş kontrol sistemleri yeteneğini geliştirerek ve düşük karmaşıklıkta sayısal gereksinimler elde ederek model tabanlı hata algılama ve tanılama çözümlerine düzeltici bir yaklaşım sunmaktadır. Geniş ölçüde endüstriyel sistemlere uygulanan model tabanlı hata algılama ve tanılama tekniklerinin başlıca amacı, gürültü, belirsizlik ya da bozulmalara göre hata algılama taslağının hassasiyetini arttırmaktır.

Tasarlanan hata algılama modeli bir Boeing 747 yolcu uçağı modeline entegre edilmiştir. Geliştirilen sistem alt sistemler bakımından temel olarak, sensör hata algılama tekniğinin etkinliğini doğrulamak için nonlineer kapalı döngü uçak modelinden, düz uçuş modunda uçağın durumlarını tahmin etmek için gözlemciden, sisteme hatalı cevapları geçirmek için hata göstericiden ve gerçek zamanlı olarak sensörden edinilen uçuş durumlarını karşılaştırarak hatalı ya da hatasız olduğunu tanımlamak için yeniden derleyiciden oluşmaktadır. Başlıca lineer gözlemci olarak Kalman filtre tasarımı kullanılarak hata algılaması başarıyla tamamlanmıştır.

Kalman filtresi taslağı model belirsizliği yayılmalarını azaltarak ani hatalara karşı hassas rezidüel meydana getirmekte ve sistem güvenilirliği için gerekli olan hata uyarısı reddini birleştirerek güvenilir hata algılaması yaklaşımını sürdürmektedir. Durum tahmininin görüntüleme devamlılığı nominal olmayan sistem davranışının gözlemlenmesine ve hatanın algılanmasına izin vermektedir. Geliştirilen metot, MATLAB Simulink'te yürütülen çoklu senaryo testlerine göre eşik değeri büyüklüğünü düşürerek daha erken kontrol yüzeyi sıkışması algılanması için uygulanabilir bir çözümdür.

Anahtar Kelimeler: elektronik uçuş kontrol sistemleri, sensör hata tespiti, durum tahmincisi, kalman filtresi, durum uzayı modelleri

To my family

ACKNOWLEDGMENTS

This study is supported primarily with my supervisor Asst. Prof. Dr. Ali Turker Kutay.

I would like to declare my honest and sincere appreciation to him for his long-term contributions covering constructive guidance, advice and major suggestions forming this considerable thesis.

I would like to present my many thanks to the committee members Prof. Dr. Ozan Tekinalp, Prof. Dr. Nafiz Alemdaroğlu, Prof. Dr. Coşku Kasnakoğlu and Assoc. Prof. Dr. İlkay Yavrucuk for their generous assistance, patience and comprehension throughout the research.

I also wish to thank to numerous instructors for their supports during my graduate studies and the personnel of METU that I could not to count their names for their helpfulness and kind manner.

Lastly, I wish to specify my deeply gratefulness to my family, especially my mother and father, for their continuous encouragement, patience, dedication and concern during my study at Middle East Technical University.

TABLE OF CONTENTS

ABSTRACT v
ÖZ vii
ACKNOWLEDGMENTS x
TABLE OF CONTENTS xi
LIST OF TABLES xiii
LIST OF FIGURES xiv
LIST OF ABBREVIATONS xvii
LIST OF SYMBOLS xviii
CHAPTERS
1. INTRODUCTION 1
1.1 Background and Motivation 1
1.2 Objective 2
1.3 Contribution of the Thesis 3
1.4 Organization of the Thesis 4
2. LITERATURE REVIEW 5
2.1 Development of Aircraft Flight Control Systems 5
2.2 History of Fault Detection Methodology 7
2.3 Fault Detection and Diagnosis Approach 10
2.3.1 Hardware Redundancy 11
2.3.2 Analytical Redundancy 12
2.3.3 Fault Detection and Diagnosis for Control Techniques 13
2.4 Fault Tolerant Control 15
2.4.1 Active Fault Tolerant Control 16
2.4.2 Passive Fault Tolerant Control 16
2.5 Diagnostic Algorithm 17
2.6 An Aircraft Control Surface: Rudder 18
2.7 Faults Classification 19
2.7.1 Sensor Faults 19
2.7.2 Actuator Faults 20

2.7.3 System Component Faults 21
2.8 Perspective of Observers and Their General Applicability 22
3. METHODOLOGY 25
3.1 Overview 25
3.2 Boeing 747 Data Analyses 30
3.3 Mathematical Modelling of Aircraft 36
3.3.1 Rigid Body Equations of Motion 36
3.3.2 Nonlinearity and Linearity Conversion 37
3.4 Fault Detection Method 40
3.4.1 Method for Linearization 42
3.4.2 Poles of the System Matrix 45
3.4.3 Gain Matrix of the Linear Observer 45
3.4.4 Design of Subsystems in Simulink 46
3.4.5 Residual Generation 54
3.5 Kalman Filtering 55
3.5.1 Kalman Filtering Theory and Formulation 58
3.5.2 Practical Problems and Extensions 62
3.6 Luenberger Observer 63
3.6.1 Luenberger Observer Theory and Formulation 64
3.6.2 Practical Problems and Extensions 65
4. SIMULATION AND RESULTS 67
5. CONCLUSION 95
REFERENCES 99
APPENDIX A 103

LIST OF TABLES

TABLES

Table 3.1 Minimum Detectable Step Input Sensor Faults 29
Table 3.2 Minimum Detectable Step Output Sensor Faults..... 30
Table 3.3 Trim Values, Lateral Oriented Mass Properties and Aerodynamic Stability Derivatives of Boeing 747 at Initial Flight Condition 33
Table 3.4 Variety of Kalman filters 57
Table 4.1 The Values of Process Noise, Measurement Noise and Estimate Error Covariance for Fault-free Case 72
Table 4.2 The Values of Process Noise, Measurement Noise and Estimate Error Covariance for Faulty Cases 78

LIST OF FIGURES

FIGURES

Figure 2.1 Threshold-based Approach for Decision Making 11
Figure 2.2 General Architecture of an FDI Unit of a Boeing 747 13
Figure 2.3 Typical Types of Sensor Faults [20] 20
Figure 2.4 Typical Types of Actuator Faults [20] 21
Figure 3.1 Aircraft Reference Frame [6] 31
Figure 3.2 Sideslip Angle vs. Time 43
Figure 3.3 Yaw Rate vs. Time 43
Figure 3.4 Roll Rate vs. Time 44
Figure 3.5 Roll Angle vs. Time 44
Figure 3.6 Block Diagram Representation of Discrete Time Boeing 747 Model 47
Figure 3.7 Block Diagram Representation of Fault Indicator Subsystem 47
Figure 3.8 Block Diagram Representation of Reconfiguration Subsystem for Kalman filter approach 49
Figure 3.9 Block Diagram Representation of Reconfiguration Subsystem for Luenberger observer approach 49
Figure 3.10 Block Diagram Representation of Kalman Filter 1 51
Figure 3.11 Block Diagram Representation of Kalman Filter 2 52
Figure 3.12 Block Diagram Representation of Luenberger Observer 52
Figure 3.13 The Entire System Architecture of the Closed-Loop Model for Kalman filter 53
Figure 3.14 The Entire System Architecture of the Closed-Loop Model for Luenberger observer 54
Figure 3.15 Usage of an Observer for Constituting Residual [29] 55
Figure 3.16 Basic Operation of a Simple Kalman Filter 59
Figure 3.17 Flow Chart Representation of Kalman Filter Algorithm 61
Figure 4.1 Top-Level Model of Boeing 747 Aircraft in Simulink [34] 68

Figure 4.2 Sideslip Angle Residual vs. Time 73
Figure 4.3 Yaw Rate Residual vs. Time 73
Figure 4.4 Roll Rate Residual vs. Time 74
Figure 4.5 Roll Angle Residual vs. Time 74
Figure 4.6 Sideslip Angle Residual vs. Time 75
Figure 4.7 Yaw Rate Residual vs. Time 75
Figure 4.8 Roll Rate Residual vs. Time 76
Figure 4.9 Roll Angle Residual vs. Time 76
Figure 4.10 Sideslip Angle Residual vs. Time 79
Figure 4.11 Yaw Rate Residual vs. Time 80
Figure 4.12 Roll Rate Residual vs. Time 80
Figure 4.13 Roll Angle Residual vs. Time 81
Figure 4.14 Fault Indicator Threshold vs. Time 82
Figure 4.15 Sideslip Angle Residual vs. Time 82
Figure 4.16 Yaw Rate Residual vs. Time 83
Figure 4.17 Roll Rate Residual vs. Time 83
Figure 4.18 Roll Angle Residual vs. Time 84
Figure 4.19 Fault Indicator Threshold vs. Time 84
Figure 4.20 Sideslip Angle Residual vs. Time 87
Figure 4.21 Yaw Rate Residual vs. Time 87
Figure 4.22 Roll Rate Residual vs. Time 88
Figure 4.23 Roll Angle Residual vs. Time 88
Figure 4.24 Fault Indicator Threshold vs. Time 89
Figure 4.25 Sideslip Angle Residual vs. Time 89
Figure 4.26 Yaw Rate Residual vs. Time 90
Figure 4.27 Roll Rate Residual vs. Time 90
Figure 4.28 Roll Angle Residual vs. Time 91
Figure 4.29 Fault Indicator Threshold vs. Time 91
Figure A.1 Airspeed vs. Time 104
Figure A.2 Angle of Attack vs. Time 104
Figure A.3 Pitch Rate vs. Time 105
Figure A.4 Yaw Angle vs. Time 105

Figure A.5 Pitch Angle vs. Time 106
Figure A.6 Aircraft Position in X-Axis vs.Time 106
Figure A.7 Aircraft Position in Y-Axis vs. Time 107
Figure A.8 Altitude vs. Time 107
Figure A.9 Airspeed vs. Time 108
Figure A.10 Angle of Attack vs. Time 108
Figure A.11 Pitch Rate vs. Time 109
Figure A.12 Yaw Angle vs. Time 109
Figure A.13 Pitch Angle vs. Time 110
Figure A.14 Aircraft Position in X-Axis vs.Time 110
Figure A.15 Aircraft Position in Y-Axis vs. Time 111
Figure A.16 Altitude vs. Time 111

LIST OF ABBREVIATONS

FDD	:	Fault Detection and Diagnosis
EFCS	:	Electronic Flight Control Systems
FCC	:	Flight Control Computer
FCL	:	Flight Control Laws
FDI	:	Fault Detection and Isolation
FTCS	:	Fault Tolerant Control Systems
SMC	:	Sliding Mode Control
EOM	:	Equations of Motion
LTI	:	Linear Time Invariant
IMM	:	Interactive Multiple Model

LIST OF SYMBOLS

V_T	True airspeed
α	Angle of attack
β	Angle of sideslip
β_e	Estimated sideslip angle
p	Body roll rate
q	Body pitch rate
r	Body yaw rate
φ	Angle of yaw
θ	Angle of pitch
$\emptyset$	Angle of roll
x_e	Distance in X_e-direction
y_e	Distance in Y_e-direction
h_e	Altitude
δ_{th}	Thrust setting
δ_e	Elevator deflection
δ_a	Aileron deflection
δ_r	Rudder deflection
b	Wing span
S	Wing area
m	Mass
g	Center of gravity
k	Time index
t_i	Instant time
t	Detection time
dt	Sample time
x	State

y	Measurement output
z	Measurement noise
w	Process noise
Q	Process noise covariance
R	Measurement noise covariance
E	Expected value
K	Kalman gain matrix
L	Luenberger gain matrix
P	Estimate error covariance

CHAPTER 1

INTRODUCTION

1.1 Background and Motivation

The aviation industry generates new and high-tech solutions which presents use of a smarter and more sustainable aircraft in the near future. The most important factor that affects flight sustainability is the weight load that aircraft exposed. For increasing the stability of the aircraft and minimizing the structural loads, it is aimed to improve the capability of the electronic flight control systems (EFCS). Aircraft design optimization has been developed to maximize the fault detection capabilities and restrict the flight control system failures. Detecting such failures in an earlier stage of occurrence has an undeniable advantage limiting the unstable condition and raising the flight performance. To accommodate a realistic resolution to diminish the overall weight problem, several techniques are developed via the revolution of the EFCS which replace the functions of the old fashioned mechanical interfaces from the pilot input to the related actuators of the control surfaces. After redundant loads are reduced in the aircraft, some improvements are provided in certain outputs such as the amount of fuel, noise, range etc**.** Industrial practices are run with redundancy-based techniques so that reliable results are acquired. Recent model-based diagnosis approaches are considered to be an appealing research field. [1]

EFCS is a reputed system implementation to control the movement of the airplane and a momentous part to supply both of the flight performance and safety of the airplane. When the sensors that measure the attitude, speed, altitude etc. are imposed due to the faults, the influenced signals transmitted from those sensors can impact both the flying and processing properties of the airplane. However, EFCS are expected to process

regularly even in such faulty conditions.

The motivation why Kalman filter is used particularly for state estimation of a civil aircraft in this study is because, it is considered to be one of the most optimum observer when noise effects that are received from sensor and model are Gaussian. Kalman filter also exposes an adaptive approach in relation to the estimation theory.

There are many similar research and studies that are revealed in the scope of longitudinal stability of the several types of aircrafts in the literature. On the other hand, surveys which focus on lateral stability take part on the sources lesser. Considering this differentiation, it is aimed to make contribution to lateral stability of a civil aircraft as a coverage of this paper.

1.2 Objective

In state estimation problems, the convenient measured data is utilized by means of prior knowledge of the physical event and the measurement equipments to generate estimates of the requested dynamic variables respectively. The aim is achieved in such a way that the error is diminished statistically. Those problems handle with the association of the model estimation and the measurements to provide more proper estimates of the system variables. [2]

State estimation issues are resolved with the Bayesian filters. According to this approach, an effort is managed to use the entire convenient data to decrease the proportion of uncertainty available in an apparently or decision-making issue. As incoming data is acquired, it is incorporated with former data to generate the principal for statistical processes. [3]

Kalman filter is a popular filtering methodology in linear systems with Gaussian noises. Expansions of Kalman filter were improved for lesser restricting conditions by applying linearization methods. Kalman filters can be a very constructive solution for applications to the complex systems with Gaussian noises among the entire techniques. [4]

In this study, Kalman filter is applied for estimating lateral states of the model of Boeing 747 in several steady state flight cases including errors in sensor measurements. Similarly, Kalman filter in the model has a function of filtering the noise on the sensors and providing outputs of the exact values of lateral states continuously throughout the simulation. The algorithms of Kalman filtering is separately integrated to the complex civil aircraft model. Linear state estimation performances are examined with a zero mean and unit covariance matrix Gaussian white noise. Performance effectiveness of Kalman filter is assorted mainly in the system after performing several flight simulation cases.

1.3 Contribution of the Thesis

The fundamental contribution of the paper is to suggest a supplement observer-based approach for sensor fault detection of a Boeing 747 as a civil airplane. This study points out that a conformable implementation of a model based approach to an aircraft model can effectively indicate the performance of flight control computer (FCC) with different types of observers that is critical for pilot to take action in any faulty condition for providing the safety of the flight. Apparent variations between Kalman filter and Luenberger observer based solutions in rapidity of the fault detection capability, amplitude response with respect to the assigned threshold level and rejection of false alarms take place in several simulation cases inside the paper.

The high-level performance of the Kalman filter as a linear observer for estimating the states of a Boeing 747 in a steady-state flight condition is indicated with performing several simulation cases. Also, the better efficiency in state estimation of Kalman-based approach is proven against Luenberger-based solution as a former study that can be found in the literature as in [5].

1.4 Organization of the Thesis

The presence of the paper is organised as below:

In Chapter 2, the literature review regarding the thesis is given mainly outlining the aircraft flight control systems, theoretical background of FDD, fault classification and types of observers.

In Chapter 3, the methodology of the study is presented with data analysis of Boeing 747, mathematical modelling of the aircraft, proposed fault detection methodology with introducing Kalman filter based algorithm and also Luenberger observer based algorithm.

In Chapter 4, simulation cases are described, implementation of the designed Kalman filter and Luenberger observer methods to Boeing 747 model are presented and simulation results based on the observer-based methods are clarified.

In Chapter 5, comments about the function of the suggested fault detection method is drawn attaching the future research aspects as a conclusion of the study.

CHAPTER 2

LITERATURE REVIEW

2.1 Development of Aircraft Flight Control Systems

EFCS was initially introduced by Wright brothers in 1902. The very first design stimulated the basis of the modern EFCS with reformative changes. By 1950's, analog FCC is released to enable artificial change of the aircraft handling properties and the fundamental autopilot stabilization functions. The Canadian Avro CF-105 Arrow interceptor equipped with an analog FCC demonstrated impressive performance capabilities. Subsequently, digital fly-by-wire technology was presented to take place of analog FCC. In 1972, the technology was possessed by an F-8 Crusader in flight tests administered by NASA. In 1987, Airbus A320 was the preliminary commercial aircraft used the fly-by-wire control systems on basic control surfaces in the civil aviation domain. Modern aircrafts contain various automatic control system that facilitates flight administration. The number and kind of aerodynamic surfaces for control regulation alters with the aircraft category [6].

Conventional mechanical control systems, as currently used in small aircrafts nowadays, have been increasingly developed to the mechanical hydraulic systems. Those hydraulic systems propagate actuator forces to move the control surfaces. Although the hydraulic system enables large forces on the control surfaces, it adds extra complexity to the already highly complex system. The fly-by-wire EFCS bring a revolutionary solution by eliminating these old-fashioned systems. The signals that are received and sent by digital FCC allow a simpler control application, thus a better handling quality. Digital fly-by-wire technology increases the flight safety, aircraft maneuverability and fuel efficiency in the means of cost [6].

EFCS failure cases can be separated to runaway and jamming with respect to the airplane moving surfaces. First definition is the moving surface deviation as its position undesirably changes. It is originated due to the FCC decomposition, electronic device deficiency or mechanical breakdown. A residual is eventuated after checking the signals. The aircraft reacts to this situation making a control surface maneuver or unwanted loads are generated. If these loads are excessive, supplemental structural reinforcement could be needed, concluded with a weighty airplane. Otherwise, in the jamming condition the moving surface stuck constantly at its present location generating a failure [1].

Mathematical models or algorithms are integrated with FCC instead of redundant hardware implementation on the aircraft. FCC architecture of a civil aircraft contains monitoring signal and command signal channels that operate interactively by monitoring each. While command channel's function is to guide the basic functions from the computer, monitoring channel assures the real time tracking of the command signals also the entire EFCS equipments. Detection is verified when the variation among the signals exceeds the devoted threshold. Monitoring technique development process is a critical matter due to detect the fault in a shorter time and reduce the detectable location of the moving surface. When a fault arises, it is informed to both autopilot and pilot to take required actions. In the status of pilot eases autopilot modes, the autopilot should be designed to satisfy characterizations on flight error and disturbance declination with less consideration on dynamic replication. An effective FDD method can diminish pilot's workload instantly in the critical time and raise flying safety.

One of the primary functions devoted to the FCC is the Flight Control Laws (FCL) computing that constitutes a command to servo control of the control surfaces. The comparison between pilot command and the state is utilized in FCL computing. Plant state is measured through a sensor set revealing the inertial measuring which modificate aircraft altitude, speed and attitude. Information is achieved applying an acquirement model generated by various devoted redundant units. This particular data

fusion procedure contains two joint steps: firstly, the computation of a singular state through valid sources and secondly, monitor the detached sources to allocate any faulty one [7].

The faults of state vector constituent, abnormous measuring, abrupt shift in measurement channel and the other complications, for instance, decline in the implement straightness or augmentation in the background noise influence the feature of standardized innovation sequence upon altering the noise [8]. A timely response to fault detection can reduce any terrific consequences with a slighter control surface deviation so that the flight performance will approach to a better level.

2.2 History of Fault Detection Methodology

Many studies about different FDI methods have been executed since 1970's and listed in the literature in detail. The success of the recommended approaches are verified and validated with real flight tests in research centers like scientific laboratories or with the help of the simulation environment. It is obvious to mention that innovative methods expose better results for recognizing the faults in some critical flight cases, however, there are still applications in which classical methods are preferred to use for proven robustness of several flight operations. The study is handled based on the accomplished studies that could be followed in the references part. Even though, these studies combine the same subject about fault detection, isolation and diagnosis at top-level, they are separated pointing out distinct approaches in circumstances. On the basis of the historical ranking, some of those studies formed for the development of the thesis can be summarized with their fundamental perspectives as below:

M. Bonfe et al. [9] express the issue of designing a set of residual generators for FDI affecting sensor states of a general aircraft. A multinomial approachment to design residual generator is proposed for realizing overall diagnosis scheme. Constitutional properties of a certain number of dynamic filters are examined for achieving decoupled disturbance, sensitivity optimization of residuals, stability of the system in relation to

noise and error. For small aircraft systems, analytical redundancy is easier to achieve, less costly and less complex to sustain so that hardware redundancy is not preferred as a primary model-based method. In the simulation, a PIPER PA30 aircraft model is used in different flight conditions, the faulty behavior is observed through a non linear flight simulation instrument imposed to the MATLAB tool. The mathematical definition of monitored airplane are determined by means of models of airplane sensor states. The aircraft is characterized by the nonlinear model in addition of the wind gust, turbulence and measurement error. It is specified that the advantage of the proposed method is clarified when its results are compared with other FDI methodologies founded upon unknown input observer, Kalman filter, non linear differential geometric methods or neural networks approaches. The cases cover sensor stuck faults at certain periods and healthy behavior of the sensors are considered.

S. Seema and T. Murthy [10] deal with the fault detection in an aircraft based on Knowledge based Neural Network approach. The method utilizes gradient decline back reproduction training algorithm of neural network. C-Star controller of F8 aircraft model is used to improve the handling qualities and detect sensor with fault for the investigation of the proposed approach in MATLAB Simulink. A normal acceleration sensor failure is considered rather than the one in either lateral or longitudinal axis due its importance in C-Star controller.

A. Gheorghe et al. [1] consider faults presented in servo-control-loop of control surface of an airplane, from FCC to control surface. Application of a smooth approach is significant for certifying the aircraft algorithms from an industrial perspective. Several FDD algorithms could not be admitted because of tuning complication and computing load. The model based approach to increase monitoring performance shows how the approach could advance FDD, meanwhile limiting those difficulties to manage the trade-off. It is stated that as a threshold-based approach, usage of a Kalman filter is a technologically viable solution for earlier fault detection in a control surface at minimum amplitude. The approach is also claimed to meet strict requirements with low computing cost. Kalman filter is implemented as a part of FCC Software of Airbus

A380. The technique is validated not only with several simulations upon simulators at Airbus test plant but also with real flight tests.

S. Singh and T. V. R. Murthy [11] examine the design of optimum control laws for a yawing damper of a linear model of an airplane to operate with a minimal cost and provide performance at an advanced level. It is presented that LQR controller elaborates in particular of rolling mode that is a related with lateral dynamic of an airplane and principally controlled on behalf of rudder, whereas aileron deflection produces rolling angle and rolling rate on airplane movement. A yaw damper executes sending commands from autopilot system to rudder to adjust the coupling effects of yaw and roll modes of flight dynamics. The movement is well-damped in a number of lightweight airplanes, yet simply yaw damper assures the reliability for certification rules. Yawing control is tested with respect to the impulse response to define the control strategy. A Boeing 747 model is used in MATLAB Simulink for the simulation.

Another study of S. Singh and T.V. R. Murthy [5] focuses on observer-based approach for analytical redundancy of the lateral dynamics model of an aircraft. A modular approach to the sensor failure detection and accommodation in EFCS is developed of a Boeing 747 jet aircraft model. The reconstructed or estimated states are derived with the observer for the feedback of the loop. It is stated that system at top-level could be analyzed for interaction of its various subsystems. The number of subsystem levels increases with system's complexity. The aircraft states are simulated for the stuck fault scenarios in MATLAB Simulink. It is attached that the faults could be detected by which uses Canberra metric as a signature of the proposed method. It is concluded that the procedure described could be useful to researchers who like to simulate any engineering state-space model for fault detection and for validation or implementation on DSP processors by using hardware in the loop simulation.

2.3 Fault Detection and Diagnosis Approach

A standard civil aircraft includes multi FCC and power supplies (both hydraulic and electric) for activation of control surfaces. There are several methods to observe fault diagnosis as built-in tests, cross checks and consistency checks. Monitoring and command channels are attached to the actuator positions or control surfaces with related sensors so that fault detection is determined with the consistence checks among two redundant signals calculated in two FCC channels. Whereas computing the identical signal with different channels, it is feasible to distinguish the contrariety because of a channel, sensor, FCC input etc. Each of the control surfaces in a civil aircraft is controlled by double actuators as actual and substitute actuators to supply the safety in the failure cases. When there is a decomposition in the actual actuator, it is switched to passive mode and the role is transposed to the substitute actuator. False alarm rate causes a handover between two actuators when triggered which means the proper actuator is out of function instead of the faulty actuator and the control of the surfaces and results with the degraded flight control as an undesired condition. Similar approaches can be appeared for sensors, whereas not as critical as the actuator faults. A fault in one of the sensors, if undetected, might cause position and attitude errors of estimation. Reconfiguration in those conditions generally depends on isolation of faulty sensor with another sensors to obtain the most desirable estimate of altitude, speed and attitude. In general, fault detection and isolation (FDI) techniques are categorised in to two classes: hardware and analytical redundancy management [1].

In multi engined aircraft where the engines exist apart from the center line, the rudder might be utilized to satisfy yaw because of the failure of the side force propagated by the rudder input associates with the asymmetric thrust vector to generate a resultant force that leads the aircraft to spoil sideways, for instance in the incident of engine failure. In addition, the rudder is used to arrange the aircraft with the runaway meanwhile take off and crosswind landing especially on large civil aircrafts.

The task of the decision system is to specify if the residuals diverge dramatically from

the pattern of zero and non zero residuals and to designate which fault is the most probable to be presented, if any. The decision making for the EFCS failure cases meets a threshold-based method as in Figure 2.1. The alarms are initiated when the signal disparity goes beyond a given threshold on a given time window as they are not equal for each of the failure detection type. A trade-off must be met among detection performance and false alarm rate. Although in a low threshold level there is a false alarm risk, faults can not be identified at minor amplitudes in a high threshold level [1].

High level fault detection methods improve the safety of the flight considered by the civil aircraft certification process and suppress the false alarms and superior loads on the aircraft. Nevertheless, certain EFCS failure conditions may affect structural loads, for instance, loss of limitations, loss of an EFCS or deterioration of a deflection rate. To achieve such faults earlier with smaller magnitudes permits a designer to keep away from strengthening the structure and save weight for supporting aircraft to accomplish sustainability purposes such as fuel burning, noise, range and influence on environment. Structure of an aircraft to be met with the aircraft certification adjustments is an unchangeable rule for the global aviation laws.

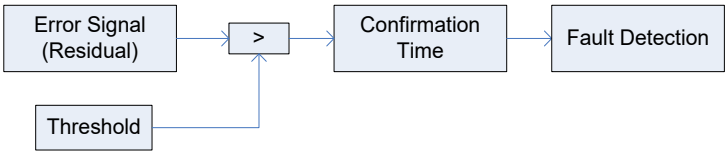

Figure 2.1 Threshold-based Approach for Decision Making

2.3.1 Hardware Redundancy

In the hardware redundancy, multiple sensors are managed for cross-monitoring, thus it is ordinarily sophisticated. The usage of dozens of sensors that makes additional hardware augmentation causes a weighty airplane with an expensive method. An extra

domain requires to relocate equipments inside restricted environment of an airplane. Application of hardware redundancy for detecting system failures and faulty actuators is generally not manageable due to repeating of constituents out of sensors is not reasonable. Hence, applicability of hardware redundancy related FDI is growingly problematical on peripheral friendlier airplane of the future. The problem correlated upon hardware redundancy prompted identification of notion of analytical redundancy related FDI. [12]

2.3.2 Analytical Redundancy

Analytical redundancy approach compares the actual plant attitude to that expected on the principal of numerical model of monitoring procedure and it is implied to model based approachment for FDI as presented in Figure 2.2. The techniques depending upon analytic redundancy are practiced with diverse estimation theories. These methods operate with parameter estimation applications, parity equations and observers. The approachments that are performed with observers designate fault detection based on actuators and comprise the fault detection filter, unknown input and adaptive observer methodologies [13]. A typical model-based FDI system is created of residual generator, residual evaluator and threshold computation with decision making. FDI unit ensures data concerning initiation, position and intensity of the fault. Residual generation reconfigures the sensor/actuator set for fault isolation and adapts the controller to associate fault impacts with respect to system inputs and outputs jointly upon failure decision data of FDI. Analytical redundancy concerns should be coherent in shortage of a fault. Thus, it can be applied for residual generation. Residual evaluation meets the object to make a correct decision for fault detection whether a fault is present or not.

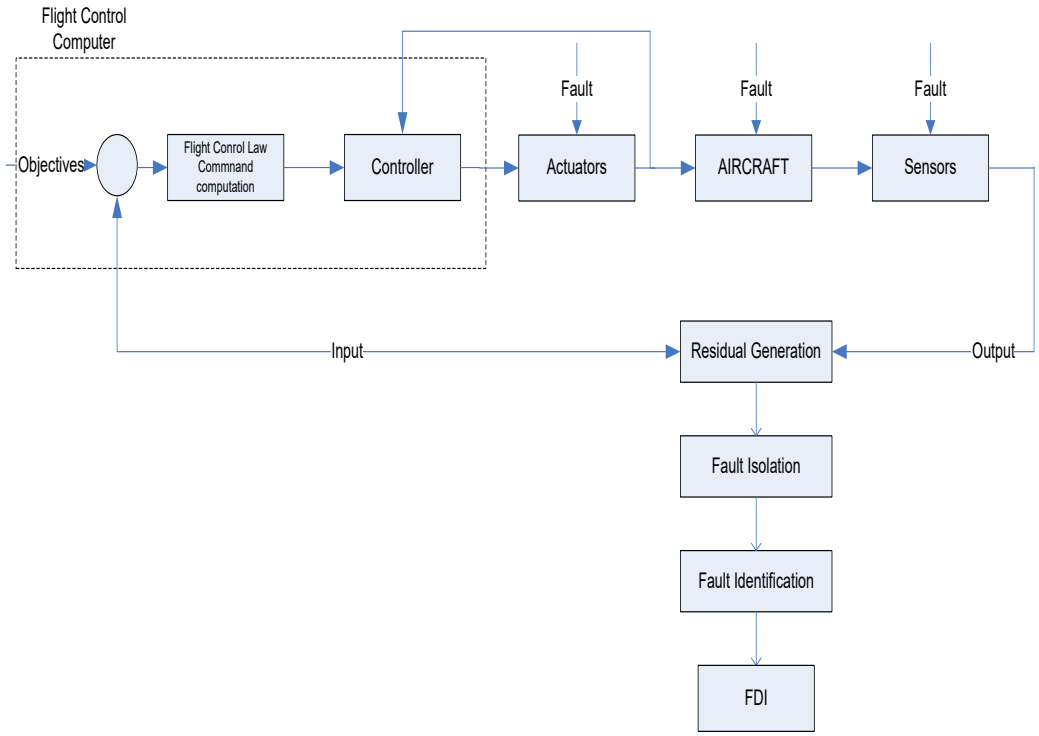

Figure 2.2 General Architecture of an FDI Unit of a Boeing 747

2.3.3 Fault Detection and Diagnosis for Control Techniques

The aircraft sensor signals usually display three basic characteristics: stochasticity (randomness), nonstationarity and serial (dynamic) dependency. Among those characteristics, stochasticity is basically because of the occurrence of noise, uncertainties, atmospheric effects (wind gusts, atmospheric turbulence etc.), and also the pilot commands. Defects in the model and measurement noises can be indicated by stochastic processes emerging as additional inputs. Stochasticity method requires to be accounted to acquire appropriate decision making under uncertainty. Variances in operating situations results in variance of aerodynamic coefficients which lead to diversity in flight dynamics. The redundant techniques employ state estimation, adaptive filtering, statistical theory, Kalman filters in a stochastic setting and Luenberger observers in a deterministic setting are very popular for generating the

signals for analytical redundancy purposes.

From the control point of view, it is approved that there is always difference between the system model and the actual system, i.e. there exists uncertainty in system model. A robust control regards this uncertainty in the synthesis of controller. There is a trade-off with performance depending on how the model could be simplified. For some sort of faults (e.g. partial loss fault), a robust control method is able to tolerate them in a particular rate, whereas, in nature, faults are coincidentally conditions for the system and they are distinct from the system model uncertainty, i.e. it is unknown even in statistical scale. These random conditions alter the system dynamics largely therefore, there is a lack of priori information on the faults for the controller. In every situation, the aircraft system is expected to operate regularly all the time when encountered the faults. Theory and practice are developed from not only to decline disturbance and suppress noise but also to be robust to parameter uncertainty and even more to be tolerant with changing dynamics because of the coincidentally incidents, e.g. faults and failures in sensors, actuators or system structure.

Control reconfiguration is needful afterwards rigid faults are taken place that lead to important structural alterations of the plant dynamics. Sensor failures are naturally simpler for detecting than actuator failures. While sensor failures interrupt the data link between the plant and the controller and make the plant partially unobservable, actuator failures distort the probabilities to affect the plant and make the plant partially uncontrollable. Under nominal situations, the measurements track estimative norms, within a tolerance specified by the amount of uncertainties presented by random system disturbances and measurement noise in the sensors. FDI assignments are generally achieved by observing the output of a failed sensor when it diverges from its estimated norm.

The principal goal of an FDD system is early detection of faults, isolation of their location and diagnosis of their reasons, facilitating correction of the faults prior to additional damage to the system or loss of service occurs. Abnormal conditions arise

when processes diverge dramatically from their normal regime while in online operation. The malfunctions can take place in the single unit of the plants, sensors, actuators or other devices and influence the attitude of the system disadvantageously. Usually, the basic requirable properties of an FDD system are:

- Early detection and diagnosis, i.e. detection delay is required to be minimized.
- Good competency to distinguish between distinct failures (isolability).
- Good robustness to several noise and uncertainty sources and their propagations via the system.
- High sensitivity and performance, i.e. high detection rate and low false alarm rate [7].

2.4 Fault Tolerant Control

The industrial and academia have developed techniques to detect such contingent events in systems in the past 40 years. The information about these contingent events is used to activate an emergence response system. Such emergence response system mostly is monitored or processed by human being. To process these events in time and properly in complicated systems, such as aircrafts, satellite, nuclear power plants and robotic systems, is beyond the reaction capability of human being. In this kind of situation, considering these events in the controller design becomes more and more important, which is the newly emerging control architecture: fault-tolerant control. The fundamental purpose of fault tolerance is to avoid errors from spreading and causing to a dangerous, hazardous or abnormal system attitude. Owing to the steadily incrementing system automation, integration and complexity degrees, industrial operations are ordinarily nonlinear. Improving fault detection and fault tolerant control techniques for nonlinear systems belong certainly to the most striking and challenging issues.

A control system that can establish faults within system components spontaneously while providing system steadiness throughout with a demanded level of entire

performance in the circumstance of system component malfunctions is presented as a fault-tolerant control system (FTCS). In the FTCS, the executable system performance is subject to the presence of redundancies in the control system in addition to the design approaches applied in the synthesis of fault-tolerant controllers. Depending on the utilization of the redundancies, FTCS is categorized into two titles, entitled, active FTCS and passive FTCS. These two methods utilize distinct design methodologies for the identical control objective. Although, the fundamental control objectives are same and indicate alike results, each method could conclude in some distinctive properties due to the margin in design approaches [14].

2.4.1 Active Fault Tolerant Control

Active FTCS deals with many types of faults and failures theoretically, however, it is costly due to the complex architecture of the combination with FDD and the reconfiguration of controller in practice. The primary restriction of the active FTCS method is the time delay from the faults existence along the FDI method and then the reconfiguration of controller based on the fault knowledge. In this process, the system is in danger of control loss because of the inconsistency of controller and system dynamics. The controller-system mismatch could also disable the FDD which may not acquire the accurate data for constructing the faulty system model if it is out of control. It shows that a sort of controller must operate for stabilizing the system during time delay.

2.4.2 Passive Fault Tolerant Control

Passive FTCS is generally a kind of robust control which establishes pre-assigned faults. It could solely deal with partial loss fault, i.e. H∞ and sliding mode control (SMC) method in FTC. domain. It sacrifices the ordinary controller performance to obtain robustness to uncertainties in the system dynamics, whereas SMC's design methodology makes it feasible to be robust to uncertainties without sacrificing excessive performance of the ordinary controller. Even more, the reaching attractor in

SMC is broaden to sliding manifold from the equilibrium in different methodologies that means there is a dynamic subsystem that sense the dynamic alteration because of the disturbances and faults [15].

2.5 Diagnostic Algorithm

The diagnostic steps of the FTC are separated using distinct names with respect to their function. They can be summarized as below:

- Fault detection step decides if fault is arised or not and identifies the time at which the system is subject to the fault.
- Fault isolation step determines in which component a fault is occurred, identifies the location of the fault and separates one fault from other.
- Fault identification and fault estimation steps determine the type of fault and also estimate its severity.

Common characteristics of the diagnostic algorithms can be clarified as below:

- The act of a dynamical system does not solely based on the input but also the initial state. In the case of the initial state of the system is immeasurable, each diagnostic problem consists of a type of state observation problem.
- The disturbance that affects the plant is generally immeasurable. As long as it affects the act of the plant, it must be considered in the consistency check [16].

Several criteria are utilized to evaluate the performance of an FDI algorithm, yet the most important are:

- Rapidity of fault detection
- Sensitivity to slowly improving faults
- False alarm rate
- Missed failure detection

- Inaccurate fault isolation [17].

2.6 An Aircraft Control Surface: Rudder

The rudder is a directional control surface of an aircraft. It is ordinarily connected to the fin or vertical stabilizer which authorizes the pilot controlling yaw related the vertical axis, for instance, the horizontal direction is replaced in which the nose indicates. The rudder enables the plane rotating on its vertical axis while it is controlled by actuators. The vertical axis runs through the top and bottom of the aircraft, intersecting the two axes. Rotation about this axis is checked by the rudder which induces the nose to move left and right that is entitled yaw [18].

As a control surface in a civil aircraft, rudder consists of three distinct hydraulic actuators running from seperate channels which indicates that the rudder carries multiple redundancy as a single control surface. There are also secondary control surfaces that could be utilized in an emergency condition which serves the same function as the primary control surface does [19].

As known the aircraft control surfaces, rudder and aileron control inputs are drived to rotate an aircraft in practice. While rudder yields yawing and satisfies an incident called adverse yawing, ailerons yield rolling. A rudder rotates a traditional fixed-wing aircraft itself as fast as possible provided that ailerons are also used in conjugation. The usage of rudder and ailerons in common generates coordinated rotations, in which the longitudinal axis of the aircraft is in alignment with the arc of the rotation, neither slipping (under-ruddered), nor skidding (over-ruddered). Favorably rotations of rudder at low velocities constitute a spin that could constitute a risk at low altitudes.

Pilots seldom actuate both rudder and ailerons in reverse directions in a maneuver called slip deliberately to get over the crosswinds and retain the fuselage in line with the runway or to lose altitude by raising drag. For instance, the pilots of Air Canada Flight 143 performed an alike technique to land the aircraft due to it was too high

above the glideslope.

One of the primary occasions ruling the loss of control of aircraft is the operational failure in the actuators, the control surfaces, such as elevators, ailerons and rudders. Aircraft rudders are subject to significant forces which specifies its position over a force or torque balance equation. In extreme conditions, these forces or torques might cause to loss of rudder controllability or even devastation of the rudder. The case of American Airlines Flight 587 on November 12, 2001 is one of the most devastating example in the flight history with the total fatality of 260 people. Another air crash due to the failure in rudder occured on September 8, 1994, in which a fault caused the kill of 133 people on board of USAir Flight 427 with Boeing 737. A McDonnell Douglas DC-8-71F lost its pitch control on takeoff, ending up with a crash and destruction of the airplane and death of three flight crew members on February 16, 2000. Another air crash due to failure in elevator occured on January 8, 2003, which killed all 19 passengers and 2 pilots aboard on an airplane Beechcraft 1900D working for US Airways Express Flight 5481. Flight simulation systems have been keeping records of faults and failures occurred in the EFCS since 1970's, many of which are caused by faults and failures in the control surfaces.

2.7 Faults Classification

Faults occur at different locations of a system and are classified according to the location of their occurrence. Faults occur in sensors, actuators and the system itself.

2.7.1 Sensor Faults

A system with sensor faults causes an incorrect measurement signal $y(t)$ that is implemented in the filter design. Some prominent and characteristic sorts of sensor faults demonstrated in Figure 2.3. Modern aircraft systems are highly instrumented with multiple redundant sensors measuring directly or indirectly all of the system state variables. Sensor faults might take place because of the breakdown in the sensor unit,

loss of accuracy and loose mounting of the sensors. The sensor faults might cause a flight control upset and contribute to the extreme behavior of the aircraft [20].

Bias refers to these faults which is a steady offset or error between the actual and measured signals.

Drift is a condition by means of the measurement errors rise over time originated from the loss of sensor sensitivity.

Loss of Accuracy happens in the condition in which the measurements do not reflect true values of the measured quantities.

Freezing of sensor signals is concluded with obtaining a steady value instead of the true value.

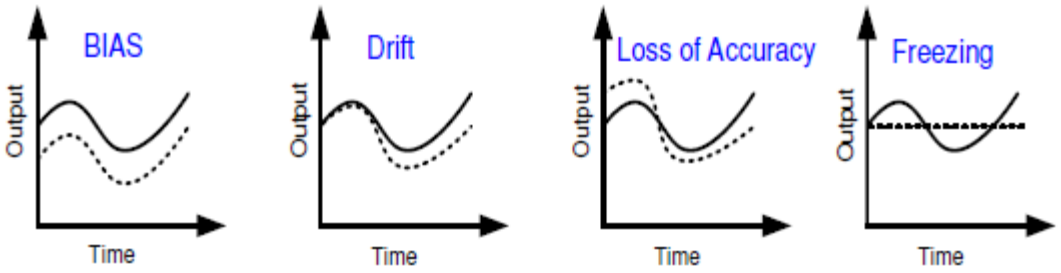

Figure 2.3 Typical Types of Sensor Faults [20]

2.7.2 Actuator Faults

Actuators are the other components in the control-action application and participate in delivering the required power to manage the controlled variable. The majority of the actuators in modern aircraft systems are hydraulic systems. Because of their power delivering capacity, actuators are mostly enormous and heavy component which limit the capability of having multiple redundant actuators to control the identical variable

in the aircraft system. Figure 2.4 represents some characteristic sorts of actuator faults in an aircraft system with respect to the time [20].

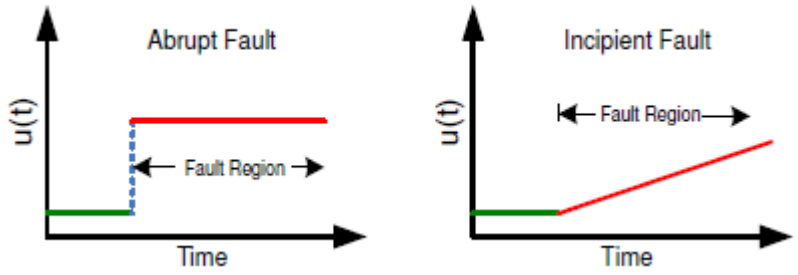

Figure 2.4 Typical Types of Actuator Faults [20]

Abrupt faults are rough faults and have a great effect on the control action. They usually emerge because of the electric short circuits or instantaneous damage of control surface with the impact of environmental agents. This type of actuator faults are easy for detection upon occurrence. Sudden and unexpected actuator struck is an ordinary sort of abrupt fault.

Incipient faults are smooth faults and have a significant influence on the control-action in the prolonged run. They usually emerge because of the leaks in hydraulic systems. This type of actuator faults are difficult for detection because of their slow change in the magnitude. When incipient faults are not concentrated for a long term, it is obvious that the performance of the aircraft is dropped off and enormous failures might be encountered in the flight circumstance.

2.7.3 System Component Faults

System component faults usually modify the elements of system matrices and aerodynamic coefficients. Component faults are difficult for detection and identification because of the spread structure of components in large-scale systems as aircraft systems. Detection of these kind of faults is considerable in high-performance

aircrafts, e.g. warplanes due permanent structural loss.

2.8 Perspective of Observers and Their General Applicability

The most commonly used technique to constitute a residual signal is observers. The main concept of the observer-based FDD includes estimating the outputs of the system from the measurement utilizing an observer and afterwards establishing residuals over directly weighted output estimation errors. In an aircraft plant, faults could happen either in the main processing component (alteration in process parameters) or in the auxiliary component (bias or drift in sensors, controller outputs, actuators, etc.). In the condition of actuator faults, the ability for controlling the system is lost across one of the actuators. Sensor faults decrease the reliability of the measurement knowledge. When there is a loss of a sensor, the system behaves less observable, whereas a fault in the process component modifies the behavior of the overall plant.

In the notion of high-rate dynamic systems, the state estimator requires to be fast and robust against extensive uncertainties, non-stationarities and heavy disturbances and unmodeled dynamics. State estimation of a dynamic state-space model is a significant factor of model-based approaches (e.g. performance monitoring, optimization, and process control). Therefore, it is a necessary practice by the time desired states could not be immediately measured. The research field was pioneered by Wiener, that conducted to Kalman's effort. Additionally, progresses in estimation and control theory enabled the evolution of observers with fast convergence characteristics together with computer science. Those observers have the potency to bring out smarter and safer systems competent to respond to real-time incidents. A high-rate estimator must also be competent to manage those matters which diversify high-rate dynamic systems from other systems. In the event of simplicity towards complexity of the estimators is referred, i.e. for computation, properties, implementation, simplicity associates to more rapid convergence rates. Nevertheless, the performance of observers is changeable with respect to the applications and the indications are subject to the kind of the scenarios [21].

Stereotype estimators quickly strike out estimating states in the case noise and uncertainties are available. In serviceable implementations, noise can originate from sensor measurements, algorithm application, spoiling estimation values, etc. A filter could be applied to compress noise if the noise function is properly established into its architecture. This noise compression forms with attached computational costs. For decreasing the convergence time, the observer gain can be augmented. Nevertheless, this may adversely affect the certainty of the estimation as the noise may be enhanced. Uncertainty is another frequent matter for several feasible implementations. A variety of techniques have been investigated to cope with system uncertainties. Generally, statistical methods could determine faults ahead probabilistic measure and can be utilized to direct prognosis by assessing the probability of faults, yet they request knowledge of probability distribution functions. The statistical features are ordinarily computed from a great number of tests, that is hard to accomplish for high-rate systems. Those methods work well when previous data is convenient to generate a great understanding of the statistical characteristics of the system's attitude. Data-driven methods could maintain proper estimations on the basis of sample identification and categorization. As an alternative, those methods request certain patterns and extended training upon convenient data set. Because of the spontaneous existence of high-rate incidents, minor cognition is assured in the exterior loads and system modifications. Those observers are favorable in case of the complicacy of a system does not permit for a proper physical representation. Model-driven methods are advantageous for supplying certain measures of damage because of the existence of models, thus making situation evaluation and system prognosis possible. Those observers generate rapid and proper estimations for systems with well specified models. Nevertheless, those observers request information of the physical model, that is a difficult assignment for real-world systems. In addition, high-rate systems can encounter modifications in the structure demanding distinct model parameters than primarily defined [21].

Filters and observers display dissimilar sensitivity properties according to the different failure modes such as system, actuator, control surface and sensor failures. The ability

to differentiate the failure effects from other signal such as noise, gust and control inputs is a significant characteristic of the filter. To give examples of some filters/observers; Kalman filter, as an optimum estimator, is sensitive to each of the failures, Insensitive observer is only sensitive to sensor failures, Robust Kalman filter is sensitive to system, actuator, unstable control surface and sensor failures, Failure Mode Sensitive observers are merely sensitive to specific failure modes. Therefore, the mentioned filters and observers could be run meanwhile in the FDI algorithm, and they could be considered for distinct functions [22].

CHAPTER 3

METHODOLOGY

3.1 Overview

The paper is actualized to improve and demonstrate the applicability of FDD algorithms for a civil aircraft plant. It is aimed to propose an alternative analytical solution for the advancement of fault detection performance proceeding a better flight profile and diagnose the sensor measurement errors of civil aircraft's specific control surface in a shorter confirmation time with a slighter detection threshold level which are originated from the closed-loop of the deterministic aircraft model and improve the responses of fault detection to prevent the extra structural loading as an undesirable condition. It is also aimed to simulate an aircraft flight control system that feeds reliable data to the pilot interface with respect to the dedicated nonlinear configurations while maintaining a steady state flight. In the simulation environment, scenarios are generated and the analysis of the system's reactions is investigated for several cases. The approach points out to a stable flight mode and presents a fast and sensitive reaction to the undesirable sensor faults. Sensor faults are related with sensors which has a function of measuring states of the system and might directly influence the procedure only in the case of measured outputs are utilized for the feed back control. In airplane control, overall states are less convenient for feed back objective than measured outputs. Exerting modern control theory, when measured outputs acquire sufficient data related system dynamic, it is feasible to apply data for estimation and observation of the overall states. Thereafter, those state estimates can be utilized for feed back objectives.

For the study, a nonlinear fixed-wing aircraft model is practiced with a proper tuning in MATLAB Simulink that computes non linear dynamics and control. An optimum

method of EFCS for a fixed wing airplane EFCS includes the flight moving surfaces,

each are controlled from the cockpit, connecting linkages and the necessary functions to control the plant.

The mathematical model for movement of an airplane is fairly complex and consists of the set of six nonlinear coupled differential as known six degrees of freedom (6 DOF) rigid body formulations which eventuate as an outcome of implemented forces and moments such as aerodynamic, thrust and gravitational. Under specific assumptions, these equations can be decoupled and linearized into the lateral and longitudinal dynamics equations. A set of regional approximates for those forces is scheduled related to the values considered by true airspeed, altitude and flight path. An aircraft has a number of varied control surfaces which are the main flight controls, i.e. roll, pitch and yaw control, originally acquired by deflection of ailerons, elevators and rudder and also the combinations of them as a coupling effect. Lateral control receives lateral stick pilot inputs and supplies anti-symmetric control requests to inner and outer control surfaces. The pilot moves the rudder sideways which controls yaw and the required yaw angle. In this paper, the control system design for yaw control is presented. Some of the states of the fully nonlinear dynamics aircraft model include the inertial position displacements, altitude, airspeed and control inputs.

The sensor fault detection model is developed at the same time and accurate links are settled with the nonlinear civil aircraft model. As a control surface, mainly rudder is considered to have a significant contribution to determine the lateral dynamics during flight stage. Lateral oriented equations of motion (EOM) include side force, yawing and rolling moment of aircraft movement. By subtracting estimated and monitored channel (the error signal) instantly, the residual is generated. Residual signal demonstrates fault emergence according to whether its value is higher or not than a threshold and decides which sensor is failed. Residual of faulty sensor exceeds threshold value, whereas residual of healthy sensor stands under threshold. Threshold value depends on residual error quantity because of the measurement errors, model

approximates and disturbance signals which are not exactly decoupled. The measured states are observed and compared with and without the faulty conditions. The proposed

FDI scheme operates with the approximation that only one sensor is in the faulty condition at a time instant, that is an acceptable approximation in practice. The decision making law could be managed for failure detection that influences the innovation sequence.

The loss of control effectiveness and sensor stuck are estimated upon the filter. If fault has not been originated, estimated states will be identical to those of the measurements. On the other hand, if fault has been originated in the system, the estimates derived from the filter will point out a value different from the measurements. In the circumstance of airplane moving surface stuck fault, it is quite hard to assure FDI scheme due to the bias effect which initiates the stuck surface that could be emerged by diverse combinations of the control surfaces. For instance, if right horizontal stabilizer stuck at 0.087 radians, impact causes stuck moving surface is nearly identical with impact causes left horizontal stabilizer stuck at -0.087 radians [13].

EFCS include intense coupling. Their sub-systems are intensely coupled as well and due to this condition, there are lacking of measured state variables. For achieving isolation procedure for those systems, application of analytical redundancy is required. For example, sensor fault detection model coupled with high fidelity aircraft model can accomplish the detection capability of bias, drift or augmented noise of nonredundant sensor in real time by means of setting analytical redundancy. The use of sensor measurements in the feedback loop of a control system makes sensors significant components in EFCS. Multiple physical redundancies have been operated in many high performance civil aircrafts, whereas analytical sensor redundancies are more appealing as it counters with higher simplicity, lower cost and weight with respect to the model accuracy.

The analytical redundancy for sensors related to the lateral dynamics model of civil

aircraft is focused. Stuck faults where sensor becomes stuck at specific ranges and erroneously yields outputs are detected by the fault indicator scope of the model. Reconfiguration with observer estimation for the failed sensor state is done as soon as

fault is detected. Reconfiguration process maintains the estimated signal from mathematical model rather than faulty sensor signal in feed back loop. The process detects fault by comparing the output of aircraft sensor value of aircraft lateral dynamics with the one obtained from the observer estimate. It also switches over to observer estimate of the output instead of faulty sensor output in shortly after fault is indicated. Reconfigurator performs the task of correcting faulty state vector in case of fault, otherwise it continues to keep aircraft sensor output in the feedback loop.

After focusing on modeling, creating algorithms, analyzing and visualizing simulations, customizing the simulation environment and introducing parameters, the whole deterministic civil aircraft model could be visualized. The subsystems composing the whole civil aircraft model are configured together in main simulation model to indicate accomplished detection and reconfiguration of sensor fault in the aircraft. Main simulation model could be examined at an advanced rate and then every subsystem block could be chosen to view ascending rates of model in detail. The approachment assures a comprehension of model organization and interaction of the system parts. System at top-level can be analyzed for interaction of its various subsystems. The number of levels increases with system's complexity.

A safe steady state flight at fixed altitude and airspeed is considered to be simulated via MATLAB Simulink. Therefore, thrust, drag, weight and lift forces balance each other in x-axis and y-axis such that an alteration in yaw and roll angle do not modify airspeed airplane under any conditions. Parameters of the simulation covering altitude, angular rates, positions and time are assigned to be compatible with the zero flight path angle during the steady level flight. An accurate determination of parameters allows to maximize reliability of responses accordingly the measuring noise or model errors, whereas maintaining fault sensitiveness features. The cruise flight case is determined

to map the input/output trim manifold independently when single fault occurs.

The navigation sensors of an aircraft identify the plant's position by measuring the acceleration and rotation changes and integrating them to speed and direction variables

and then feed the data to the pilot even during flight. Due to small inaccuracies in the measurements, the position errors grow over time. The sensor faults are expected to be the major element rather than the faults originated from wind, turbulence or severe temperature changes. The sensor noise (e.g. bias or white noise) can influence the FDI scheme severely. Due to faulty signal has alike characteristic with sensor noise, it is not easy to separate these signals.

Concerning the implementation scope of common aviation airplanes, the detection delay values, reported in Table 3.1 and
Table *3.2* are estimated in terms of time obtained by slowest residual to surpass the established threshold as worst case outcomes of a PIPER PA30 aircraft [9]. Moreover, the fault sizes are relative to the condition in which the fault occurrence is detected and isolated at the earliest.

Table 3.1 Minimum Detectable Step Input Sensor Faults

Input sensor	**Fault magnitude**	**Detection delay**
Rudder deflection	4°	8 s
Aileron deflection	3°	6 s
Elevator deflection	2°	18 s
Throttle aperture	%2	15 s

Table 3.2 Minimum Detectable Step Output Sensor Faults

Output sensor	**Fault magnitude**	**Detection delay**
Roll rate	2°/s	24 s
Yaw rate	3°/s	29 s
Roll angle	5°	5 s
Yaw angle	6°	20 s

The main criteria handled to remark the variables with respect to their severity is subject to dynamic of parameters that are monitored. Particularly, time scale of the altered parameter is quicker means the violence of the correlated fault is significantly superior. On the other hand, faults on the angular rate are less critic, although their time scales are not the slowest. In terms of parameters on tables above, comparatively reliable filters are applied to the FDI method to increase the critical sensor estimations.

3.2 Boeing 747 Data Analyses

The aircraft model examined in this study is a Boeing 747 which is an inter continental wide body transportation via four turbofan engines which makes it an excellent representative for any of the civil aircrafts serving nowadays thereby, provides a conformable test bed with versatile of modeling and design techniques. It has a range of greater than 11,000 kilometers, a cruise airspeed more than 965 km/h and an attitude of 13,716 m. [23]. The diversity with other Boeing aircrafts are generally relevant with developments in the structure and payload.

The center of the study is about lateral tendency of an aircraft. The precise equations leading the motion of an aircraft are lateral and nonlinear. Lateral oriented dynamics are decoupled of longitudinal dynamic, whereas they are coupled with lateral directional dynamics. Due to the numerical model of airplane covers decoupled small perturbations, transfer functions related longitudinal input parameters to lateral output

parameters are not presented. A movable rudder with a single component and an engine thrust could be used to manage the lateral axis motion [24].

On the contrary to the longitudinal dynamic, explication of lateral oriented dynamic is not very simple due to stability means are not quite different. It generally causes a considerably larger magnitude of coupling [25].

Nonlinear model of Boeing 747 introduces entire aerodynamics nonlinearity. Yawing control could be acquired by changing the lift on the rudder. Deflection of a control surface not only alters the angular rate but also alters moment of center of gravity (g).

Aircraft reference frame is indicated in Figure 3.1 with respect to the body-fixed frame F_E. F_O represents origin at g of the aircraft, F_W represents wind axes reference frame, F_S represents stability axes reference frame and F_B represents boxy fixed reference frame. Angular rate alteration affects the sideslip and roll angle immediately. In addition, coupling effects on moving surfaces presents within aircraft. For instance, yaw rate (r) could be shifted due to the deflection of partial/entire of the control surfaces.

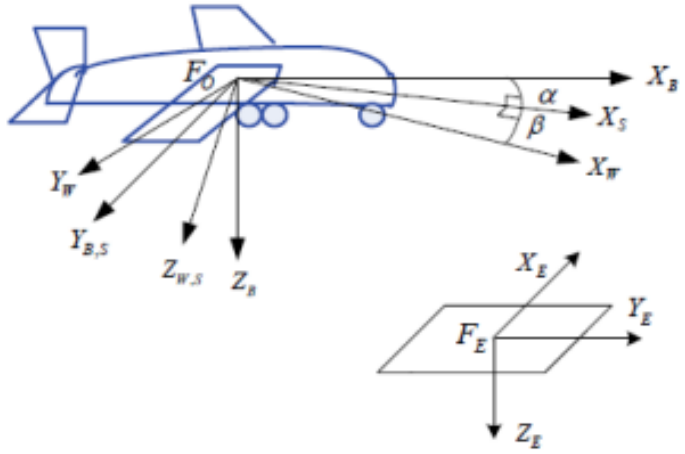

Figure 3.1 Aircraft Reference Frame [6]

The linear time-invariant (LTI) systems of Boeing 747 are introduced for linear estimation method. LTI systems are utilized in the design phase, whereas superior constancy non linear model is utilized in the closed loop experiments. LTI models are assured by means of linearization of non linear aircraft on trim points at true airspeed 0.44 Mach and altitude 20,000 ft. The parameters represent less severe faults at trim points.

Aircraft trim analysis is significant process to assess the aircraft attitude. As a part of the analysis, the trim routine is utilized to meet an equilibrium point of the plant under a given set of constraints. The purpose of the trim routine is to solve the aircraft nonlinear EOM (first-order differential equations) to receive state and control vectors that assure the time derivatives of state variables are equal zero or remain constant. In some cases, equilibrium points may not be unique.

The trim analysis restores the deflection inputs and other states of the airplane based on a motion case in which time derivatives of angular velocities are all equal to zero. There are different alternatives for trimming of the aircraft. They can be summarized as steady level, level turn, push-over/pullover, beta trim, thrust-stabilized turn and specific power turn. Each situation demands distinct limitations and detached variables, i.e. mainly flight controls, aircraft and engine states [6].

The modification of dynamic and kinematic parameters of Boeing 747 is applied upon the deterministic aircraft model in MATLAB Simulink. Boeing 747 aircraft model is obtained specially in the steady state level flight of 0.44 Mach true airspeed and altitude of 20,000 ft. The nonlinear model is linearized around this flight condition as the trim and linearization routines. Trim values, lateral oriented mass distribution and aerodynamic stability characteristics of Boeing 747 at initial flight condition is given in Table 3.3 [24]. The physical parameters such as mass and inertia are stable to their nominal values. A fault is regarded non compensable when flight trajectory of the airplane passes to a non-trimmable region.

Table 3.3 Trim Values, Lateral Oriented Mass Properties and Aerodynamic Stability Derivatives of Boeing 747 at Initial Flight Condition

Initial Flight Condition of Boeing 747	**Cruise (low)**
State and Control	**Value**
V_T	492 ft/s
α	0.0436 rad
β	0 rad
p	0 rad/s
q	0 rad/s
r	0 rad/s
φ	0 rad
θ	0.0436rad
$\emptyset$	0 rad
x_e	0 ft
y_e	0 ft
h_e	20,000 ft
δ_{th}	0.75 rad
δ_a	0 rad
δ_e	0 rad
δ_r	0 rad

Table 3.3 (continued)

Geometry and Intertias	**Value**
S	5500 ft^2
b	196 ft
m	636,636 lbs
I_{xx}	18.2×10^6 slug-ft^2
I_{zz}	43.1×10^6 slug-ft^2
I_{xz}	0.97×10^6 slug-ft^2
Lateral Directional aerodynamic stability derivatives	**Value**
$c_{l\beta}$: rolling moment due to sideslip angle derivative	-0.160
c_{lp} : rolling moment due to roll rate derivative	-0.340
c_{lr} : rolling moment due to yaw rate derivative	0.130
$c_{l\delta a}$: rolling moment due to aileron deflection derivative	-0.013
$c_{l\delta r}$: rolling moment due to rudder deflection derivative	0.008
$c_{n\beta}$: yawing moment due to sideslip angle derivative	0.160
c_{np} : yawing moment due to roll rate derivative	-0.026
c_{nr} : yawing moment due to yaw rate derivative	-0.280
$c_{n\delta a}$: yawing moment due to aileron deflection derivative	-0.001
$c_{n\delta r}$: yawing moment due to rudder deflection derivative	-0.100
$c_{y\beta}$: side force due to the side slip derivative	-0.900
c_{yp} : side force due to roll rate derivative	0
c_{yr} : side force due to yaw rate derivative	0
$c_{y\delta a}$: side force due to aileron deflection derivative	0
$c_{y\delta r}$: Side force due to rudder deflection derivative	0.120

To solve the equations defining lateral directional aircraft motions, all the coefficients should be estimated for the derivatives of L, N and Y with respect to the appropriate independent variables v, p and r.

c_{l_β} (dihedral effect) is a measure of the preliminary inclination of an airplane to roll when disturbed in β. It has a significant role in determining the lateral static stability of the airplane. However, it is hard to quantify since it depends on many elements including wing dihedral, wing sweep and wing/fuselage/fin geometry.

c_{l_p} (roll damping) is mainly originated by the wings and tail. As the aircraft rolls, the impact on one wing is increased which constitutes more lift and the impact on the other wing is decreased which generates less lift. The identical effect occurs when the aircraft yaws, but c_{l_r} is much smaller in magnitude than c_{l_p}. Positive values for c_{l_p} cause the system to roll uncontrollably and diverge.

c_{l_r} (cross-coupling) is primarily contributed by two sources as the wings and vertical tail from the fact that, when the airplane is yawed, α is changed and the lift force is propagated.

$c_{l_{\delta_r}}$ (roll due to rudder) is negative whether, the center of pressure (cp) of the vertical tail is above the center of gravity (cg), as with a conventional vertical tail.

$c_{l_{\delta_a}}$ (lateral control power) has a great significance since it represents the effect of deflecting the ailerons which is the main roll control mechanism. A rolling moment can also be constituted by deflecting the rudder as an outcome of the alteration of the lift distribution, but this effect is much smaller in magnitude than the aileron effect.

c_{n_β} (static directional stability/ weathercock stability) is described as the preliminary inclination of an airplane to return to or depart from its equilibrium β (normally equal to zero) when disturbed. It is principally responsible for the aircraft directional

dynamic stability. The total value of c_{n_β}, at any β, is specified by contributions from the vertical tail, fuselage and wing.

c_{n_p} is another potentially significant moment which is originated from the differential drag constituted by the wings as they roll.

c_{n_r} provides weathercock damping analogous to c_{m_q} in pitch.

$c_{n_{\delta_r}}$(rudder power) is of major importance since it represents the impact of deflecting the rudder. It is the main yaw control mechanism, but there is a potential for aileron deflection to constitute a yawing moment which comes from the differential drag between the left and right ailerons when they are deflected.

3.3 Mathematical Modelling of Aircraft

3.3.1 Rigid Body Equations of Motion

A number of assumptions must be established to derive the EOM. These assumptions could be summarized as below:

- The aircraft is a rigid body
- The earth is flat and non-rotating
- The aircraft mass characteristics are stationary and any mass variety is inconsiderable
- The aircraft has a plan of symmetry in the $X_B Z_B$ plan which denotes that moment of inertia I_{xy} and I_{yz} are equal to zero. This assumption is eligible for an undamaged aircraft. In the case of the aircraft is influenced from asymmetric damage, the assumption does not work anymore.

Aircraft EOM could be derived from Newtons Second Law. The external forces

consist of thrust forces, gravity forces, aerodynamic forces and the external moments consist of the engine moments and the aerodynamic moments. The external forces could be derived in Eq. (1), Eq. (2), Eq. (3) and the external moments could be derived in Eq. (4), Eq. (5) and Eq. (6) with respect to [6] in terms of aerodynamic coefficients.

$$F_x = \frac{1}{2}\rho {V_t}^2 S(-c_D \cos\alpha + c_L \sin\alpha) + F_{T_x} - mg\sin\theta \tag{1}$$

$$F_y = \frac{1}{2}\rho {V_t}^2 S c_Y + F_{T_y} - mg\cos\theta\sin\emptyset \tag{2}$$

$$F_z = \frac{1}{2}\rho {V_t}^2 S(-c_D \sin\alpha - c_L \cos\alpha) + F_{T_z} - mg\cos\theta\cos\emptyset \tag{3}$$

$$M_x = \frac{1}{2}\rho {V_t}^2 S b c_{lb} + M_{engx} \tag{4}$$

$$M_y = \frac{1}{2}\rho {V_t}^2 S \bar{c} c_{mb} + M_{engy} \tag{5}$$

$$M_z = \frac{1}{2}\rho {V_t}^2 S b c_{nb} + M_{engz} \tag{6}$$

3.3.2 Nonlinearity and Linearity Conversion

The primary concept of linearization is to convert a non linear model into an exactly or partially linear model firstly and apply common linearization design techniques for completing control design subsequently. This attempt is utilized to solve numerous feasible non linear flight control issues. It can be implemented to significant classes of nonlinear systems, i.e. so-called input state linearization or minimal phase models requiring complete state measuring [26].

The EOM of a rigid airplane are non linear. It is a form of 12 non linear first order normal differential equations. Within 12 equations, 6 equations are dynamic and other 6 equations are kinematic. Dynamic equations originate from 3 force and 3 moment equations, whereas kinematic equations originate from 3 navigation equations and 3 Euler angles equations. Navigation equations are decoupled with other nine equations, in this way the other 9 equations could be taken as a set and the navigation equations could be taken independently.

Among the resulting nine nonlinear equations, lateral dynamics equations that is investigated in this study, including the set of aerodynamic coefficients, is linearized around steady state trim point and then used in the simulations to evaluate the sensor fault detection performance of the Kalman filter. Linearization is acceptable in such flight scenarios covering a climb, level cruise, coordinated turn, power approach or even in a pull up, in which the aircraft functions mostly near around the equilibrium point. Whatever the case is, proposed FDI scheme manages the flight parameters that is utilized for fault identification. In case of FDI scheme detects a failure when any parameter is out of identified gap, FDI scheme notifies an error. However, it must affirm the fault notice following warnings when flight parameters are in identified gap.

Nonlinear equations can be linearized by means of small-disturbance theory. In accordance with the theory, each variable in these equations is changed with a reference value and also a disturbance or perturbation. Technically, robustness is referred to how the system can struggle with the perturbations of the system model, meanwhile releases disturbance and measurement noise to other properties such as stability and sensitivity. For simplicity, the reference flight situation is considered to be symmetrical and pushing forces are considered to stand stable. Entire structure of airplane is concerned with the sensor faults. A sum of the differential nonlinear equations of Boeing 747 for the lateral motion are extracted from [6] and given as in Eq. (7), Eq. (8), Eq. (9), Eq. (10).

$$\dot{\beta} = \frac{1}{mV_t}\Big(-F_x \cos\alpha \sin\beta + F_y \cos\beta - F_z \sin\alpha \sin\beta - mV_t(-p \sin\alpha + r \cos\alpha)\Big) \tag{7}$$

$$\dot{r} = \left(\frac{\left(I_{xx} - I_{yy}\right) I_{xx} + {I_{xz}}^2}{I_{xx} I_{zz} - {I_{xz}}^2} p - \frac{\left(I_{xx} - I_{yy} + I_{zz}\right) I_{xz}}{I_{xx} I_{zz} - {I_{xz}}^2} r\right) q + \frac{I_{xz}}{I_{xx} I_{zz} - {I_{xz}}^2} M_x + \frac{I_{xx}}{I_{xx} I_{zz} - {I_{xz}}^2} M_z \tag{8}$$

$$\dot{p} = \left(\frac{\left(I_{yy} - I_{zz}\right) I_{zz} + {I_{zz}}^2}{I_{xx} I_{zz} - {I_{xz}}^2} r - \frac{\left(I_{xx} - I_{yy} + I_{zz}\right) I_{xz}}{I_{xx} I_{zz} - {I_{xz}}^2} p\right) q + \frac{I_{zz}}{I_{xx} I_{zz} - {I_{xz}}^2} M_x + \frac{I_{xz}}{I_{xx} I_{zz} - {I_{xz}}^2} M_z \tag{9}$$

$$\dot{\emptyset} = p + \tan\theta\,(q \sin\emptyset + r \cos\emptyset) \tag{10}$$

The equations above could be approximated to partially linear systems as an outcome of the nonlinear functions transformed to linear functions using small-disturbance theory. The assumption covers the motion of the aircraft includes small deviations about a steady flight condition. The model will be defined as nonlinear if the primary variables are subject to the state or control. Conversely, the model is linear when the primary variables are free from the state and control. The system matrices of the aircraft can be computed according to the specified flight cases in the scenarios with the following equations as in Eq. (11), Eq. (12), Eq. (13), Eq. (14), Eq. (15) [27]. Basically, a transformation is linear if its output is proportional to its input which means the linear relationships between variables are maintained. On the other hand, if a transformation does not satisfy this characteristic, it is termed as nonlinear as correlation between the variables are changed. The aircraft model used in this study consists of many complex nonlinear equations identifying force, moment and motion of the platform. Considering the state estimators also used for the comparison approach are both linear estimators, so the linear transformation is required specific to the lateral

states. Eq. (11) is the matrix representation of partial derivatives of the lateral states and figures out the linear transformation that takes a small change in the input of a function to the corresponding small change in the output supplied that several partial derivatives exist and deal adequately well.

$$\begin{bmatrix} D\beta \\ D\hat{p} \\ D\hat{r} \\ D\emptyset \end{bmatrix} = \begin{bmatrix} \frac{c_{y_\beta}}{2\mu} & \frac{c_{y_p}}{2\mu} & \frac{c_{y_r} - 2\frac{\mu}{A}}{2\mu} & \frac{c_{w_e} cos\gamma_e}{2\mu} \\ \frac{c_{l_\beta}}{I'_x} + I'_{zx} c_{n_\beta} & \frac{c_{l_p}}{I'_x} + I'_{zx} c_{n_p} & \frac{c_{l_r}}{I'_x} + I'_{zx} c_{n_r} & 0 \\ I'_{zx} c_{l_\beta} + \frac{c_{n_\beta}}{I'_z} & I'_{zx} c_{l_p} + \frac{c_{n_p}}{I'_z} & I'_{zx} c_{l_r} + \frac{c_{n_r}}{I'_z} & 0 \\ 0 & \frac{1}{A} & \frac{1}{A} tan\gamma_e & 0 \end{bmatrix} \begin{bmatrix} \beta \\ \hat{p} \\ \hat{r} \\ \emptyset \end{bmatrix} + \begin{bmatrix} \frac{\Delta c_{y_c}}{2\mu} \\ \frac{\Delta c_{l_c}}{I'_x} + I'_{zx} \Delta c_{n_c} \\ I'_{zx} \Delta c_{l_c} + \frac{\Delta c_{n_c}}{I'_z} \\ 0 \end{bmatrix} \tag{11}$$

$$I'_x = A(\hat{I}_x \hat{I}_z - \hat{I}_{zx}{}^2)/\hat{I}_z \tag{12}$$

$$I'_z = A\left(\hat{I}_x \hat{I}_z - \hat{I}_{zx}{}^2\right)/\hat{I}_x \tag{13}$$

$$I'_{zx} = \hat{I}_{zx} / A(\hat{I}_x \hat{I}_z - \hat{I}_{zx}{}^2) \tag{14}$$

$$\begin{bmatrix} \Delta c_{y_c} \\ \Delta c_{l_c} \\ \Delta c_{n_c} \end{bmatrix} = \begin{bmatrix} c_{y_{\delta r}} & 0 \\ c_{l_{\delta r}} & c_{l_{\delta a}} \\ c_{n_{\delta r}} & c_{n_{\delta a}} \end{bmatrix} \begin{bmatrix} \delta_r \\ \delta_a \end{bmatrix} \tag{15}$$

3.4 Fault Detection Method

A simplified trim model of the lateral axis LTI Boeing 747 model in a cruise flight

used in the simulation has mainly four states (x) which consist of sideslip angle (β), yaw rate (r), roll rate (p) and roll angle ($\emptyset$) as given in Eq. (16) and two inputs (u) which consist of the rudder deflection (δr) and aileron deflection (δa) as given in Eq. (17) [11]. The main states of the aircraft can be summarized mainly in the true airspeed (V_T), angle of attack (α), sideslip angle (β), angular rates (p, q, r), Euler angles ($\varphi, \theta, \emptyset$), positions in earth-fixed reference frame (x_e, y_e) and altitude (h_e). For the study, β is accepted as faulty sensor state, whereas other states are healthy. Therefore, the lateral dynamic effect of the sideslip angle is represented efficiently.

Controller and pilot commands associated with the autopilot system separately carry signals to the feed the required inputs to the actuator dynamics system. Sensors are accepted to be optimal, thus inputs of aircraft body form a feedback straightly to observer design. In other words, the controller within the autopilot model is disrupted by noise in the sensors during simulation. Detecting the error in sideslip is critical because it augments parasite drag due to the efficient frontal cross-section area of the plant is augmented and it leads to a decrease in lift due to the blanking impact of the fuselage. Related to the sideslip angle, errors can be divided to two groups as calibration error influencing the sensors and additional white noise modeling the sensor defectiveness.

$$x = [\beta, r, p, \emptyset]^T \tag{16}$$

$$u = [\delta_r, \delta_a]^T \tag{17}$$

In this study, the steady state function is designed and tested with different simulation cases. For carrying out the design, a linearized model is developed in an equilibrium point. The cruise flight is proceeded at altitude of 20,000 ft and Mach 0.44. The lateral dynamic approachment of the airplane is used to design observer as a model-based FDD. The linear state-space equations are given in Eq. (18) and Eq. (19). Here, as the linearization purpose, state-space equation demonstrates that system model does not change over time which means system matrices A and B remain constant. On the other

hand, the nonlinearity of the aircraft model of Boeing 747 is not affected with this conversion. The lateral attitude of the aircraft is examined with the fault effects on the lateral states.

$$\dot{x} = Ax + Bu \tag{18}$$

$$y = Cx + Du \tag{19}$$

3.4.1 Method for Linearization

For the study, linear analysis tool of MATLAB is used to find the system matrices as the state matrix (A), input matrix (B), output distribution matrix (C), feed forward matrix (D), given as Eq. (20), Eq. (21), Eq. (22), Eq. (23) are matched for the plant's trim values in a steady state flight at $20{,}000$ ft altitude and 0.44 Mach true airspeed. After adding input perturbation to deflections and open loop output to any of the lateral states of the aircraft model in Simulink and run the complete model, those system matrices are correctly found.

$$A = \begin{bmatrix} -0.1345 & -1.0040 & 0.0459 & 0.0653 \\ 0.9460 & -0.3314 & -0.0559 & -0.0006 \\ -2.7057 & 0.4002 & -1.1620 & 0.0018 \\ 0.0267 & 0.0428 & 1.0117 & 0 \end{bmatrix} \tag{20}$$

$$B = \begin{bmatrix} -0.0001 & 0.0132 \\ -0.0157 & -0.6222 \\ -0.2241 & 0.1070 \\ 0.0023 & -0.0008 \end{bmatrix} \tag{21}$$

$$C = \begin{bmatrix} 1 & 0 & 0 & 0 \\ 0 & 1 & 0 & 0 \\ 0 & 0 & 1 & 0 \\ 0 & 0 & 0 & 1 \end{bmatrix} \tag{22}$$

$$D = \begin{bmatrix} 0 & 0 \\ 0 & 0 \\ 0 & 0 \\ 0 & 0 \end{bmatrix} \tag{23}$$

To prove that the acquired system matrices conform with the nonlinear aircraft model of Boeing 747, the states of measurements can be compared with the state-space of the system. The results of lateral states are demonstrated as in Figure 3.2, Figure 3.3, Figure 3.4 and Figure 3.5.

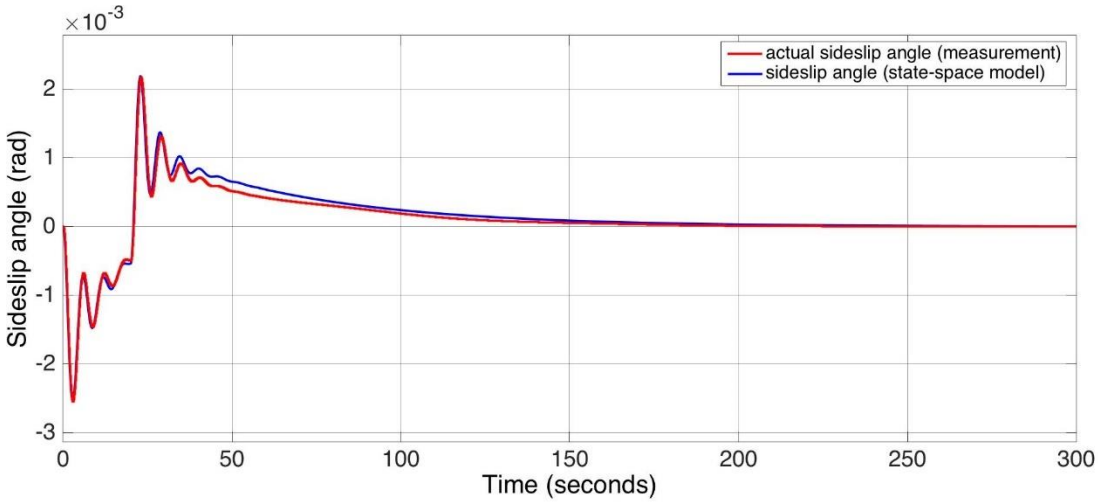

Figure 3.2 Sideslip Angle vs. Time

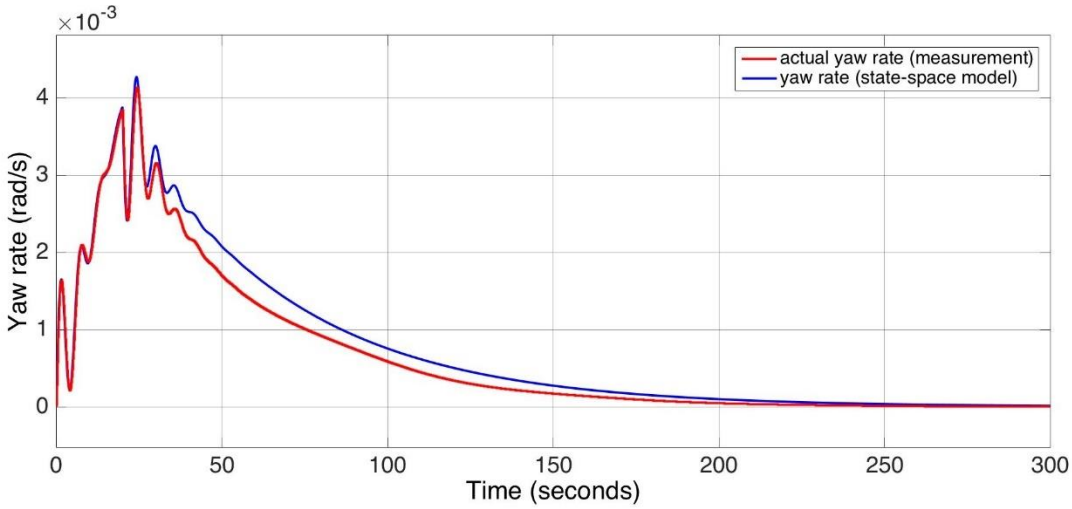

Figure 3.3 Yaw Rate vs. Time

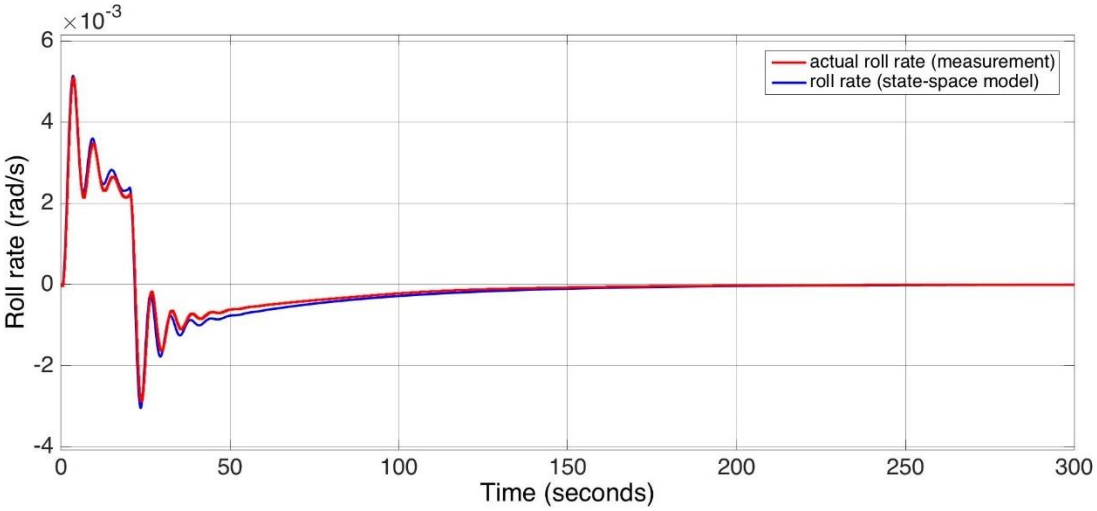

Figure 3.4 Roll Rate vs. Time

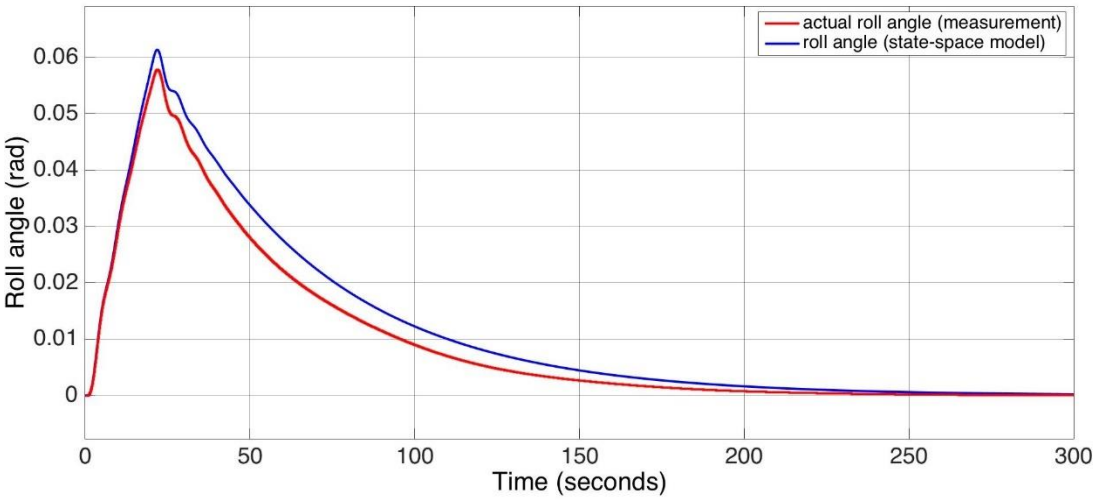

Figure 3.5 Roll Angle vs. Time

When rudder input $\delta r = 0.01$ rad, the identical states of state-space model are observed to converge with the sensor measurements. This condition verifies that the system model is linearized accurately and can be used with linear observers effectively.

The alterations in the platform parameters at any flight situation are regarded as a fault that should be detected with state estimation. For instance, if it is not corrected, a sensor failure will lead to false estimation of variation in parameters of A matrix or an

actuator failure will lead to false interpretation in parameters of B matrix. With another example, plant variation because of the loss of the aircraft structure could lead to false values of system matrices A, B, C, D. [28].

3.4.2 Poles of the System Matrix

Eigen values of the system matrix A is solved to find the modes of the system and also the poles of the transfer function. The poles of the system are calculated in MATLAB after determining the system matrix A. The poles reveal that the system is stable as they exist in the left side of the y-axis. The poles are listed as below:

Dutch roll (oscillatory): $-0.1843 + 1.0749i$, $-0.1843 - 1.0749i$

Roll damping (fast real): $-1.2390 + 0.0000i$

Spiral mode (slow mode): $-0.0203 + 0.0000i$

3.4.3 Gain Matrix of the Linear Observer

The gain matrix of Luenberger observer is also calculated in MATLAB. Luenberger gain matrix (L) is chosen such that $(A - LC)$ has stable eigen values placed further away (negatively) from the eigen values of system matrix A. As a well-known method of Modern Control, Pole Placement technique is used to find the observer gain matrix. The poles in the closed-loop transfer function may be placed in desired locations to assure satisfactory transient response. They are accepted approximately 4-5 times greater for faster estimation by the observer. Pole matrix used for gain matrix calculation can be seen in Eq. (24). With the change of gain, the system poles and zeros move around the S-plane. Root-locus allows to graph the locations of the poles and zeros for every value of gain. L is found by $place$ command in MATLAB as in Eq. (25).

$$p = [-5 \quad -1+i \quad -1-i \quad -0.1] \tag{24}$$

$$L = \begin{bmatrix} 0.8655 & 1.9460 & -2.7057 & 0.0267 \\ -2.0040 & 0.6686 & 0.4002 & 0.0428 \\ 0.0459 & -0.0559 & 3.8380 & 1.0117 \\ 0.0653 & -0.0006 & 0.0018 & 0.1000 \end{bmatrix} \tag{25}$$

3.4.4 Design of Subsystems in Simulink

Diverse analysis processes are used attached to the methods applied to propagate the residual. A well-established n process to analyze residual propagated by devoted observers for identifying failures is threshold sense. A basic threshold logic to analyze the residual signal is:

$$\begin{Bmatrix} \|t_i(t)\| < t; & \text{healthy case} \\ \|t_i(t)\| \geq t; & \text{faulty case} \end{Bmatrix}$$

that $t_i(t)$ represents instant time while t represents the detection time given in Eq. (26) that can be confirmed within the MATLAB Simulink blocks while performing the simulation cases.

$$t \; = \; N \; x \; dt \tag{26}$$

Fault indicator subsystem is applied to reveal stuck fault of sideslip angle (β) sensor. Sideslip angle (β) is taken out from other states using Demux so as to fault indication. β sensor signal is transferred through fault introducer and faulty signal β is multiplexed with other three healthy sensor states using Mux in Fault indicator subsystem to form $xFaulty$ as a faulty state vector. The architecture of the overall model also meets the task of reconfiguring corrected β (β_{out}) that is applied to correct faulty state vector $xFaulty$ in case of fault. Reconfigured or corrected β (β_{out}) is multiplexed with the other three states of $xFaulty$ and also other thirty-six auxiliary healthy states to form corrected state vector, which is then fed back to nonlinear Boeing 747 aircraft

subsystem model. Block diagram representation of Discrete Time Boeing 747 model is shown in Figure 3.6. β sensor state from xFaulty is terminated with the use of

Terminator block [5]. Block diagram representation of Fault Indicator subsystem is shown in Figure 3.7.

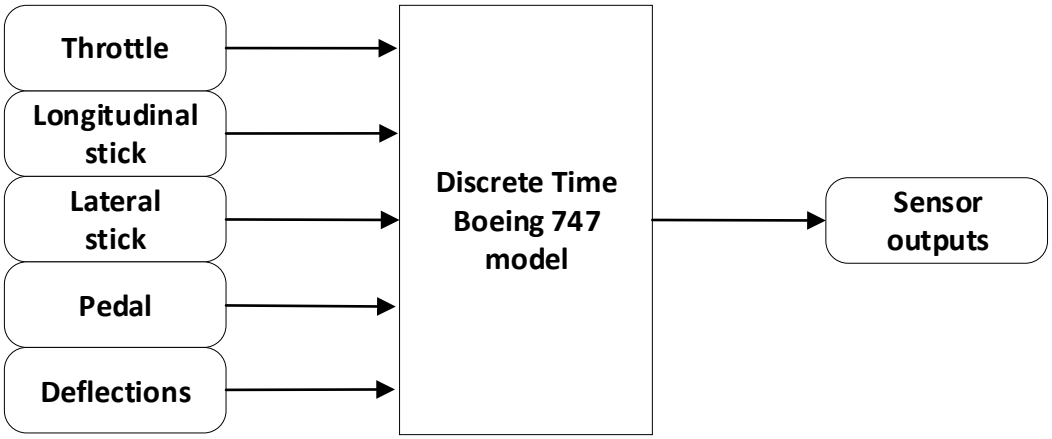

Figure 3.6 Block Diagram Representation of Discrete Time Boeing 747 Model

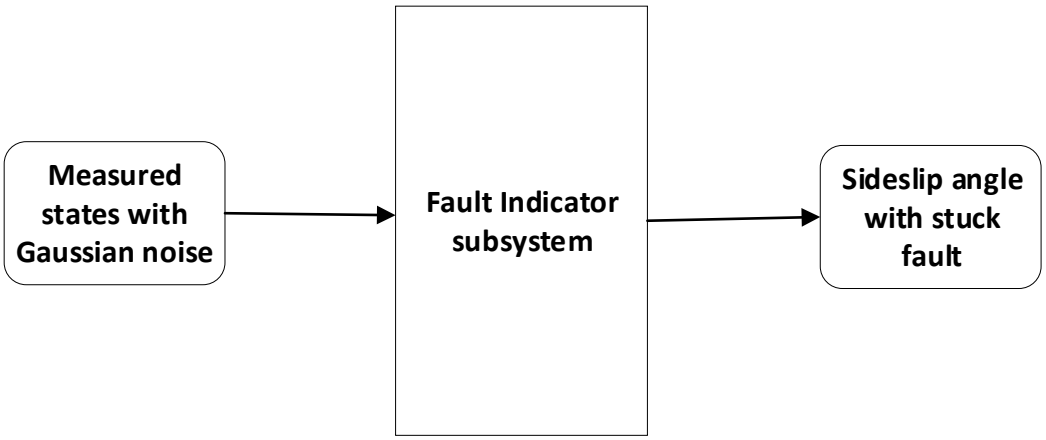

Figure 3.7 Block Diagram Representation of Fault Indicator Subsystem

Fault introducer is performed by means of N-Sample Switch as a Simulink block. Sample Switch N is assigned to 100 in the model. Stuck fault is introduced at $t = 2\ s$, i.e. $(Nxdt)$ of the faulty cases in the model. It is expressed with if-else condition. If $t < 2$ s, output = healthy signal else if $t \geq 2$ s, output = stuck signal. N Sample Switch

block generates the signal connected to the healthy signal gate. N is indicated in Switch count variable [10].

Threshold value for the sensor fault signal is determined when the fault indicator signal is emerged instantly in the detection time. The fault indicator signal could be used as control signal for reconfiguration operation. The simplest approach will be the usage of correction signals when estimation of fault surpasses a prior determined threshold value. The selected threshold value needs to be greater than the normal variations in fault estimation signals for avoiding false alarms, yet not too great that can cause missing the faults. In the simulation stage of the study, the threshold value is decided to assign to '0.8'. This identification establishes a minimal that is well-overcomed while analyzing the proposed filter algorithm in fault schemes [10].

Reconfiguration block maintains the estimated sensor signal (from mathematical model) rather than faulty sensor signal in the feedback loop. This is modeled by Reconfiguration subsystem which is managed for two goals: First objective is to detect and demonstrate fault in Fault Indicator. This is done by comparing aircraft sensor output β with observer estimate β_e in Reconfiguration subsystem. The second objective is to switch over to observer estimate β_e rather than faulty sensor output β when fault is indicated. Block diagram representation of Reconfiguration subsystem for Luenberger observer approach is shown in Figure 3.8. On the other side, switch occurs between the estimated lateral states of Kalman filter1 and Kalman filter2 according to the threshold value '0.8' for Kalman filter approach which is demonstrated in Figure 3.9. Detailed information can be followed in the explanation section of the simulation cases in Chapter 4.

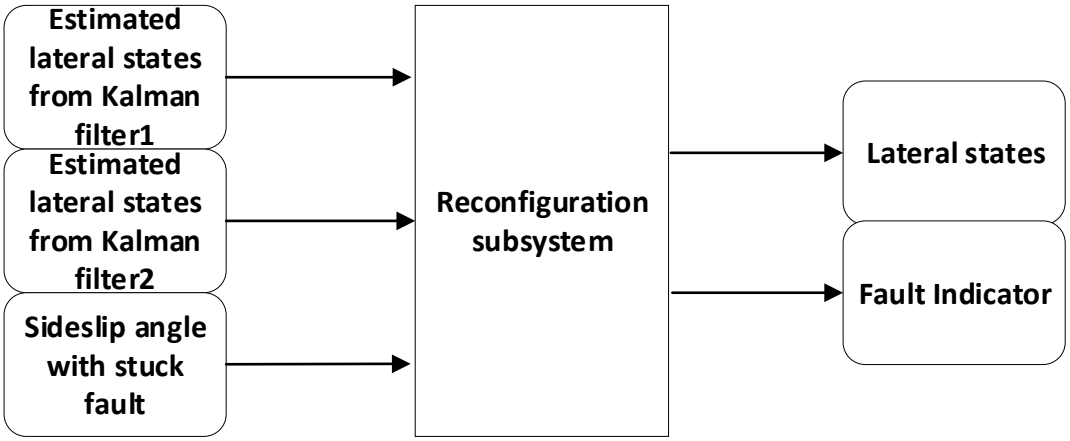

Figure 3.8 Block Diagram Representation of Reconfiguration Subsystem for Kalman filter approach

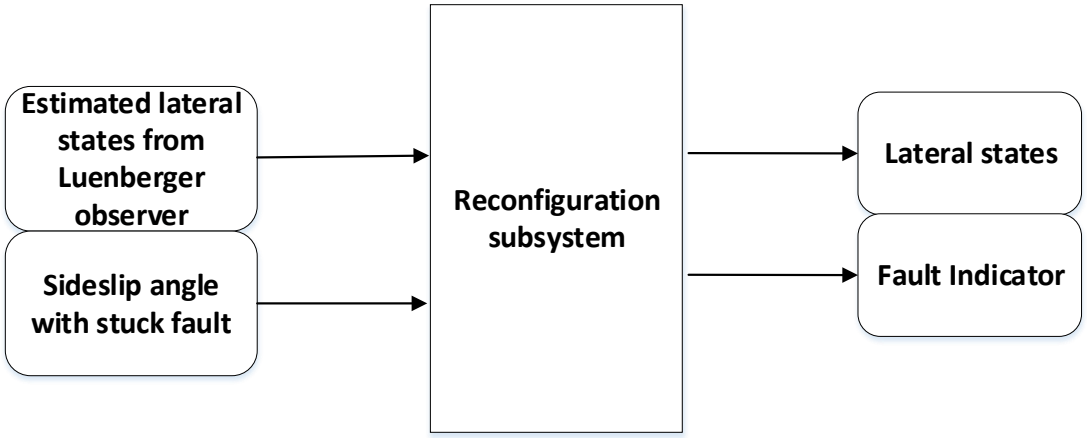

Figure 3.9 Block Diagram Representation of Reconfiguration Subsystem for Luenberger observer approach

The fault detection and reconfiguration is accomplished with the application of an observer to the system model and additionally using Canberra metric in the Reconfiguration subsystem. Fault detection model detects the stuck fault that utilizes Canberra metric. Canberra is a distance metric and useful for similarity or dissimilarity comparison. The generalized equation is given in the form of Eq. (27). The nominator in the metric equation specifies the difference and the denominator normalizes the difference.

$$Canberra\ Metric = \frac{|observed - measured|}{|observed| + |measured|} \tag{27}$$

Canberra metric compares β signal from Fault Indicator subsystem and β_e signal from Observer subsystem and generates signal 'S' as a part of the reconfiguration process. It enables to observe how much β signal differs from the β_e signal. Signal 'S' creates an input to the transfer function block of Simulink which treats as a filter so that it is smoothened. The mathematical phrase of Canberra metric with respect to the sideslip angle β is indicated in Eq. (28) [5].

Canberra metric has only one singularity condition that it is both β and β_e is equal to 0. In this condition, the singularity in the algorithm is overcomed with equalizing Canberra metric to 0.

$$S(t) = \frac{|\beta(t) - \beta_e(t)|}{|\beta(t)| + |\beta_e(t)|} \tag{28}$$

Eq. (28) is simulated along with $Switch$ and Abs blocks in MATLAB Simulink to form Reconfiguration subsystem. Abs block smooths Signal 'S' and outputs the absolute value of the input in Reconfiguration subsystem. Threshold value which is equal or higher than '0.8' of this block demonstrates the fault incident. The fault indicator signal is also applied as control signal for reconfiguration in switch. This control signal of Switch is the output of Abs block. Switch operates the following equation [5].

$$\beta_{out} = \begin{Bmatrix} \beta, & |Control\ signal| < 0.8 \\ \beta_e, & |Control\ signal| \geq 0.8 \end{Bmatrix}$$

It is actualized with the subsequent if-else statement of Switch block in Simulink.

If $|Control\ signal| \geq 0.8,\ \beta_{out} = \beta_e$, else $\beta_{out} = \beta$; Reconfiguration is done as

soon as fault is detected by switching over to estimated β_e from the proposed observer subsystem.

Observer subsystem consists of both Kalman filter and Luenberger observer respectively. It estimates the sensor states of sideslip angle (β), yaw rate (r), roll rate (p) and roll angle ($\emptyset$). It also uses healthy sensor outputs from the nonlinear closed-loop aircraft model for estimating the sensor states. Block diagram representation of Kalman filters are shown in Figure 3.11 and Figure 3.11, while, block diagram representation of Luenberger observer is demonstrated in Figure 3.12

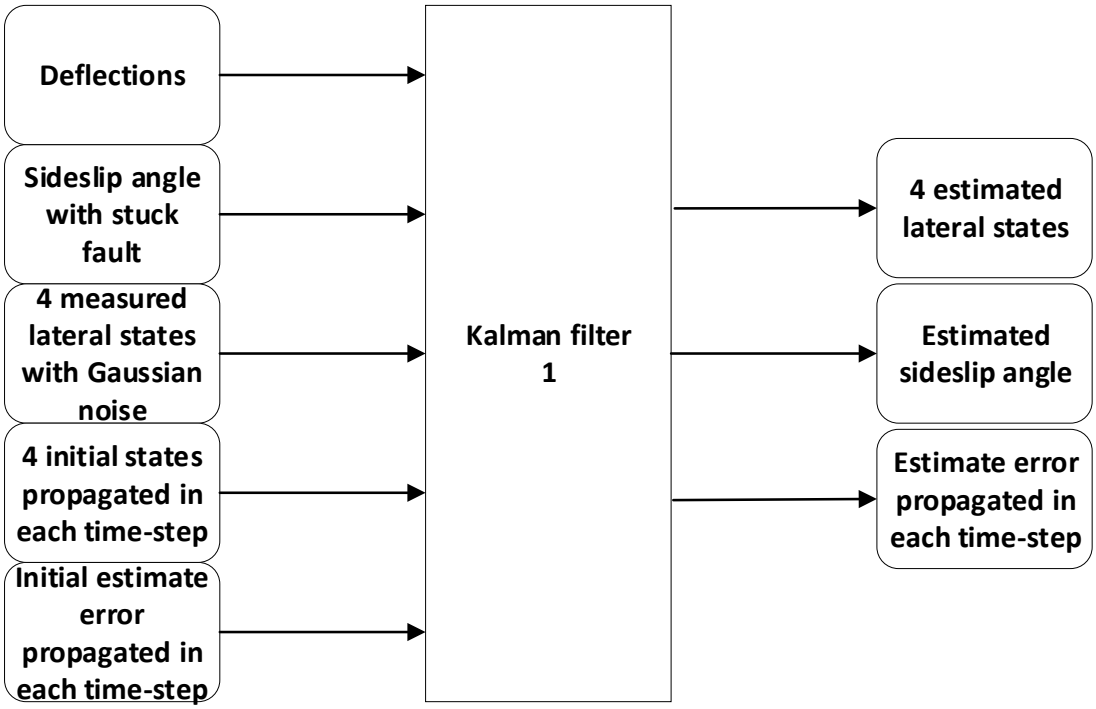

Figure 3.10 Block Diagram Representation of Kalman Filter 1

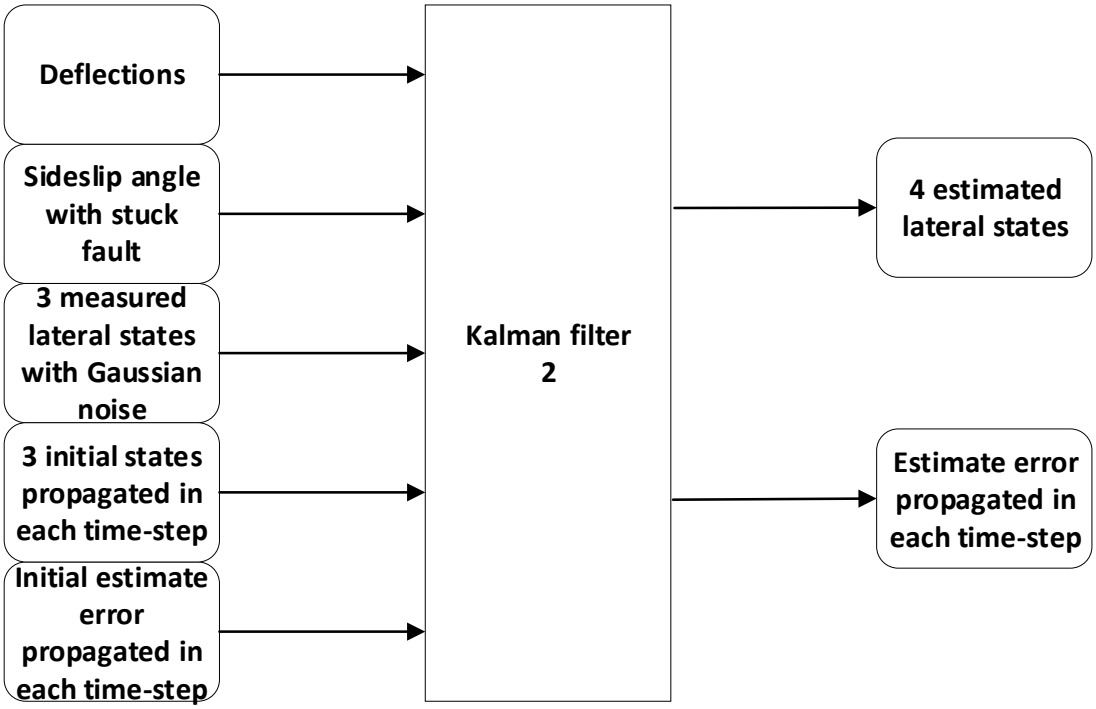

Figure 3.11 Block Diagram Representation of Kalman Filter 2

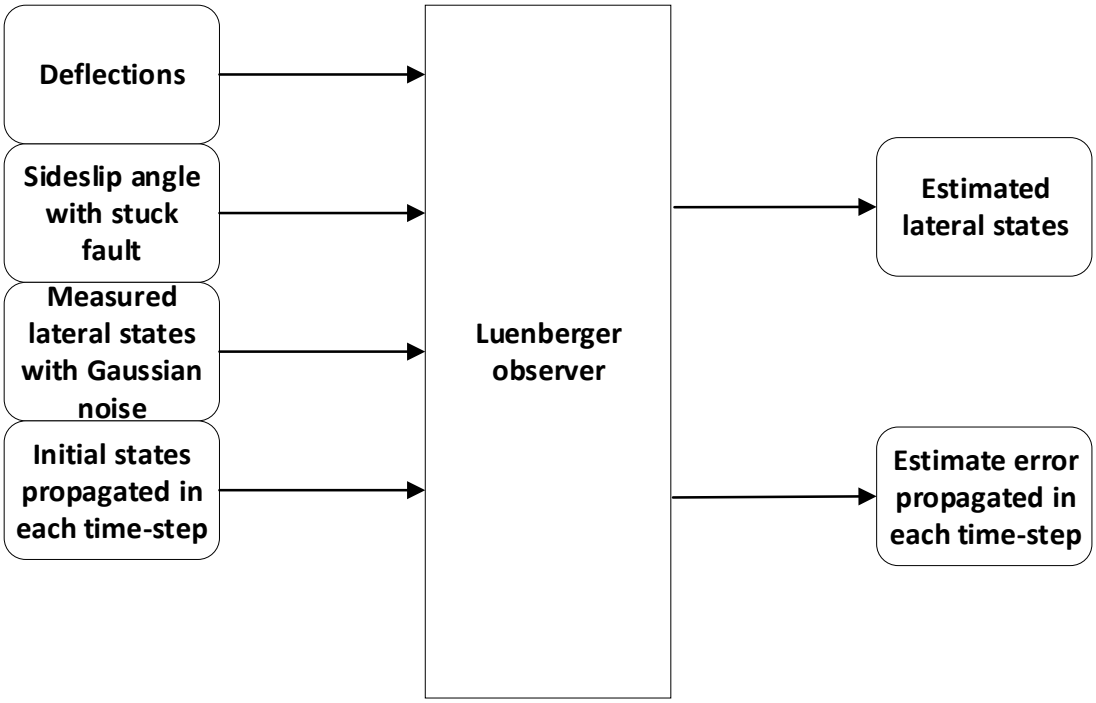

Figure 3.12 Block Diagram Representation of Luenberger Observer

Associating the subsystems above, the entire system architecture of the closed-loop aircraft model covering the fault detection and observer-based state estimation models in MATLAB Simulink is indicated in Figure 3.13 for Kalman filter and in Figure 3.14 for Luenberger observer.

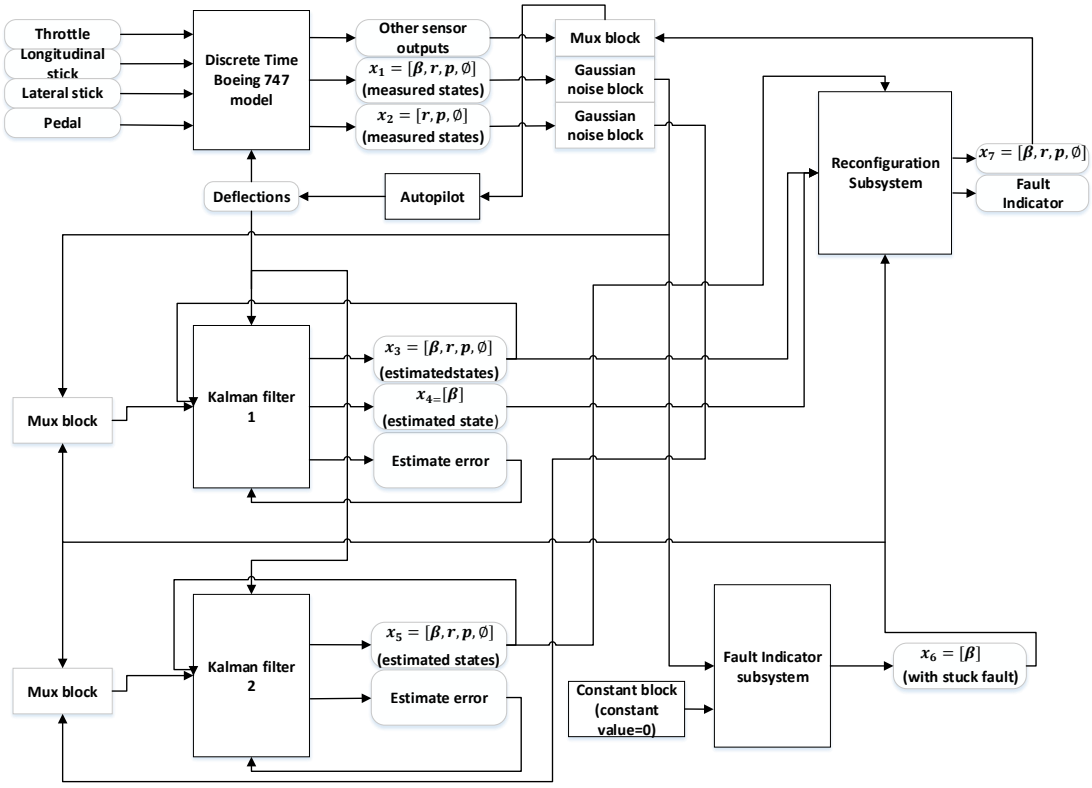

Figure 3.13 The Entire System Architecture of the Closed-Loop Model for Kalman filter

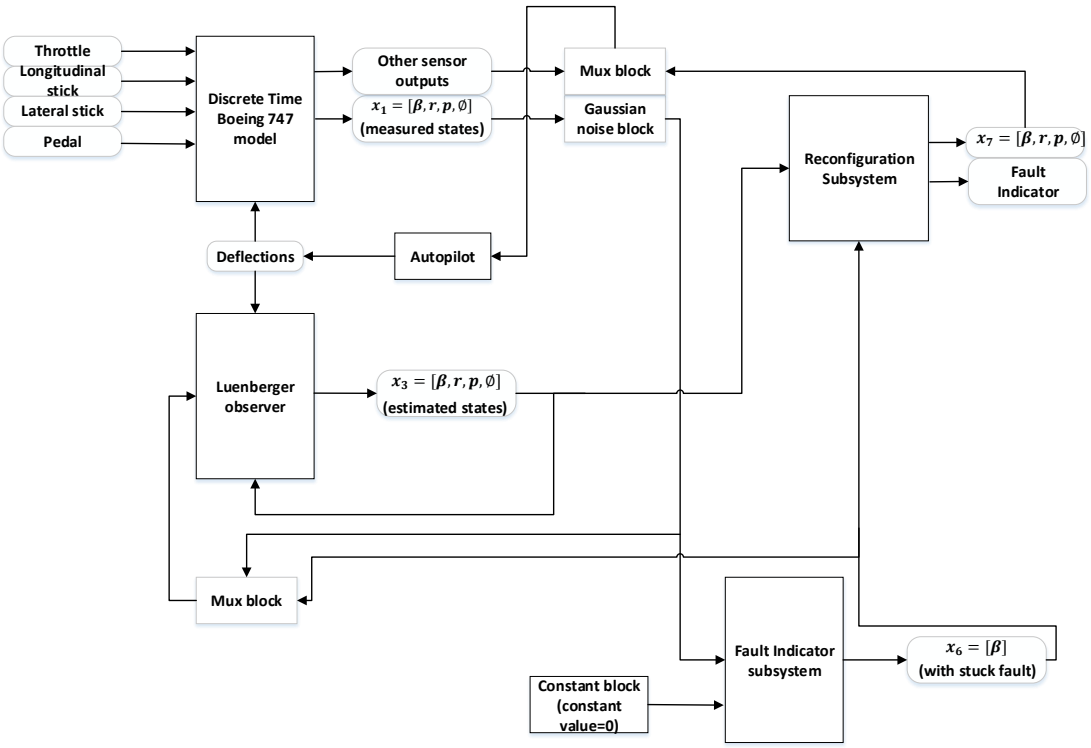

Figure 3.14 The Entire System Architecture of the Closed-Loop Model for Luenberger observer

3.4.5 Residual Generation

The observer-based approach can be applied for only online measurement processes unlike other approaches yield more design freedom. The aim of the observer-based fault detection technique is to specify a residual. The usage of an observer for specifying residual can be followed in Figure 3.15.

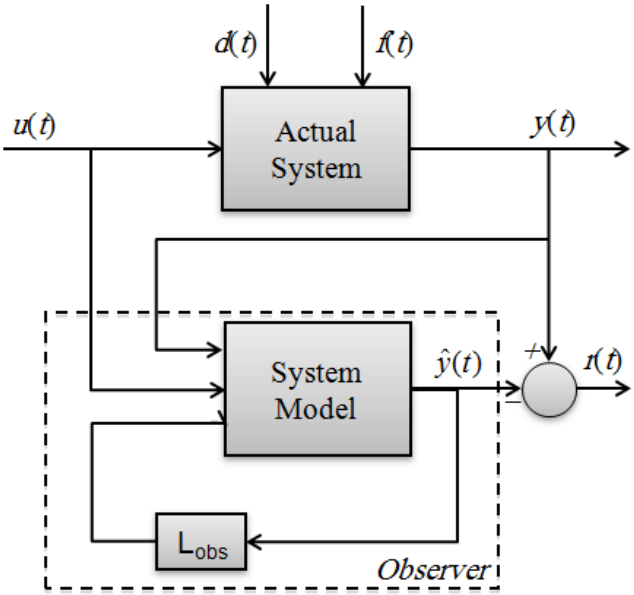

Figure 3.15 Usage of an Observer for Constituting Residual [29]

3.5 Kalman Filtering

Kalman filter is a notable methodology as a well-known observer type. The Kalman filter was originated in the 1960's by R. Kalman. The filter achieved popularity by its implementation of the spacecraft navigation for well-known NASA Apollo programme. Subsequently, Kalman filter was applied in various engineering systems and fields covering navigation, computer vision, image processing, radar, manufacturing, neural network or fuzzy logic [19].

As an optimum observer-based on indirect, inaccurate and uncertain observations thanks to minimizing the mean square error of the estimated states coming from the Gaussian noise. Kalman filters not only ensure fairly accurate results because of its structure and optimality but also have a recursive property which enables new measurements to be processed as they reach for real-time digital processing. Kalman filter treat like an estimator and thus it is utilized for fault detection by generating residuals by checking real and estimated outputs.

Kalman filter's main objective is estimating the variables which can not be measured

directly. The algorithm usually occurs in prediction and correction steps and due to algorithm's repetitive structure, the algorithm could be practiced in real time operations applying current measuring, formerly computed variables and their uncertainty matrices. Prediction uses a preceding knowledge of how the system thrives over time, i.e. the further variable values are approximated to outcome their current variable values by multiplying them with particular system matrices. The matrices are specified according to the designed system model. When the result of subsequent measure is considered, the predicted values are updated with the help of a weighted average. Further weight being given to the estimated values causes higher certainty in the model. Correction uses existing measurements. After identifying how the measurements are involved with the estimated variables, the actual measurements could be compared to the predicted measurements. The residual of the measurements is multiplied by a Kalman gain matrix and the acquired values are added to the predicted values to straighten them. Supposing that the designed system model is roughly reasonable up to certain additive Gaussian noise with known variance, then the Kalman filter convergence to the steady state regardless of the initial conditions could be proven. This verifies the particular interest is concentrated on the estimation of the noise variance, in other words, variance matrices and covariance matrices belong to the state model and the measurement model.

The advantage that Kalman filters get ahead against other observers is that Kalman gain matrix is computed in an optimal way. The standard Kalman filter is not adaptive which means that it does not spontaneously regulate Kalman gain matrix by actual error statistics compromised in the designed model. Kalman filter is charming due to it is the one which minimizes the estimation error variance beside all other possible filters. Kalman filter is generally applied to control systems due to the fact that proper estimations of the process variables are primarily requested in a control operation.

There is variety of Kalman filters based on the characteristic of the model linearity, type of assumed distribution and magnitude of the computational cost as given in Table 3.4

Table 3.4 Variety of Kalman filters

State Estimator	**Model**	**Assumed Distribution**	**Computational cost**
Kalman filter	Linear	Gaussian	Low
Extended Kalman filter	Locally Linear	Gaussian	Low (if Jacobians need to be computed analytically)
Unscented Kalman filter	Nonlinear	Gaussian	Medium

A state-space model of the linear system is simply defined in subsequent expression in Eq. (29). Accounting the measurement uncertainty that results from the inaccuracy of the model or inaccuracy of the input values, a zero mean and unit covariance matrix Gaussian white noise is introduced to model as given in Eq. (30). State equation can be indicated as in Eq. (30) and Eq. (31) and output equation can be indicated as in Eq. (31).

$$x_{k+1} = Ax_k + Bu_k \tag{29}$$

$$x_{k+1} = \mathrm{A}x_k + Bu_k + w_k \tag{30}$$

$$y_{k+1} = Cx_{k+1} + z_k \tag{31}$$

where k represents the time index, A implies state transition matrix that concerns the state from former time step, B implies input matrix that links the control input u with x. x implies state, u implies known input, y implies measurement output, w implies

process noise, z implies measurement noise. All quantitatives are vectors in general,

thus, each of them comprises at least two elements. State (x) comprises entire data over system's current value, but it is not possible to measure x can not be measured straightly. Instead, the measurement output $(y)$is measured and disrupted by measurement noise (z). The measurement output (y) helps for gain estimation for state (x), however, the information can not be taken from measurement output (y) due it is affected by noise. Process noise (w) is presumed as a zero mean and unit covariance matrix Gaussian white noise. In practice, the value of the variance is unknown and it must have been estimated. The measurement noise (z) is introduced by the means of measurements and also assumed to be modeled with a zero mean and unit covariance matrix Gaussian white noise.

The conventional Kalman filter could be accepted to be perfectly tuned due to the residual of actual states and estimated states. Generally, complexity reduction of modeling is invoked because of the fact that there are various unknown parameters in a model. Hence, in real applications, the certain noise covariances R and Q are not known. On the other hand, all variables are presumed to be known within the study. When the residuals in Kalman filter does not conform with the actual process with respect to the nature of noise parameter, the filter diverges or converges to an extensive boundary [30].

3.5.1 Kalman Filtering Theory and Formulation

An estimator should satisfy two criteria: First requirement is to make sure of the equality between the average value of state estimation and real state instead of being deviated in any way. Numerically, the expected value of estimation must be identical to the one of state. Secondary requirement is to make sure of the minimum convergence of state estimation from real state. Numerically, estimator with minimum possible error variance is expected to be found.

The Kalman filter is a state estimator that satisfies the criteria mentioned above. The filter is used in the condition where the dynamics of a system being estimated and

modelled as linear and time-invariant. The basic outline is pointed out in Figure 3.16. However, Kalman filter solution is merely applicable when precise assumptions about the noise are satisfied which influences the system model. Process noise covariance matrix (Q) and measurement noise covariance matrix (R) are described in Eq. (32) and Eq. (33).

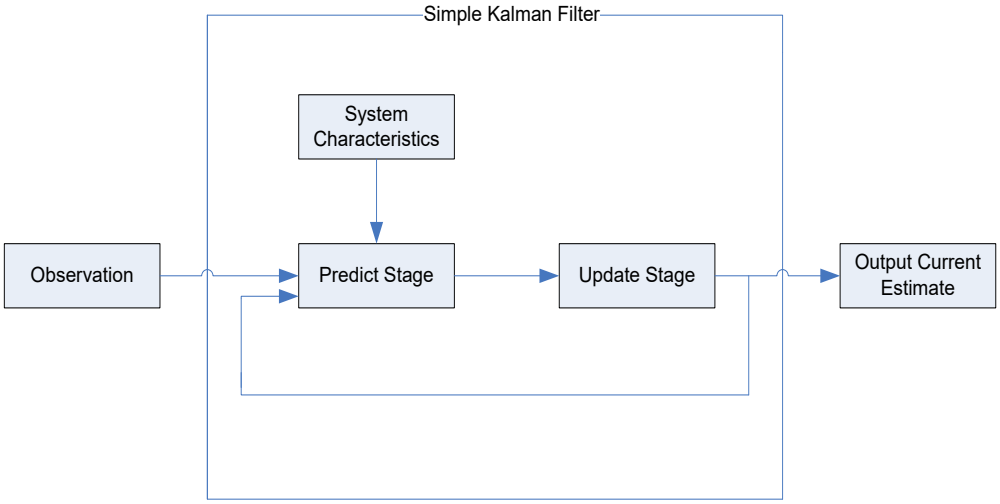

Figure 3.16 Basic Operation of a Simple Kalman Filter

$$Q = E(w_k w_k^T) \tag{32}$$

$$R = E(z_k z_k^T) \tag{33}$$

that w^T and z^T demonstrate the transpose operation of noise matrices w and z and E illustrates expected value. Kalman filter mainly consists of prediction and correction stages.

For prediction stage, observer states are predicted as well as the covariance matrix. A

covariance matrix could be considered as an indication of how well the estimation is or as an estimation error. K implies Kalman gain matrix while P implies the estimate error covariance. Prediction stage is illustrated by following equations as followed in

Eq. (34), Eq. (35) and Eq. (36).

$$\hat{x}_{k+1} = (A\hat{x}_k + Bu_k) \tag{34}$$

$$P_{k+1} = AP_kA^T + Q \tag{35}$$

$$K_k = P_{k+1}C^T (CP_{k+1}C^T + R)^{-1} \tag{36}$$

in which $^{-1}$, ^{T}, $\widehat{\ }$ superscripts show inversion, transposition, estimate value, respectively. State estimate ($\hat{x}_k$) is quite intuitive and reproduces with time. Correction function implies the quantity in which to straighten reproduced state estimation because of the measure. In Eq. (36), Kalman gain matrix (K) indicates that covariance of the noise will increase simultaneously with measurement noise therefore, Kalman gain matrix (K) will decrease while sufficient reliability could not be supplied to the measured output (y) in step of computing the next state $\hat{x}$.

The measurement residual can be demonstrated as in Eq. (37).

$$\text{residual} = y_{k+1} - C\hat{x}_{k+1} \tag{37}$$

For the correction stage, the updated state estimate of the observer and covariance matrix are determined in Eq. (38) and Eq. (39) for a stochastic system.

$$\hat{X}_{k+1} = \hat{x}_{k+1} + K_k(y_{k+1} - C\hat{x}_{k+1}) \tag{38}$$

$$\hat{P}_{k+1} = P_{k+1} - (K_kCP_{k+1}) \tag{39}$$

The flow chart representation of Kalman filter algorithm is shown in Figure 3.17.

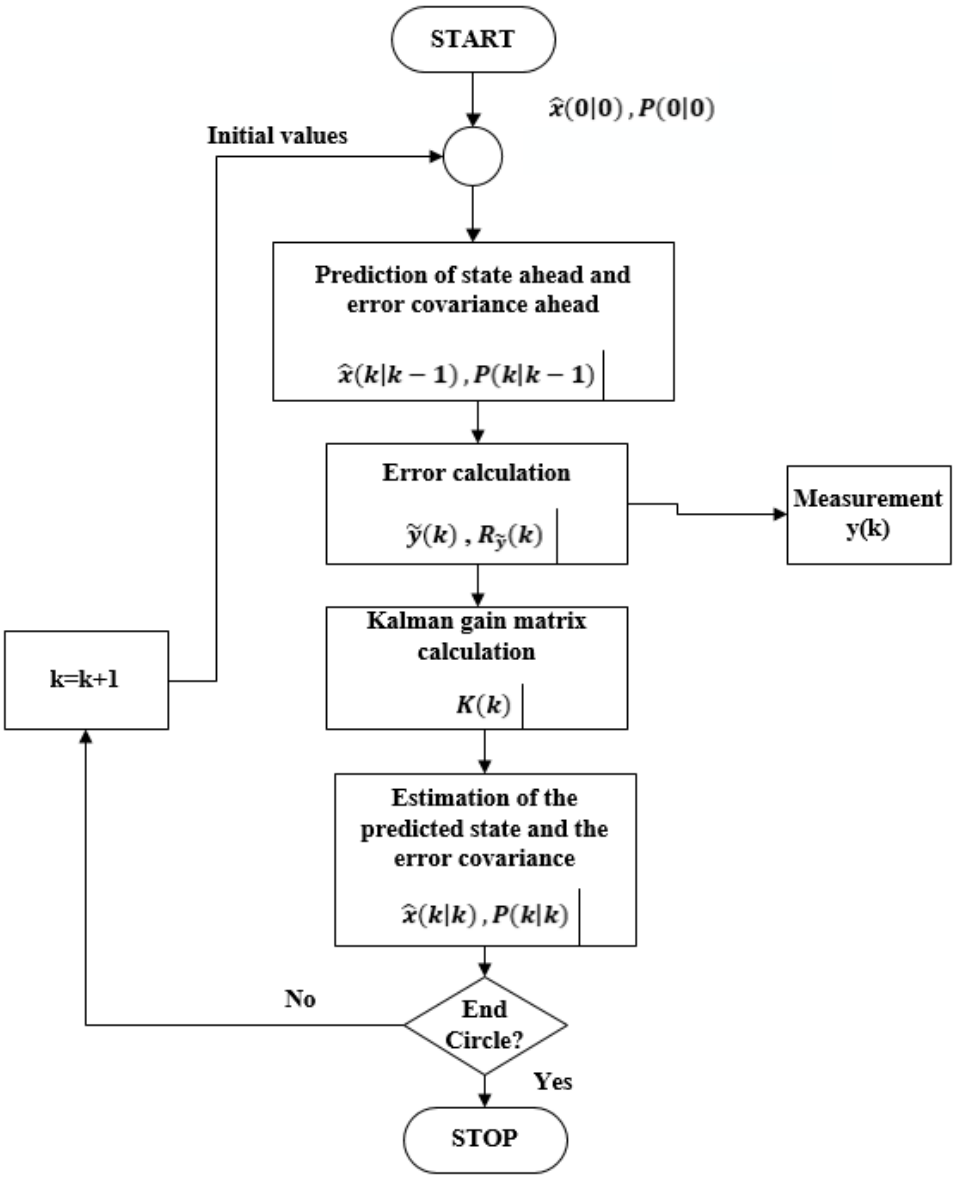

Figure 3.17 Flow Chart Representation of Kalman Filter Algorithm

The dynamic model and the stochastic data ensured to the Kalman filter must be correct for actualizing a high performance from the filter. Hence, it is efficient to settle the stochastic model for locating the changes in aircraft dynamics and environmental conditions. Unlike other types of filters, Kalman filter requires to be maintained with

a correct initial state and initial covariance of the civil aircraft. If this precondition can not be provided, it is inevitable that Kalman filter will fail during the steady state flight of the aircraft.

3.5.2 Practical Problems and Extensions

Systems with multi states could exceed the computational effort which is correlated upon matrix inversion is in proportion with n^3 (n represents matrix size) which implies when count of states in the filter triples, computation effort will increase to twenty-seven times. Kalman filter maintains high performance in estimation and decreases computational effort. K_k matrix and P_k matrix are stable in steady-state Kalman filter. In real time operations, equations that include additional steps should be applied.

The fact that nearly overall engineering operations are nonlinear was acknowledged for Kalman filters and cause the improvement of Extended Kalman Filter as an expansion of conventional Kalman filter to the nonlinearity. State estimation is discussed for a civil aircraft system in the study through the states could be simply approximated by a linear system.

Kalman Filter could estimate a state not only in a time step but also along an overall time history, e.g. the trajectory reconstruction of the aircraft in a steady state flight is illustrated within this study. The Kalman filter proceeds a smoother estimate of the system behavior.

Kalman filter is a theoretically attractive observer by minimizing the variance of the estimate error. The formulation depends on a prior knowledge for available noise statistics and requires the covariances of noise R and Q to be known. Kalman gain matrix (K) could be taken out from output signals, yet the covariance of the state error could not have judged without any information of covariances of measurement noise (R) and process noise (Q). The covariance function of the innovations from any steady filter and the output measurements have attracted most in accordance with the linear

relations between the matrices within the techniques that have been improved to the noise covariances Q and R from measurements.

3.6 Luenberger Observer

The theory of Luenberger observer is originated in the middle of the 1960's. According to Luenberger, any system driven by the output of the dedicated system can serve as an observer for that system. [31]

General class of compartmental systems are defined in Eq (40).

$$\frac{dx}{dt} = Ax(t), \qquad y(t) = Cx(t), \qquad x(0) \geq 0 \tag{40}$$

The state observation of dynamic systems using a classical Luenberger observer contains the integration of the linear differential equations, beginning from equal initial cases of the following dynamic system in Eq. (41).

$$\frac{d\Theta}{dt} = (A - LC)\Theta(t) + Ly(t) \tag{41}$$

The observer design is based on choosing a matrix L that gives a closed-loop stability and performance. This design is ordinarily based on placing the eigen values of the matrix $A - LC$ in desired positions. Once L is chosen, it is only required to integrate Eq. (41), beginning from equal initial cases to obtain estimations that converge to the real state. This simpliness of concept and implementation has made Luenberger observers favorable for those practical applications where the system can be definetely defined by a dynamical system. [32]

3.6.1 Luenberger Observer Theory and Formulation

The steps of Luenberger observer formulation can be followed as below [31]:

- Correcting the estimation equation with a feedback from the estimation error $y(k) - \hat{y}(k)$

$$\hat{x}(k+1) = A\hat{x}(k) + Bu(k) + L(y(k) - C\hat{x}(k)) \tag{42}$$

where $L \in R^{n \times p}$ is the observer gain and $L(y(k) - C\hat{x}(k))$ is feedback on estimation error

- The dynamics of the state estimation $\tilde{x}(k) = x(k) - \hat{x}(k)$ is

$$\tilde{x}(k+1) = Ax(k) + Bu(k) - A\hat{x}(k) - Bu(k) - L[y(k) - C\hat{x}(k)] \tag{43}$$

$$\tilde{x}(k+1) = (A - LC)\tilde{x}(k)$$

and then $\tilde{x}(k) = (A - LC)^k(x(0) - \hat{x}(0))$

- Applying the identical notion for continuous-time systems $\dot{x}(t) = Ax(t) + Bu(t)$

$$\frac{d\hat{x}(t)}{dt} = A\hat{x}(t) + Bu(t) + L[y(t) - C\hat{x}(t)] \tag{44}$$

The dynamics of the state estimation error are

$$\frac{d\tilde{x}(t)}{dt} = (A - LC)\tilde{x}(t) \tag{45}$$

3.6.2 Practical Problems and Extensions

Luenberger observer in Eq. (41) does not take into account the fact that the system in Eq. (40) is compartmental, so nonrealistic outcomes could be obtained for some of the states.

Furthermore, it is significant to assure higher and/or lower bounds on the real states in many applications, yet conventional Luenberger observers do not assure that the estimated states converge from above or below to the real states.

Another problem of classical observers is that the initial state or the uncertainty in the system parameters might not be easily incorporated into the observer. [32]

CHAPTER 4

SIMULATION AND RESULTS

Design and Development Environment Tool

MATLAB, abbreviation of Matrix Laboratory, is an open and expanded software environment ordinarily used for engineering or academic purposes and distributed worldwide. It simplifies the calculations for various kinds of algorithms, particularly in terms of matrix manipulation and obtains helpful methods to display data applying the matrix being a core object, the vector as a particular case. This feature makes MATLAB especially practical as a modelling tool, as a means of processing data and by means of its graphical facilities, a particularly good visualisation package. Simulink is a front-end for MATLAB that authorizes complicated algorithms and systems to be demonstrated diagrammatically. As well as helping the design of systems, it corresponds for simulating and analysing the systems [33]. Owing to these features, MATLAB Simulink is chosen to develop the simulation environment expressed in this chapter of the study.

Test Bed: A Boeing 747

Modelling and simulation software takes a significant part in the development of sensor fault detection in EFCS. Hence, an insight to sensor EFCS system using MATLAB Simulink for a civil aircraft is submitted. For compensating the requirement to generate a closed-loop aircraft and maintaining its compatibility with the fault detection model, a reliable electronic source, Airlib, is benefited from modeling and simulation and accepted to obtain a completely accurate civil aircraft model. Airlib is a wide airplane model library generated in MATLAB. It consists of multi blocks for application of continuous and discrete time nonlinear common airplane models. [34]

The aircraft model of Boeing 747 is improved to maintain the nonlinear system to the decentralized data fusion. The preliminary idea is choosing the appropriate environment in which sensors can extract their data to model sensors for data fusion. In the frame of autonomous control, this requires a sufficiently complicated model of an actual system therefore, sufficient data flows are ensured for an environment where sensors are operated. A Boeing 747 aircraft model is chosen for this aim due to it is known that many models have been developed in Simulink, thus it would keep a diverse collection of data sources for a sensing system.

Figure 4.1 demonstrates the main structure for a Simulink model of Boeing 747 obtained by the Airlib toolbox. The model receives several modifications including input parameters to steer the aircraft in a desired steady state flight. This condition is assigned to sustain a more common sort of motion that would be experienced in flight.

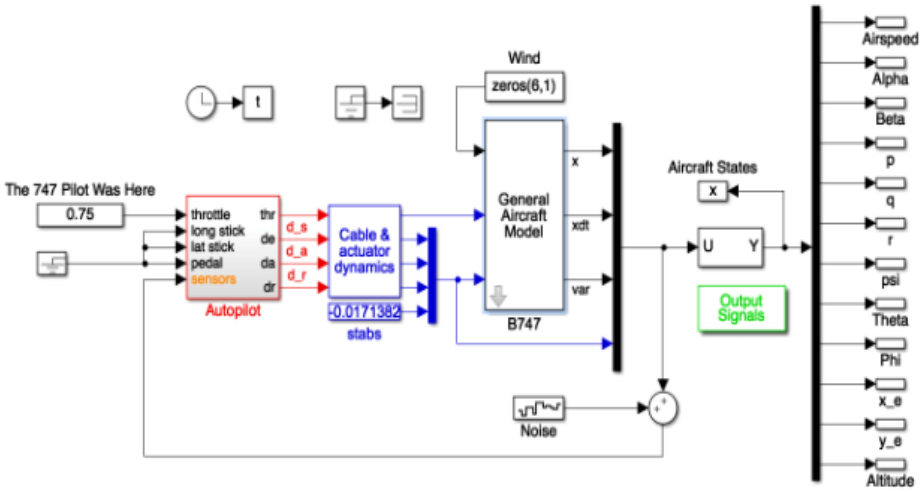

Figure 4.1 Top-Level Model of Boeing 747 Aircraft in Simulink [34]

In this section, further step is taken to qualify proposed filtering algorithm in order to consider the estimation performance for the stuck faults traced by the sensors. The

effectiveness of the filtering algorithm and the accuracy of the design paradigm submitted in earlier sections are revealed in this section by means of several simulation cases. The effectiveness of the observer in the closed-loop setting and the reliability of the nonlinear state-feedback control method is evaluated.

As a scope of the validation of the proposed observer-based fault detection approach, a number of simulations were performed utilizing a nonlinear Boeing 747 model in MATLAB Simulink. Following the model design, the residuals, also considered as errors, are propagated by transferring the input data through the observer. The thresholds for the FDD are adjusted by evaluating the highest values attained by the residuals upon a sequence of tests. In the case of residual value surpasses an exact threshold, it initiates a fault alarm. Fault parameterization in the simulation model of the filters intents to receive the angle at which the extension of the control effectiveness is lost. The plant orientation modifies wind constituents [35]. The wind effect and turbulence impact are assumed to be zero as ineffective components in the simulation cases run of the study.

For revealing the performance and examining the reliability of suggested FDD methodology, three flight scenarios are introduced with distinctness in the states. Flight cases are examined in a steady-state phase. For each combination of the flight and aircraft parameters, uncertainties are also incorporated.

Case I. Fault-free (nominal) case
Case II. Stuck fault of the sensor case at $\mathrm{t} = 2$ s with an initial $\beta = 0.2$ rad
Case III. Stuck fault of the sensor case at $\mathrm{t} = 2$ s with a rudder input as a square wave $\delta_r = 0.25$ rad for 10 s

The simulations are carried out for the nominal and faulty conditions where all regions are trimmable. All of the experiments are performed considered as a steady state flight of a Boeing 747 aircraft at $20{,}000$ ft altitude and 0.44 Mach true airspeed. Also, the simulation period is arranged to 20 seconds for the simulation cases. The sampling

time (dt) is arranged to 0.02 seconds for all of the cases of the simulations. For each run of the simulation cases, a number of seven graphics of the results are plotted. In Appendix A, the behavior and rate of changes of the other Boeing 747 states apart from the lateral states ($\beta, r, p, \emptyset$) are introduced, respectively.

The feedback controller that is processed for the several cases acquires the value of sideslip angle (β) in each iteration. The primary sources of noise in the aircraft are sensors. The wind disturbance and turbulence impact are omitted instantly of the flight. The various values which are regulated for measurement noise (z) belong to the sensor noise. When sensor fault is detected, the controller directs a dominant rudder deflection immediately that alternately propagates high tips in φ and r states. The measurement noise (z) is attached to measured sideslip angle that is obtained of the nonlinear aircraft model and transferred to the observer model.

CASE I. Fault-free case (Nominal) case:

The fault-free performance of the Kalman filter and Luenberger observer are indicated when there is no fault in the system. The initial value of β is assigned to 0.2 radians. The demonstrations are followed in order of the separately computed lateral states β, r, p, $\emptyset$ respectively as Figure 4.2, Figure 4.3, Figure 4.4 and Figure 4.5 for Kalman filter and Figure 4.6, Figure 4.7, Figure 4.8 and Figure 4.9 for Luenberger observer. Red curve represents measurement of state with noise, blue curve represents estimate of state, magenda curve represents measurement of state with stuck fault and green curve represents true state.

The sample switch (N) is assigned to be $100{,}000$ as quite a large value to slide the fault to the preliminar instant of the simulation which means that there is no fault triggered at all. Gaussian noise in sensors are applied using a Simulink block of white noise in MATLAB with a mean zero, noise power $5x10^{-6}$ and sample time 0.02 seconds. The noise power is given by the variance of the noise. The noise variance is calculated as in Eq. (46).

$$Noise\ variance = sqrt(Noise\ power/Sample\ time) \quad (46)$$

$$Noise\ variance = 1.5 \times 10^{-2}\ (\text{deg}^2)\ \text{(for angles)}$$

$$Noise\ variance = 1.5 \times 10^{-2}\ (\text{deg/s})^2\ \text{(for angular rates)}$$

Considering that there is no relation between the noise covariance matrices, the process noise (w), the measurement noise (z) and estimate error covariance (P) are set to the optimum levels as given in Table 4.1 after a couple of simulation experiments on MATLAB. It is important to underline that the larger value of the measurement noise (z) imposes filter to rely on the model itself, whereas lower value of the measurement noise (z) imposes filter to rely on the measurements. When measurement noise covariance matrix (R) approaches to zero (0), the designed filter relies more on the state measurements. The process noise covariance matrix (Q) is chosen more approximate to measurement noise covariance matrix (R) to also rely on the measurements.

Table 4.1 The Values of Process Noise, Measurement Noise and Estimate Error Covariance for Fault-free Case

Noise	**Mean**	**Covariance Matrix**
Process Noise (w)	0	$\begin{bmatrix} 5x10^{-7} & 0 & 0 & 0 \\ 0 & 5x10^{-7} & 0 & 0 \\ 0 & 0 & 5x10^{-7} & 0 \\ 0 & 0 & 0 & 5x10^{-7} \end{bmatrix}$
Measurement Noise (z)	0	$\begin{bmatrix} 1.5 \times 10^{-2} & 0 & 0 & 0 \\ 0 & 1.5 \times 10^{-2} & 0 & 0 \\ 0 & 0 & 1.5 \times 10^{-2} & 0 \\ 0 & 0 & 0 & 1.5 \times 10^{-2} \end{bmatrix}$
Estimate Error Covariance (P)	0	$\begin{bmatrix} 5x10^{-6} & 0 & 0 & 0 \\ 0 & 5x10^{-6} & 0 & 0 \\ 0 & 0 & 5x10^{-6} & 0 \\ 0 & 0 & 0 & 5x10^{-6} \end{bmatrix}$

Results of Kalman-based Approach:

True state of β converges to the estimated state of β carried from the observer model as in Figure 4.2. The actual β has a rise time of less than 3 seconds. By considering a sample set of values of initial β as 0.2 radians as a reference, then actual β does not surpass almost 0.2 radians. Actual β decreases gradually from 0.2 radians to -0.08 radians and increases gradually over -0.08 radians to 0.01 radians. β settles between 0.2 and -0.08 radians within 3 seconds in the steady cruise flight.

The distinction of residuals are not required to be precisely zero because of the existence of Gaussian noise on sensors that measure β, r, p, ∅ and also the errors in the filter design parameters. As observed from Figure 4.2, Figure 4.3, Figure 4.4 and Figure 4.5, residuals are minor in the nominal case.

It can be observed from Figure 4.2, Figure 4.3, Figure 4.4 and Figure 4.5 that Kalman filter assumes the fault is not detected due to estimated states approximately converge

to the measured states at $t = 10$ s as the normal fault-free condition. The estimation error is minor since the actual value of the engine thrust. The error norm remains in the no-fault region and false alarms are avoided.

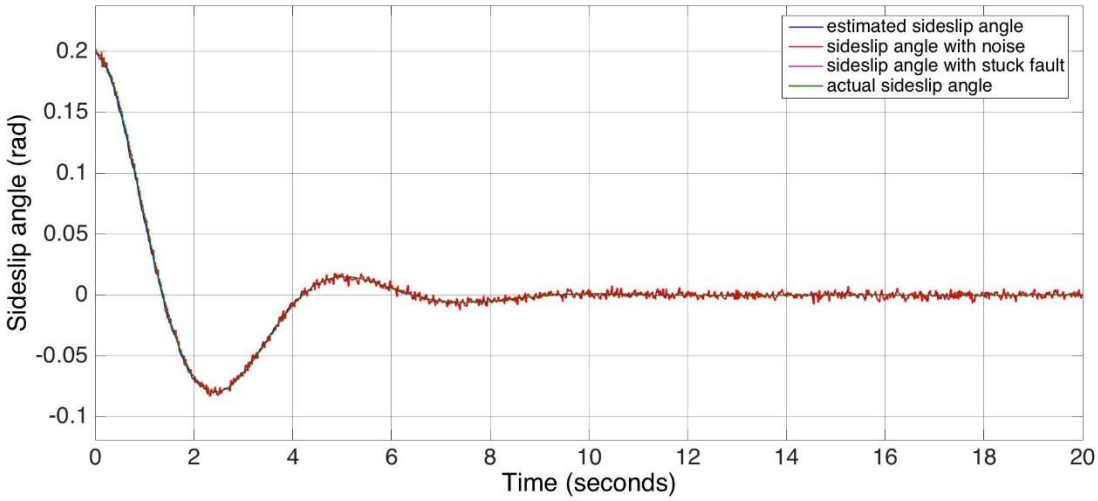

Figure 4.2 Sideslip Angle Residual vs. Time

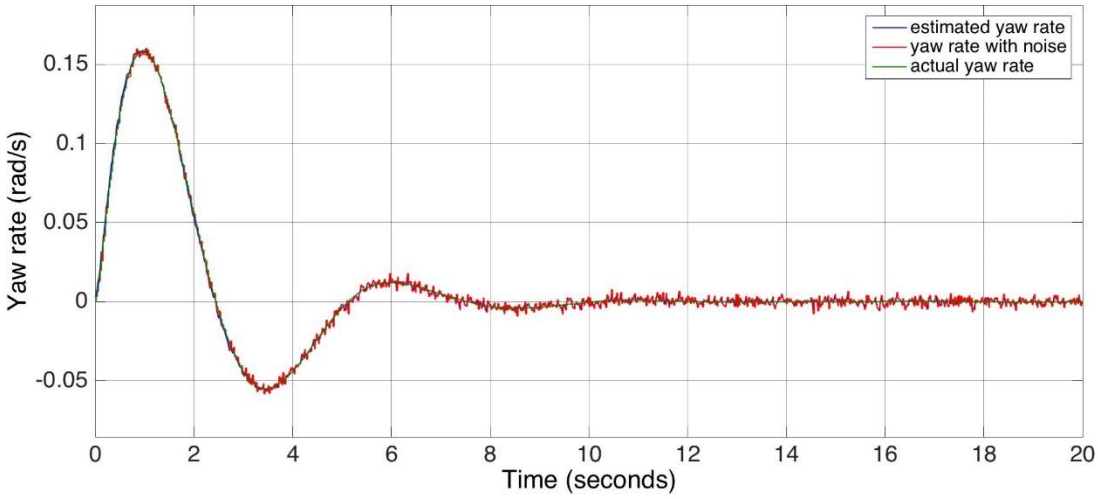

Figure 4.3 Yaw Rate Residual vs. Time

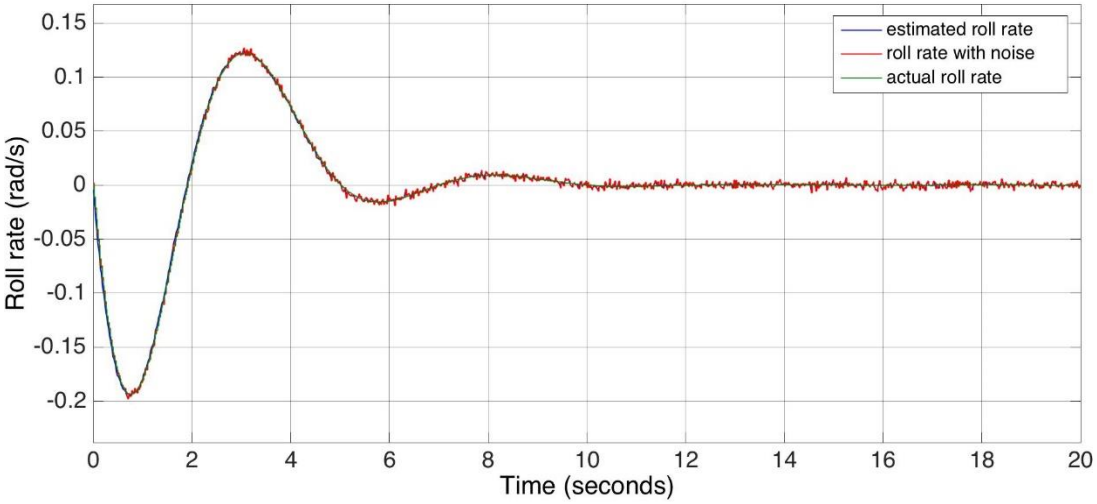

Figure 4.4 Roll Rate Residual vs. Time

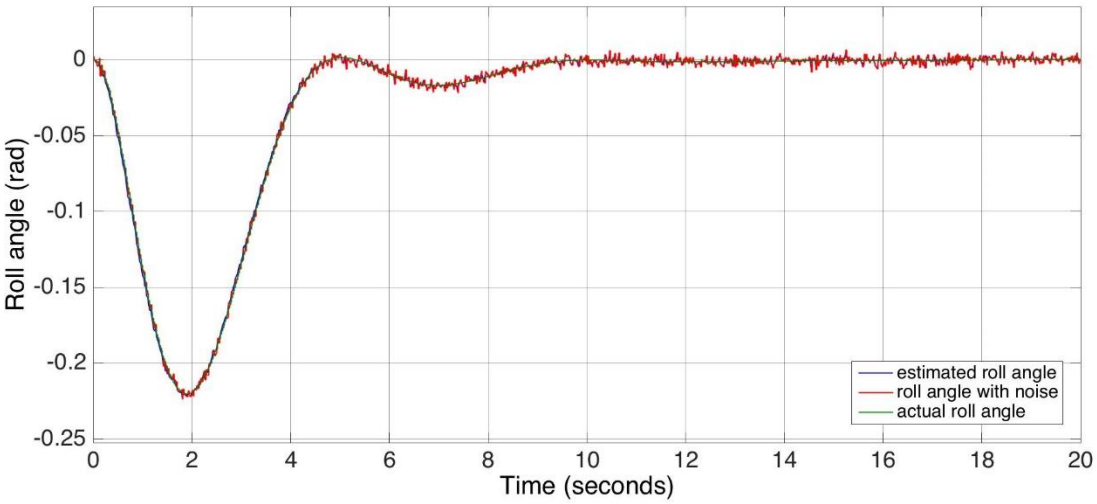

Figure 4.5 Roll Angle Residual vs. Time

Results of Luenberger-based Approach:

For the same uncertainty conditions, measured states of β and $\emptyset$ converge to their estimations in Figure 4.6 and Figure 4.9 while, measured states of r and p display a similar attitude as in Figure 4.7 and Figure 4.8. In Figure 4.6 and Figure 4.7, the residuals between the actual and estimated sideslip angle curves are seen clearly before $t = 3$ s.

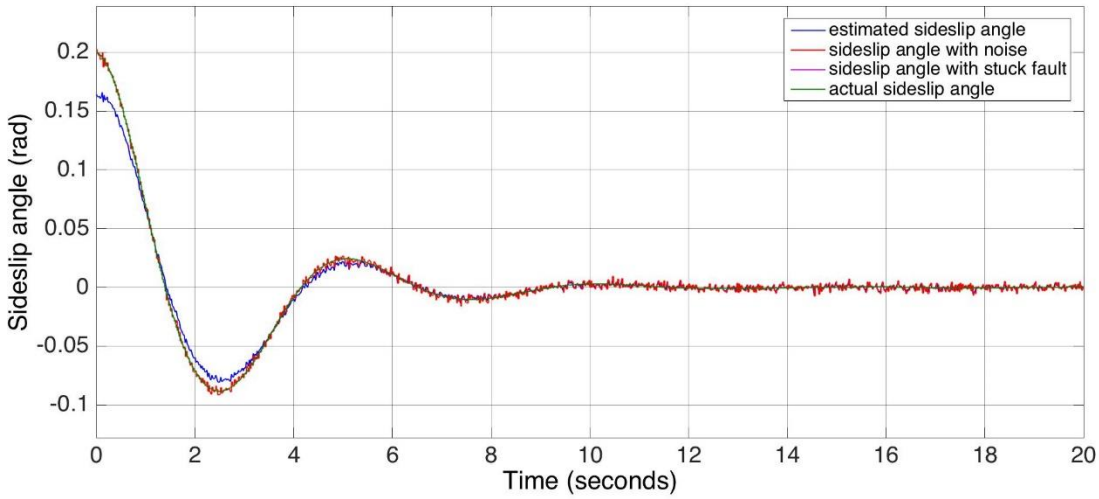

Figure 4.6 Sideslip Angle Residual vs. Time

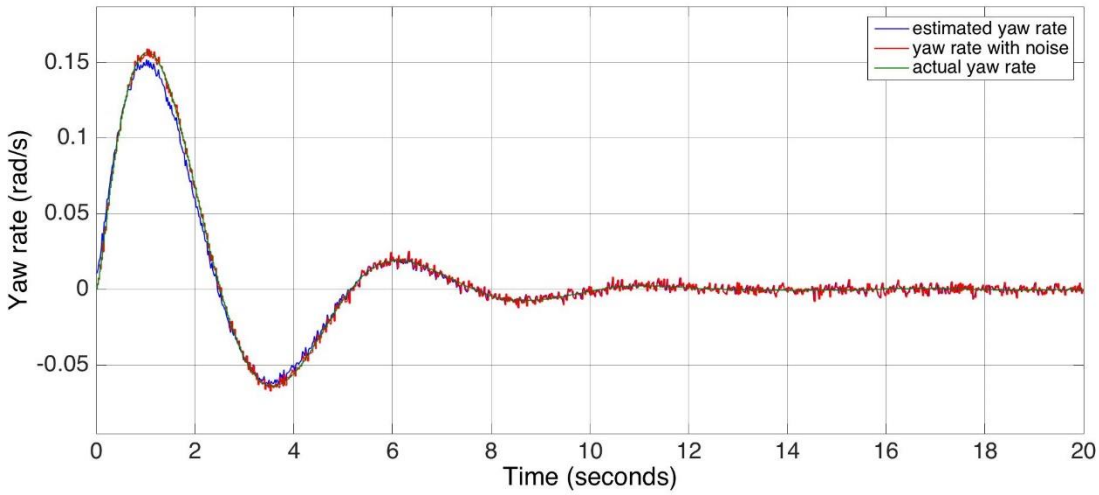

Figure 4.7 Yaw Rate Residual vs. Time

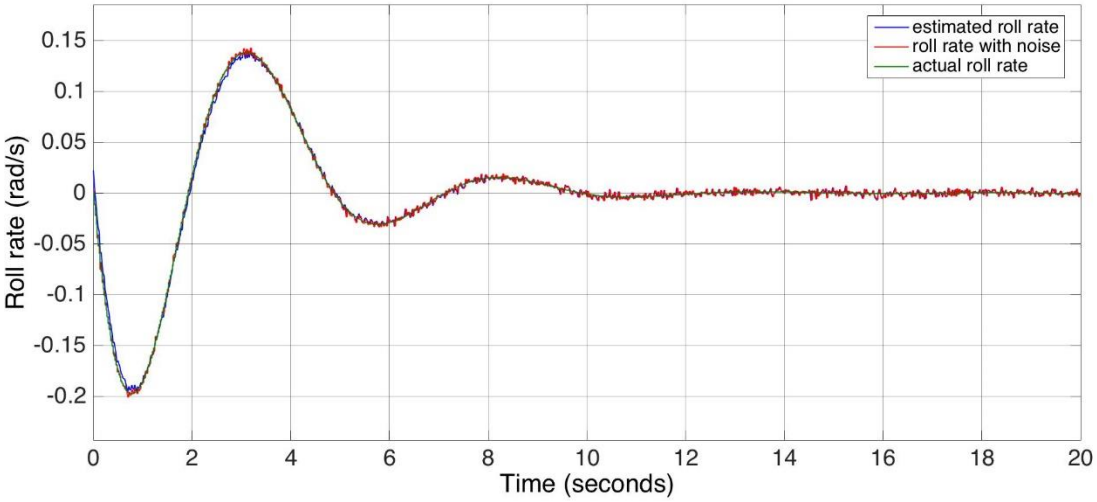

Figure 4.8 Roll Rate Residual vs. Time

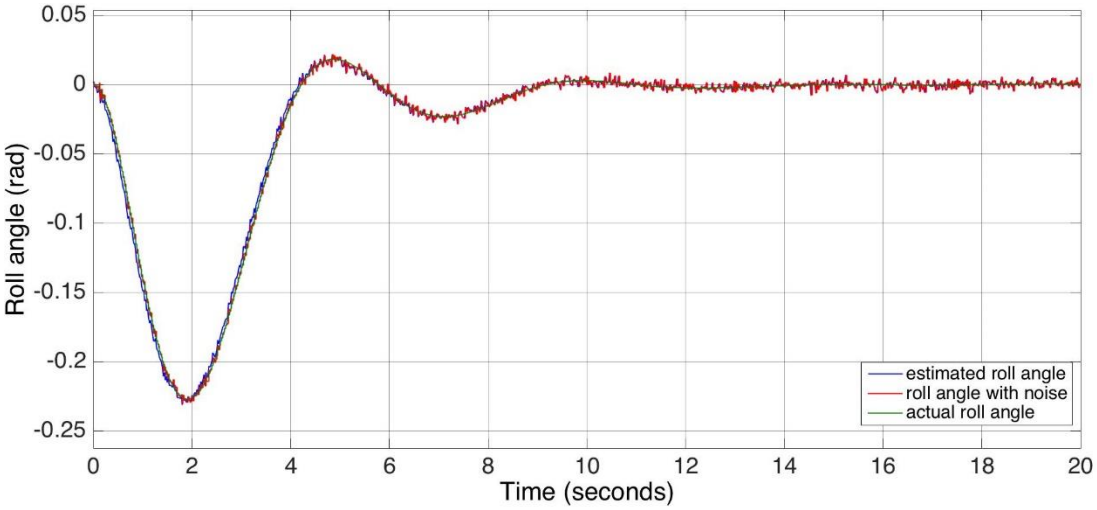

Figure 4.9 Roll Angle Residual vs. Time

CASE II. Sensor stuck fault case at $t = 2$ s with an initial $\beta = 0.2$ rad

The performances of the Kalman filter and Luenberger observer in the faulty case are pointed out when there is stuck fault in the system. The initial value of β is assigned to 0.2 radians. The demonstrations are followed in order of the separately computed lateral states β, r, p, ∅ respectively as Figure 4.10, Figure 4.11, Figure 4.12 and Figure 4.13 for Kalman filter and Figure 4.15, Figure 4.16, Figure 4.17 and Figure 4.18 for

Luenberger observer. Red curve represents measurement of state with noise, blue curve represents estimate of state with all sensor measurements included, purple dashed curve represents estimate of state except sideslip angle sensor measurement, magenda curve represents measurement of state with stuck fault and green curve represents true state. The fault indicator response of the faulty scenario could be traced in Figure 4.14 for Kalman filter and Figure 4.19 Luenberger observer.

Stuck fault is modelled in the Fault Indicator block and applied to the measurement states regarded as a fault input. The sample switch (N) is assigned to be 100, thus β sensor is observed to be stuck at $t = 2$ s, mathematically. Gaussian noise in sensors are applied using a Simulink block of white noise in MATLAB with a mean zero, noise variance 1.5×10^{-2} radians and sample time 0.02 seconds.

Unlike the nominal case, two Kalman filters are modelled for the observer subsystem in faulty case which provides a distinct point of view to the observer objectives:

First Kalman filter is identical with the one used in Case I. as there are four inputs that consist of the measurements of lateral states β, r, p, ∅ and the outputs are the estimations of those lateral states. Once β sensor is stuck, other states estimate the signal of faulty sensor β.

On the other hand, second Kalman filter has three inputs that consist of the measurements of the same lateral states except β, which means there is no any input signal from the β sensor, then other three states support the estimation of β with their measurement data assuming there is no β sensor in the system.

As a result of this approach, the lateral states β, r, p, ∅ which are the outputs of the Reconfiguration subsystem feeding back to the autopilot system are flexible between two discrete Kalman filters with respect to the threshold approach.

Considering that there is no relation between the noise covariance matrices, the process

noise (w), the measurement noise (z) and estimate error covariance (P) are set to the optimum levels as given in Table 4.2 after a couple of simulation experiments on MATLAB. Comparing to the covariance matrices in the fault-free case, it is considered a 100 times decline in the magnitude of process noise covariance matrix (Q) which means the designed filter relies on the system model itself on a noisy environment instead of the state measurements.

Table 4.2 The Values of Process Noise, Measurement Noise and Estimate Error Covariance for Faulty Cases

Noise	**Mean**	**Covariance Matrix**
Process Noise (w)	0	$\begin{bmatrix} 5x10^{-9} & 0 & 0 & 0 \\ 0 & 5x10^{-9} & 0 & 0 \\ 0 & 0 & 5x10^{-9} & 0 \\ 0 & 0 & 0 & 5x10^{-9} \end{bmatrix}$
Measurement Noise (z)	0	$\begin{bmatrix} 1.5 \times 10^{-2} & 0 & 0 & 0 \\ 0 & 1.5 \times 10^{-2} & 0 & 0 \\ 0 & 0 & 1.5 \times 10^{-2} & 0 \\ 0 & 0 & 0 & 1.5 \times 10^{-2} \end{bmatrix}$
Estimate Error Covariance (P)	0	$\begin{bmatrix} 5x10^{-8} & 0 & 0 & 0 \\ 0 & 5x10^{-8} & 0 & 0 \\ 0 & 0 & 5x10^{-8} & 0 \\ 0 & 0 & 0 & 5x10^{-8} \end{bmatrix}$

Results of Kalman-based Approach:

Although, sideslip angle (β) can not be measured accurately after stuck fault and continuously feedbacks faulty responses as 0 rad as in Figure 4.10, true state of β converges to the estimated state of β carried from the filter model. It can be seen that the actual β has a rise time of less than 3 seconds. By considering an initial sample value of β as 0.2 radians as a reference, then actual β does not surpass almost 0.2 radians. Actual β decreases gradually from 0.2 radians to -0.07 radians and increases gradually over -0.07 radians to 0 radians. β settles between 0.2 and -0.07 radians

within 5 s in steady cruise flight.

It can be observed from Figure 4.10, Figure 4.11, Figure 4.12 and Figure 4.13 that the overall lateral states are estimated properly before and after the existence of the stuck fault of β sensor. The error norm does not scale up to critical level owing to the detection performance of Kalman filter and tracks the faulty behavior through the simulation period. The measured states oscillate for a while and converge to their estimations approximately at $t = 10$ s and reach to the trim values. The estimation error is minor since the actual value of the engine thrust. Hence, it is reasonable within the considered stuck magnitude.

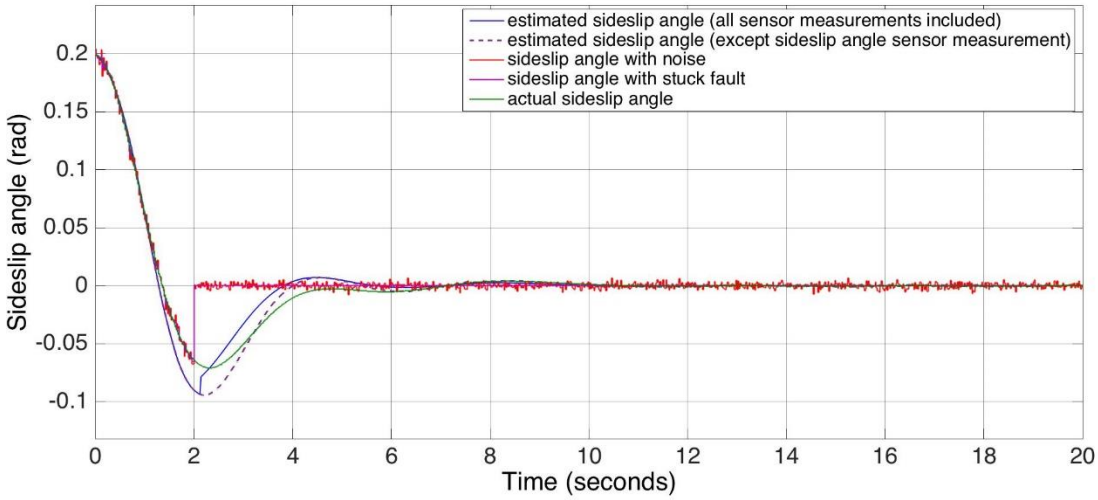

Figure 4.10 Sideslip Angle Residual vs. Time

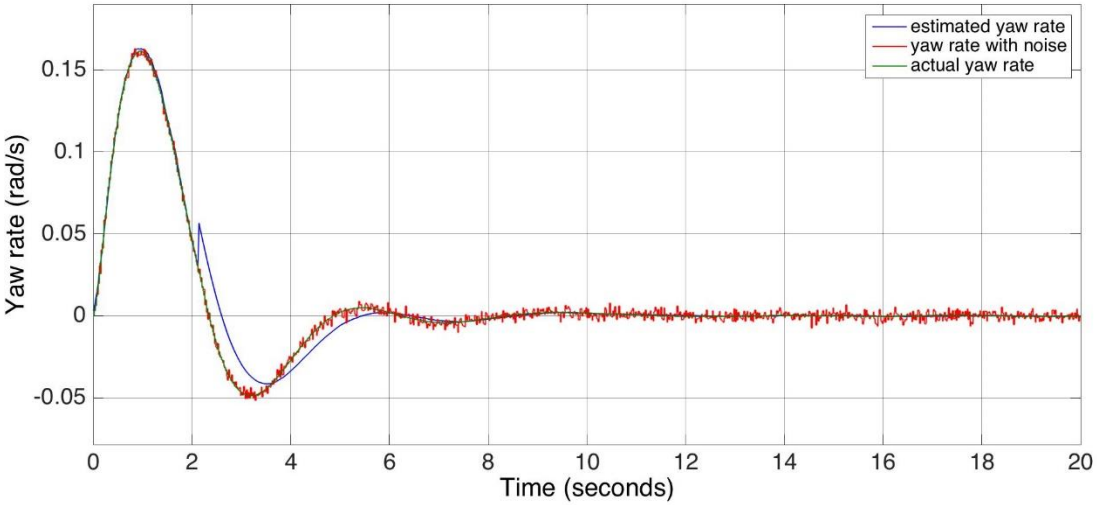

Figure 4.11 Yaw Rate Residual vs. Time

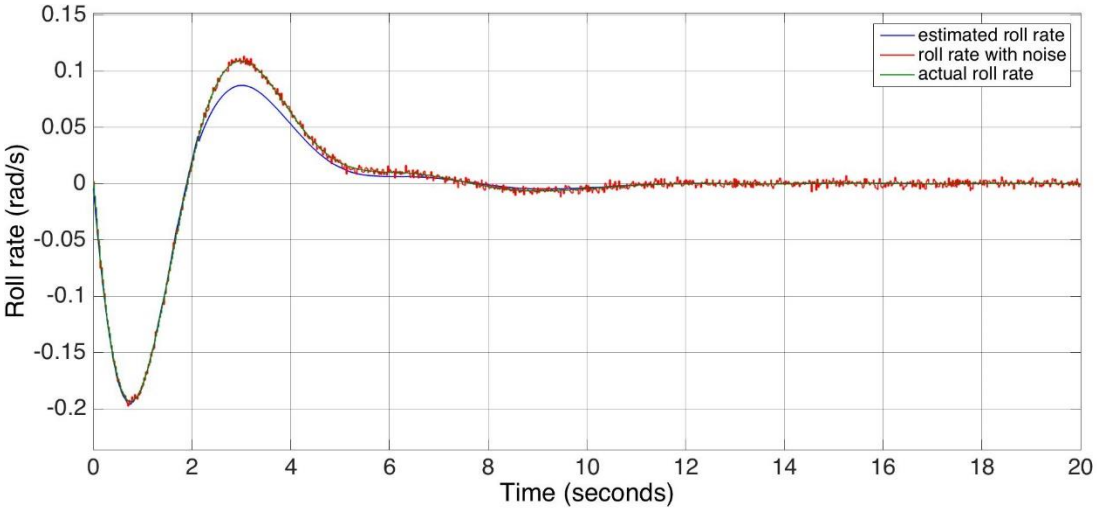

Figure 4.12 Roll Rate Residual vs. Time

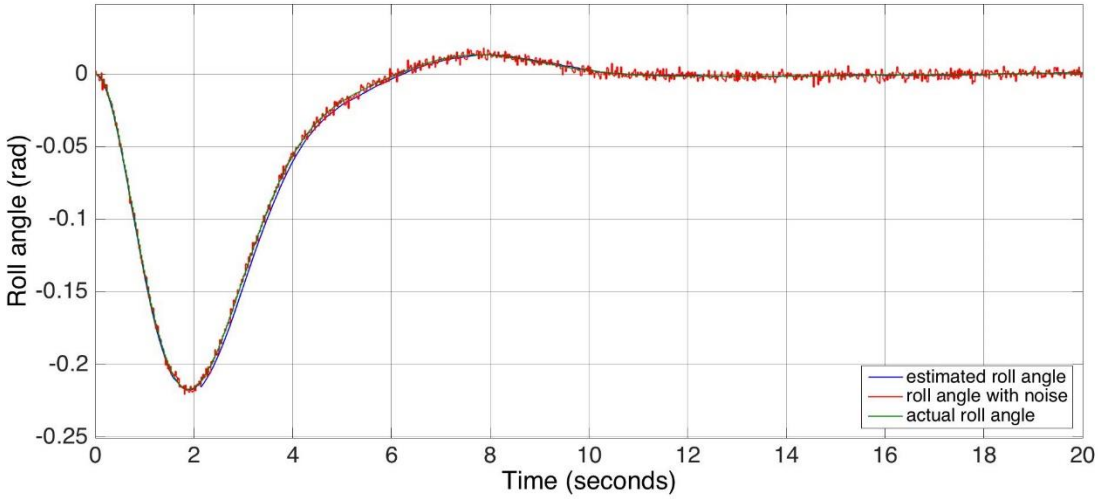

Figure 4.13 Roll Angle Residual vs. Time

In Figure 4.14, fault indicator threshold value on y-axis as '1' shows the fault is at its maximum while, its value as '0' shows that there is no fault. When the threshold value exceeds '0.8', then it is accepted to point out the value as '1' on y-axis as a design decision which refers the fault is not able to be eliminated from that point. In other words, it indicates that β sensor can not measure any signal within the faulty region.

The same figure illustrates that fault indicator signal exceeds the threshold magnitude value of '0.8' due to the uncertainty and fault effect on β sensor. Accomplished fault reconfiguration is directly considered in existence of stuck fault as there is no shift in β signal as the corresponding control channel after $t = 2$ s following the fault indicator response. Thereafter, the control designation is implemented which affirms that the sensor is failed at $t = 2$ s.

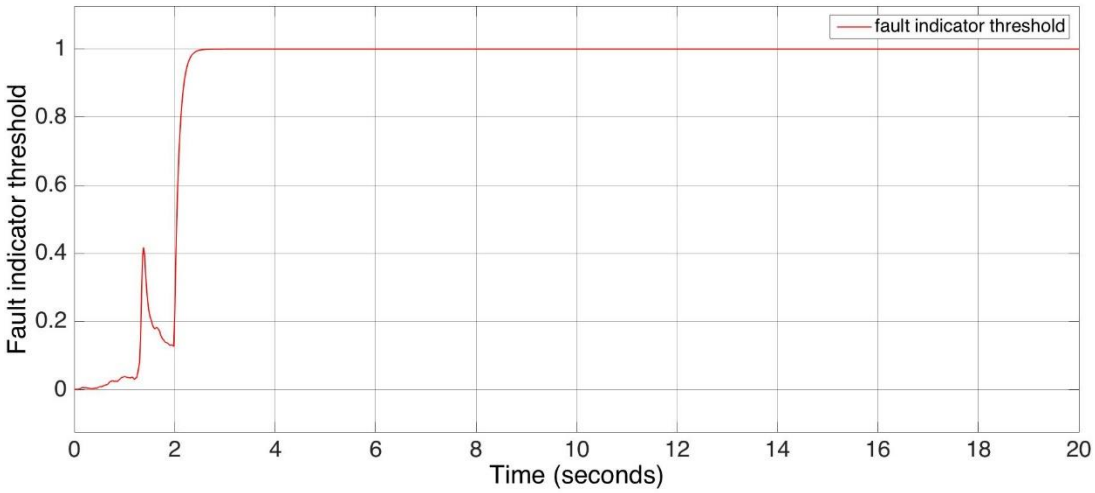

Figure 4.14 Fault Indicator Threshold vs. Time

Results of Luenberger-based Approach:

For the same uncertainty conditions, it is observed that actual state of β can not converge to its estimation and there is a considerable difference in residual as in Figure 4.15 while, measured states of r, p and $\emptyset$ display an opposite attitude since getting accurate measurements as in Figure 4.16, Figure 4.17 Figure 4.18.

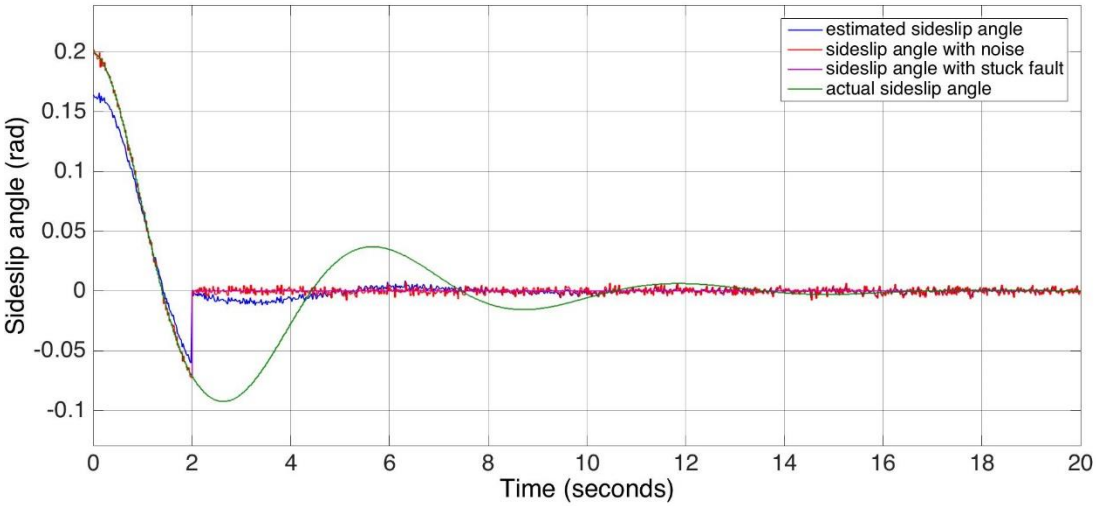

Figure 4.15 Sideslip Angle Residual vs. Time

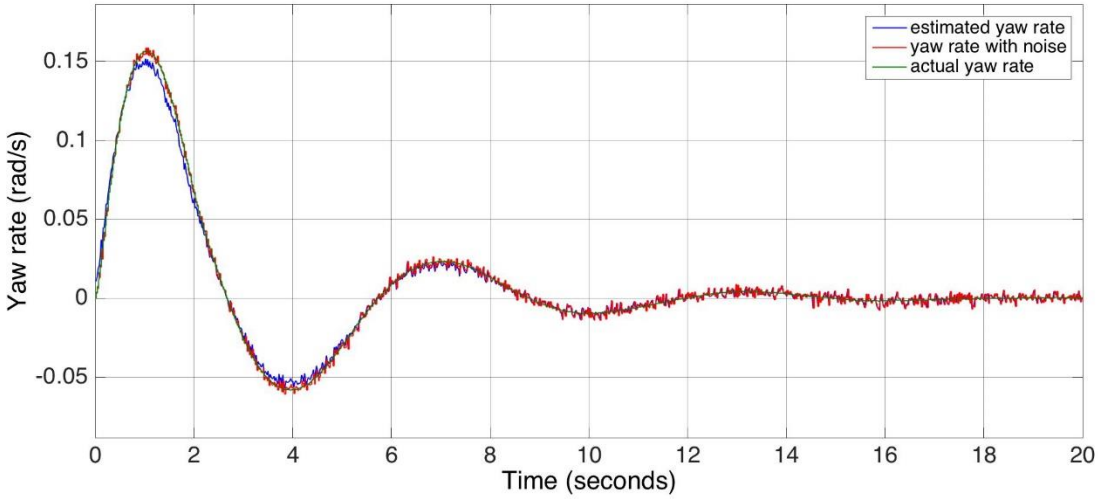

Figure 4.16 Yaw Rate Residual vs. Time

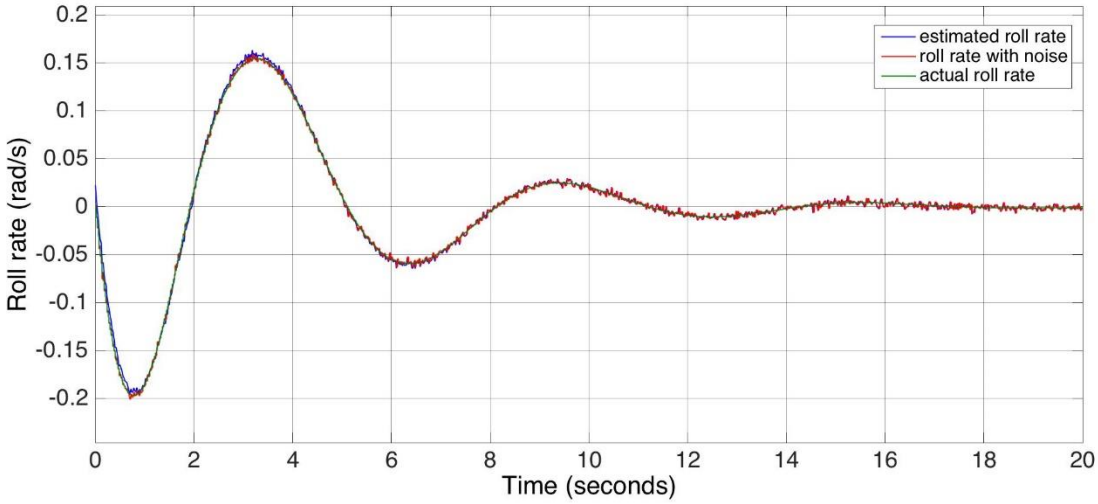

Figure 4.17 Roll Rate Residual vs. Time

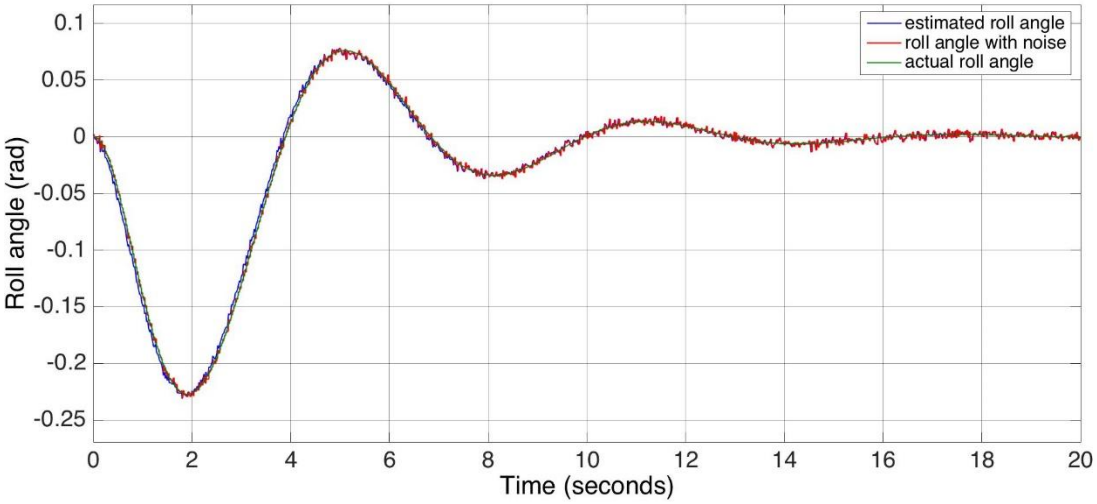

Figure 4.18 Roll Angle Residual vs. Time

Figure 4.19 points out that the fault indicator signal also exceeds the threshold magnitude value of 0.8. However, a false alarm is observed before $t = 2$ s due to the rigid uncertainty condition. Fault reconfiguration is directly considered in existence of stuck fault as there is no shift in β signal as the corresponding control channel after $t = 2$ s following the fault indicator response.

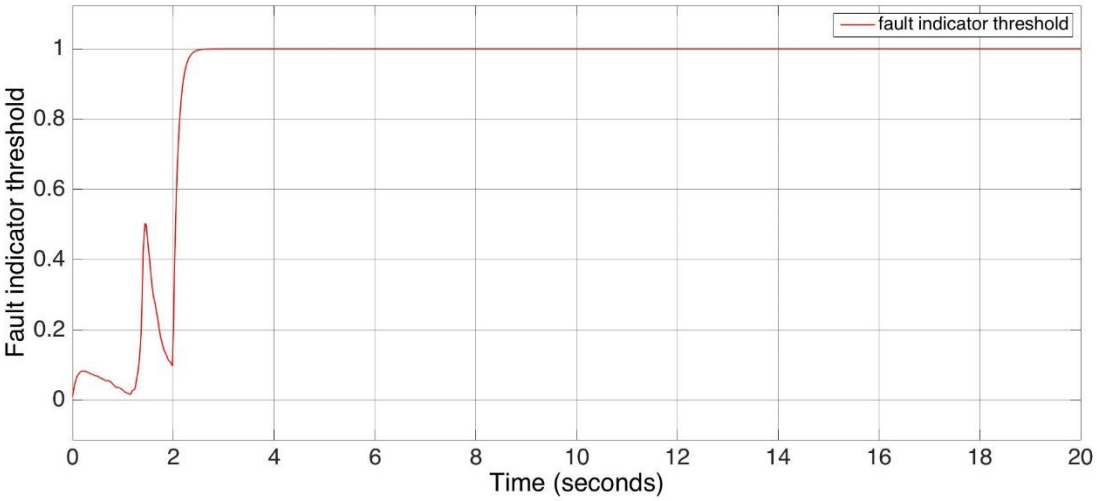

Figure 4.19 Fault Indicator Threshold vs. Time

CASE III. Stuck fault of the sensor case at $\mathbf{t = 2}$ s with a rudder input as a square wave $\boldsymbol{\delta_r = 0.25}$ rad for 10 s

The secondary faulty case compensates to the sensor stuck fault at the same test circumstances with Case II. However, there is an additional rudder deflection effect as a square wave with a magnitude of 0.25 rad for 10 s. After that time, the value of the rudder input turns back to 0 rad.

The performances of the Kalman filter and Luenberger observer in the faulty case are pointed out when there is both a stuck fault and rudder input in the system. The initial value of β is assigned to 0.2 radians. The demonstrations are followed in order of the separately computed lateral states β, r, p, ∅ respectively as Figure 4.20, Figure 4.21, Figure 4.22 and Figure 4.23 for Kalman filter and Figure 4.25, Figure 4.26, Figure 4.27 and Figure 4.28 for Luenberger observer. Red curve represents measurement of state with noise, blue curve represents estimate of state with all sensor measurements included, purple dashed curve represents estimate of state except sideslip angle sensor measurement, magenda curve represents measurement of state with stuck fault and green curve represents true state. The fault indicator response of the faulty scenario could be traced in Figure 4.24 for Kalman filter and Figure 4.29 for Luenberger observer.

The sample switch (N) is also assigned to be 100, thus β sensor is observed to be stuck at $t = 2$ s, mathematically. Gaussian noise in sensors are applied with a mean zero, noise variance 1.5×10^{-2} radians and sample time 0.02 seconds. The process noise (w) and the measurement noise (z) are set to the same values as given in Table 4.2.

In Case III, the same method of dual Kalman filters is used for the simulation as in Case II.

Results of Kalman-based Approach:

Although, sideslip angle (β) can not be measured accurately after stuck fault and continuously feedbacks faulty responses as 0 rad as in Figure 4.20, true state of β converges to the estimated state of β carried from the filter model. It can be seen that the actual β has a rise time of less than 3 seconds. By considering an initial sample value of β as 0.2 radians as a reference, then actual β does not surpass almost 0.2 radians. Actual β decreases gradually from 0.2 radians to -0.08 radians and increases gradually over -0.08 radians to 0 radians. β settles between 0.2 and -0.08 radians within 5 seconds in steady cruise flight.

The actual β and estimate of β are damped to 0 rad until 10 s and when the effect of rudder deflection angle is removed from the autopilot system, the attitude of actual β and estimate of β change to an oscillation status in less than 8 s to adapt the stabilized flight condition.

It can be observed from Figure 4.20, Figure 4.21, Figure 4.22 and Figure 4.23 that the overall lateral states are estimated properly before and after the existence of the stuck fault of β sensor. The error norm does not scale up to critical level owing to the detection performance of Kalman filter and tracks the faulty behavior through the simulation period. The measured states oscillate for a while and converge to their estimations approximately at $t = 7$ s until the effect of rudder input ceases and reach to the trim values. The estimation error is minor since the actual value of the engine thrust. Hence, it is reasonable within the considered stuck magnitude.

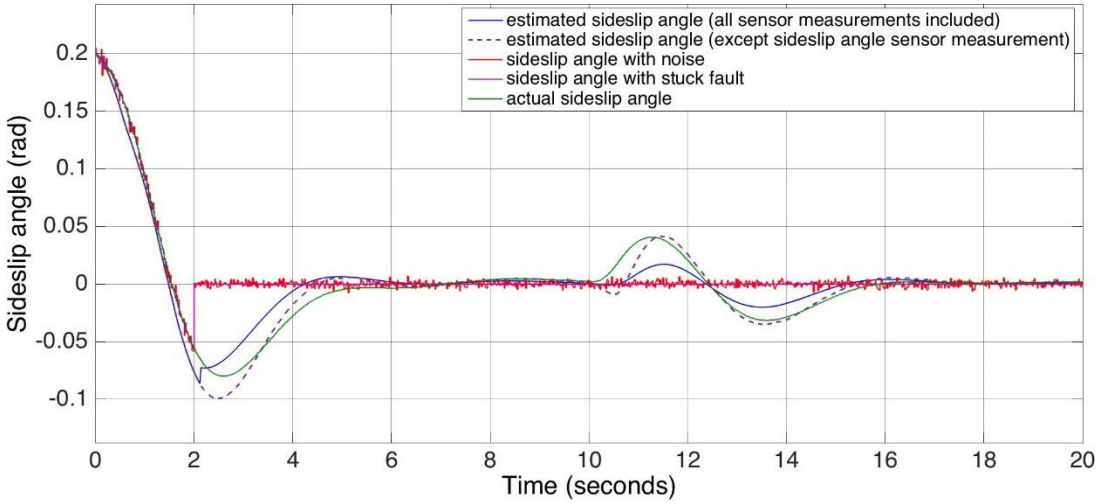

Figure 4.20 Sideslip Angle Residual vs. Time

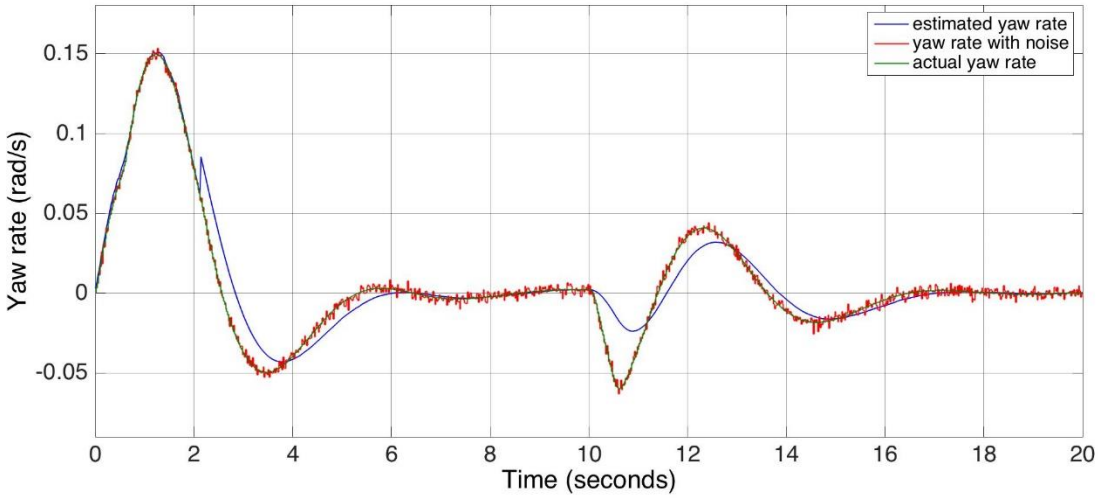

Figure 4.21 Yaw Rate Residual vs. Time

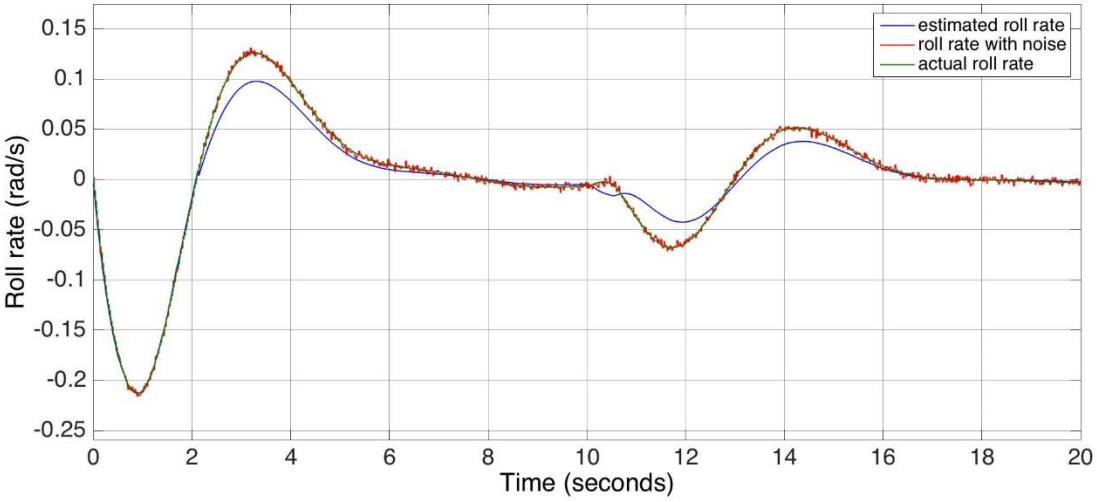

Figure 4.22 Roll Rate Residual vs. Time

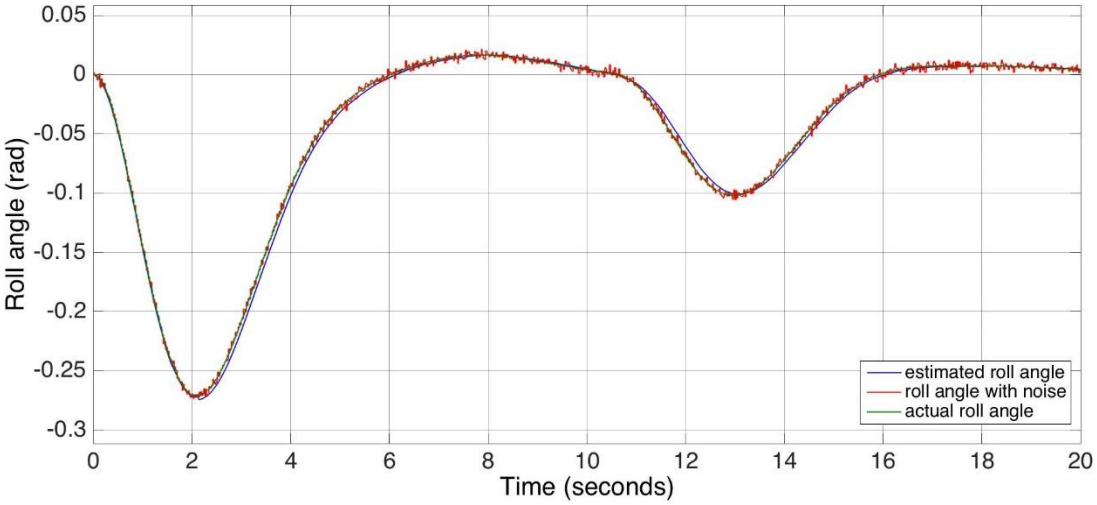

Figure 4.23 Roll Angle Residual vs. Time

As illustrated in Figure 4.24, fault indicator signal exceeds the threshold magnitude value of 0.8 due to the uncertainty and fault effect on β sensor. Accomplished fault reconfiguration is directly considered in existence of stuck fault as there is no shift in β signal as the corresponding control channel after $t = 2$ s following the fault indicator response. Thereafter, the control designation is implemented which affirms that the sensor is failed at $t = 2$ s.

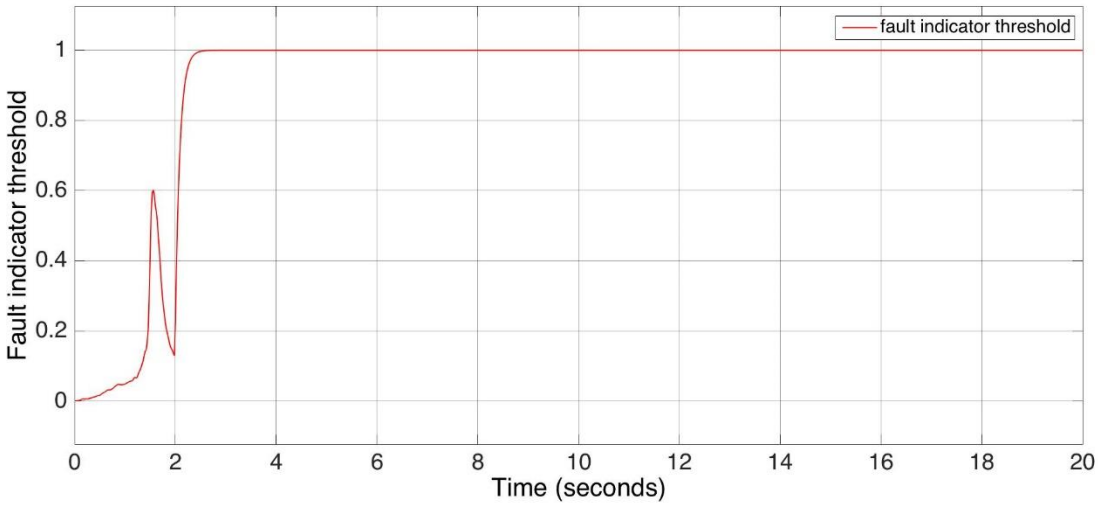

Figure 4.24 Fault Indicator Threshold vs. Time

Results of Luenberger-based Approach:

For the same uncertainty conditions, it is observed that actual state of β can not converge to its estimation and there is a considerable difference in residual as in Figure 4.25 while, measured states of r, p and $\emptyset$ display an opposite attitude since getting accurate measurements as in Figure 4.26, Figure 4.27 and Figure 4.28.

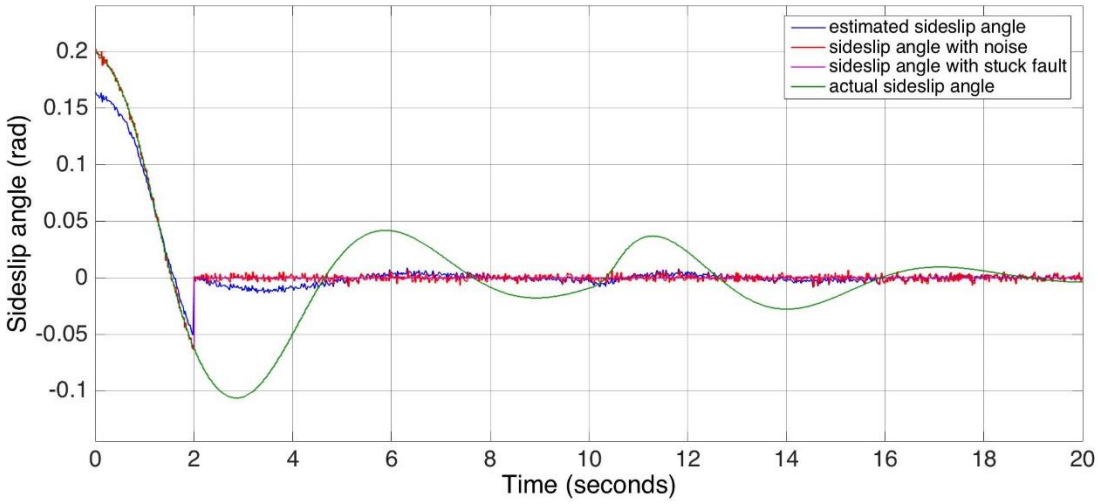

Figure 4.25 Sideslip Angle Residual vs. Time

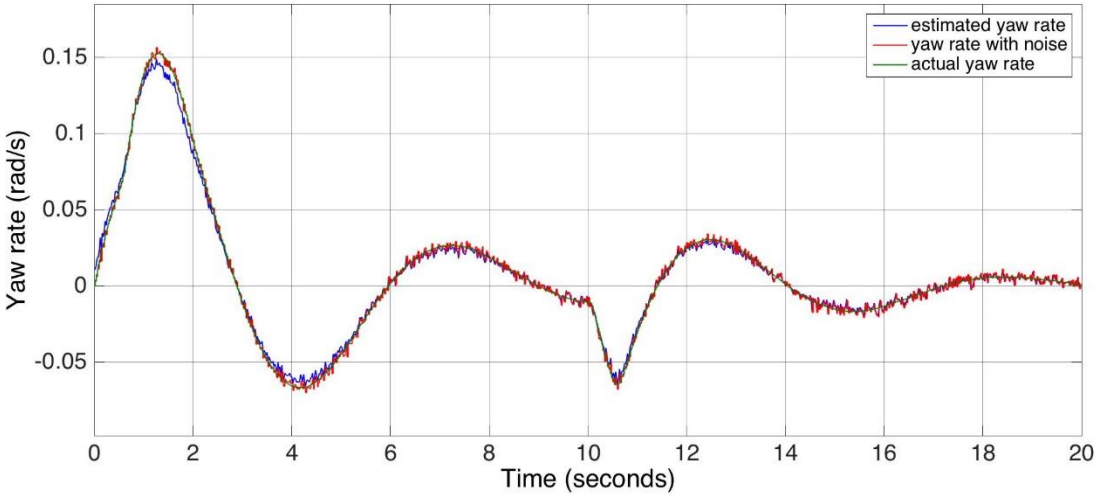

Figure 4.26 Yaw Rate Residual vs. Time

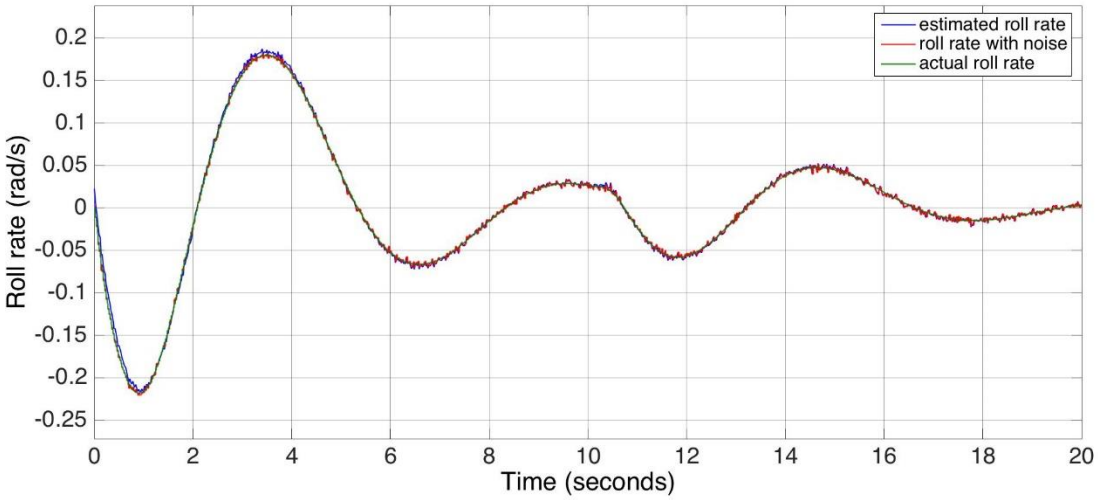

Figure 4.27 Roll Rate Residual vs. Time

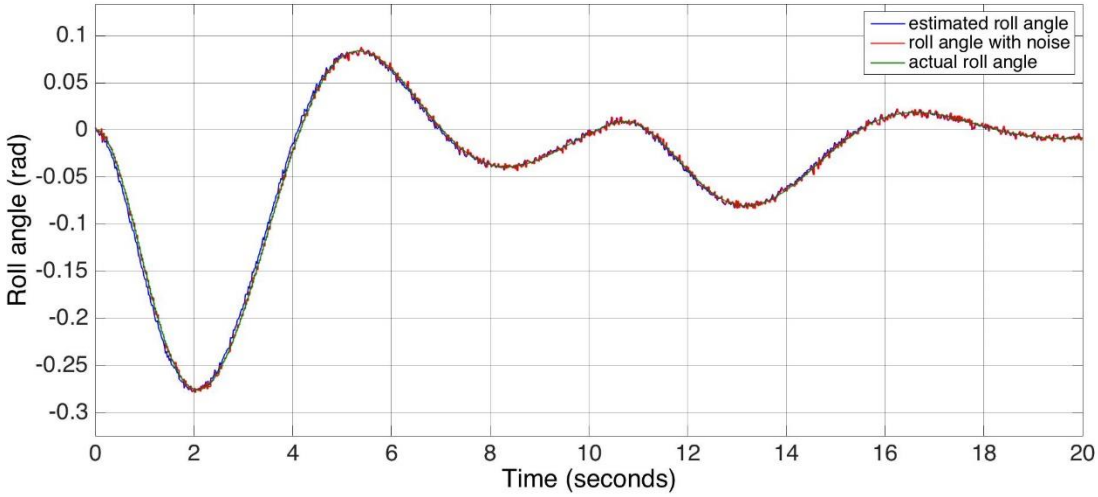

Figure 4.28 Roll Angle Residual vs. Time

Figure 4.29 points out that the fault indicator signal also exceeds the threshold magnitude value of 0.8. However, a false alarm is observed before $t = 2$ s due to the rigid uncertainty condition. Fault reconfiguration is directly considered in existence of stuck fault as there is no shift in β signal as the corresponding control channel after $t = 2$ s following the fault indicator response.

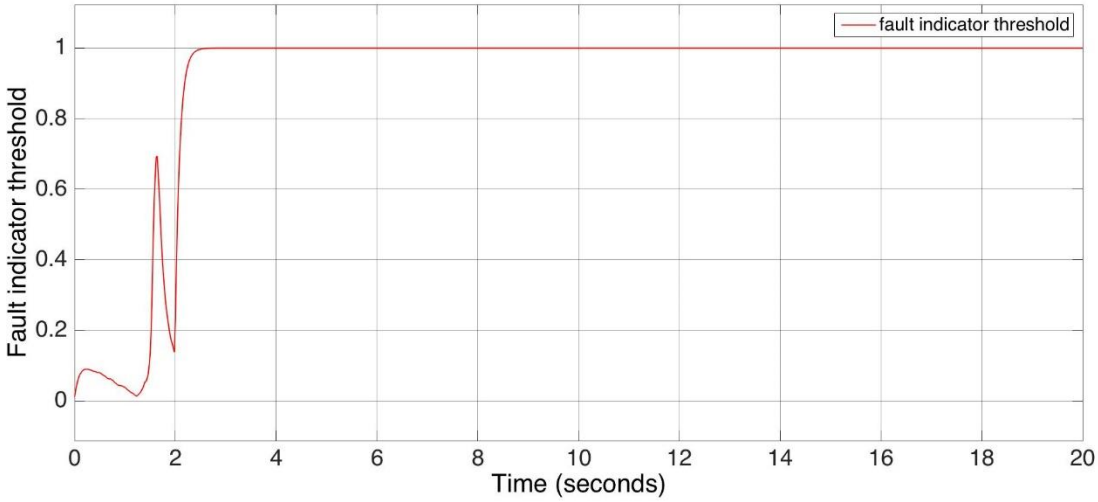

Figure 4.29 Fault Indicator Threshold vs. Time

To summarize the simulation results, a conventional Kalman filter and Luenberger observer were used to estimate the magnitude of stuck faults for a Boeing 747 aircraft

model. The simulation cases were performed to estimate the lateral states of a civil aircraft during a cruise flight. Kalman filter successfully detects the magnitude of the fault even it is set to quite small magnitudes. Kalman filter was indicated to be stable under certain situations. Then, it was observed that it does not only minimize the expected value, but it also minimizes the estimation variance in noisy environments. Kalman filter displayed a more remarkable estimation performance than Luenberger observer on the simulation cases that are introduced by means of faster convergence and trim rates with smaller error norms upon the states of the aircraft.

Including a white Gaussian noise effect to the aircraft model causes an uncertainty case that increases the false alarm in the system. As a control surface reaction, state measurements showed that the rudder may become extremely effective against the faults. However, high performance estimation of Kalman filter against the noise effects, the false alarm was limited.

The deflection inputs were supplied such that the loss of effectiveness and the estimation of fault magnitudes could be succeed for a limited region. It was clearly observed that the trim point remains stable fairly soon assuring the plant stability until the end of the observations. Hence, the controller was not required to be redesigned to take care of uncertainty.

Kalman filter has modelled a zero mean and unit covariance matrix Gaussian white noise accurately. If the aircraft model was not integrated in exact accuracy level due to any inaccuracy in the system matrices A and B, this condition would give incorrect results in different flight scenarios such as a coordinated turn, a power approach or even in a pull up. Kalman filter is said to be an effective observer for performing the function of estimation on the faulty sensor measuring the sideslip angle (β) with the information carried from other accurate state measurement channels.

After regulating several parameters and variables on the entire MATLAB Simulink model, it is achieved to get prominent results with respect to the figures that are

discussed above on similar scales. The proposed method is proven to offset the stuck faults immediately after they emerge and limit the variation between the state measurements and state estimations. The improvement in handling the faults in a slighter detection threshold level, shorter confirmation time, better false alarm rate elimination or getting a better flight performance of the aircraft is presented as the main purpose of the study.

CHAPTER 5

CONCLUSION

This study presents the concept and results of a FDD method based on state estimations of a stochastic observer model in the continuous-time framework. The introduced design framework covers a flight control law to struggle with undesired faulty conditions of the sensors of a civil aircraft. The sensor fault detection application was supported to verify with multi simulation tests and the control effectiveness of a complex dynamic systems was confirmed with several faulty and fault-free cases. The parameters were optimized to the relevant values for different flight cases. Stuck faults were introduced in a certain time by the fault indicator. Stuck fault arised from the faulty sensor signal was investigated by presenting several faulty schemes additionally a nominal (no fault) scheme and carried out sequentially. It can be observed that stuck fault in sensor that measures sideslip angle also affects the sensor measures roll angle as a coupling effect. This is owing to faulty state vector in feedback loop through controller. For achieving realistic simulation results, the simulation model of the aircraft should consist of straight stability derivatives. The principle is separated to two different approaches to evaluate the performance of the designed FDD scheme with a Luenberger observer and a Kalman filter as a more conventional estimator. The simulation results pointed out that the aircraft maintains the trim conditions of airspeed, altitude and Euler angles. The observer performances of the schemes were considered for comparison objectives in the same flight conditions.

As the basic stage of the study using Kalman filter, the linearization of the nonlinear lateral states was introduced. An FDI scheme was improved for analytical redundancy for mainly the sideslip angle (β) sensor of lateral dynamics model of Boeing 747 civil aircraft. The subsystems were designed and connected appropriately in the simulation

model to indicate the overall architecture of the system. The proposed FDI system can operate for stuck faults at any time instant. It is important to consider that the nonlinearity of the aircraft should be straightly integrated to the observer design to allow correct state estimations including more severe faulty cases.

In the Kalman filter approach, it can be clearly seen that the resultant state estimator is unbiased, stable and minimum variance in exact assumptions. The Kalman filter algorithm is said to be pretty good in estimating the states successfully and also detecting stuck faults in the system. The simulation result for fault-free case is also successful since the filter tunes for no fault condition. Although this study covers a representation for Boeing 747 aircraft, the overall FDD process can be implemented for other kinds of civil and military aircrafts and also for the platforms that operate on space services. The performance of the Kalman filter analytically shows that the approach is effective in predicting the states of the system quite accurately. As a theoretical point of view, this can be explained as observer gain matrix is adaptive for Kalman filter. Kalman filter is considered to be an optimum observer in the case of noise that are received from sensor and model are Gaussian [36].

The figures shown in the previous sections are representative results of numerical simulation samples for those stuck fault and fault-free cases. The residual generated for the stuck fault case is originated with respect to the variation between the measurement and estimation channels. The magnitude of the residual was reduced and fault detection at a small magnitude was detected. The detection delay limitation is clearly observed for the comparison objective. Furthermore, in the fault-free situation for a specified threshold and confirmation time, the method gave no false alarms.

As an outcome, the proposed Kalman filtering methodology is very sensitive to the faults and has a good performance with respect to the slight detection threshold level, short confirmation time and good false alarm rate limitation. The model could quickly

detect even slight changes in the measurement channel and is suitable for real-time fault detection. The residuals are monitored to be limited in a restricted gap for the developed fault detection method. If detection of fault and reconfiguration does not take place, aircraft will cross the limits of safe operation. This explains that sensor fault detection must be diagnosed in time. Otherwise, it could lead to closed-loop instability and unrecoverable flight conditions. Likewise, the results of the experiment demonstrate that the proposed filter ensured a significant profit and safety in estimation performance with small computational effort to measurement uncertainties in a certain scale of the study. The facility of generating similar estimation features of the Kalman filter can be verified in extensive applications virtually with the results of this combined study in aircraft sensor fault detection approaches. From the industrial case, a realistic solution was considered worthy by improving the performance level of the aircraft.

Future research could focus on the integration of an interactive multiple model (IMM) ensemble Kalman filter instead of a single Kalman filter model to the FDI scheme to get more accurate state estimation. IMM Kalman filter is originated from a dual Kalman model that uses the equations of the filter. It decides which one to use by computing the probability and weight accounts upon the measurement data considering the model. Therefore, the need for calibrating the ideal values of covariances will be set by the filter automatically.

The significance of the study could contribute to the real-time flight incidents as a noticeable augmentation to the aircraft performance that is evaluated with the fuel consumption, noise level reduction and raise of range respectively. The educational and research objectives were also considered in aircraft flight control systems that operates MATLAB Simulink to run the observer-based fault detection scheme under several simulation tests that is proposed in the paper.

REFERENCES

[1] A. Gheorghe, A. Zolghadri, J. Cieslak, P. Goupil, R. Dayre, and H. Le Berre, "Model-Based Approaches for Fast and Robust Fault Detection in Aircraft Control Surface Servo-loop," *IEEE Control Systems*, 2013, vol. 33, Iss. 3, pp. 20–84, DOI: 10.1109/MCS.2013.2249417.

[2] H. Fang, N. Tian, Y. Wang, M. Zhou, and M. A. Haile, "Nonlinear Bayesian Estimation: From Kalman Filtering to a Broader Horizon," *IEEE/CAA Journal of Automatica Sinica*, 2018, vol. 5, Iss. 2, pp. 401-417. DOI: 10.1109/JAS.2017.7510808.

[3] J. Zhang, K. You, and L. Xie, "Bayesian Filtering with Unknown Sensor Measurement Losses," *IEEE Transactions on Control of Network Systems*, 2018, DOI: 10.1109/TCNS.2018.2802872.

[4] A. Valade, P. Acco, P. Grabolosa, and J. Y. Fourniols, "A Study about Kalman Filters Applied to Embedded Sensors," *Sensor (Basel)*, 2017, vol. 17, Iss. 12, DOI: 10.3390/s17122810

[5] S. Singh and T. V. R. Murthy, "Simulation of sensor failure accommodation in flight control system of transport aircraft: a modular approach," *World Journal of Modelling and Simulation*, vol. 11, no. 1, pp. 55–68, 2015.

[6] G. X. Xu, "Nonlinear Fault-Tolerant Guidance and Control for Damaged Aircraft," University of Toronto, Graduate Department of Aerospace Science and Engineering, 2011.

[7] A. Zolghadri, D. Henry, J. Cieslak, D. Efimov, and P. Goupil, "Fault Diagnosis and Fault-Tolerant Control and Guidance for Aerospace Vehicles," DOI 10.1007/978-1-4471-5313-9, 2014.

[8] F. Caliskan and C. M. Hajiyev, "Sensor fault detection in flight control systems based on the Kalman filter innovation sequence," *Proc. Instn. Mech. Engrs*. vol. 213, Part I, IMechE, 1999.

[9] M. Bonfe, P. Castaldi, W. Geri, and S. Simani, "Fault detection and isolation for on-board sensors of a general aviation aircraft," *International Journal of Adaptive Control and Signal Processing*, 2006, vol. 20, pp. 381–408, DOI: 10.1002/acs.906.

[10] S. Singh and T. V. R. Murthy, "Neural Network based Sensor Fault Detection for Flight Control Systems," *International Journal of Computer Applications*, vol. 59, no. 13, pp. 1–8, 2012.

[11] V. Sridhar, H. S. Sheshadri and M. C. Padma, "Emerging Research in Electronics, Computer Science and Technology," *Proceedings of International Conference*, vol. 248, pp. 801–810, 2014.

[12] S. Kim, Y. Kim, C. Park, and I. Jung, "Hybrid Fault Detection and Isolation Techniques for Aircraft Intertial Measurement Sensors," *AIAA Guidance, Navigation and Control Conference and Exhibit*, 2014, DOI: 10.2514/6.2004-5419.

[13] Y. Han, S. Oh, B. Choi, D. Kwak, H. J. Kim, and Y. Kim, "Fault detection and identification of aircraft control surface using adaptive observer and input bias estimator," *IET Control Theory Appl.*, 2012, vol. 6, Iss. 10, pp. 1367–1387, DOI: 10.1049/iet-cta.2010.0724.

[14] J. Jiang and X. Yu, "Fault-tolerant control systems: A comparative study between active and passive approaches," *Annual Reviews in Control*, vol. 36, pp. 60–72, 2012.

[15] T. Wang, "Sliding Mode Fault Tolerant Reconfigurable Control against Aircraft Control Surface Failures," Concordia University, Department of Mechanical and Industrial Engineering, 2012.

[16] M. Blanke, M. Kinnaert, J. Lunze, and M. Staroswiecki, "Diagnosis and Fault-Tolerant Control," 2016, DOI 10.1007/978-3-662-47943-8.

[17] M. J. L. Levesque, "Fault Detection and Isolation for the Bluebird Test Bed Aircraft," Naval Postgraduate School, Department of Electrical Engineering, 1993.

[18] G. N. Vishnu, M. V. Dileep, and K. R. Prahalad, "Design of Fuzzy Logic Controller for Lateral Dynamics Control of Aircraft by Considering the Cross-Coupling Effect of Yaw and Roll on Each Other," *International Journal of Computer Applications*, vol. 47, no. 13, pp. 44–48, 2012.

[19] H. Alwi, C. Edwards, and C. P. Tan, "Fault Detection and Fault-Tolerant Control Using Sliding Modes," 2011, DOI 10.1007/978-0-85729-650-4.

[20] P. K. Rachinayani, "Robust Fault-Tolerant Control for aircraft systems," Graduate Faculty of the Louisiana State University and Agricultural and Mechanical College, Department of Electrical and Computer Engineering, 2006.

[21] J. Hong, S. Laflamme, J. Dodson, and B. Joyce, "Introduction to State

Estimation of High-Rate System Dynamics," *Sensors*, 2018, vol. 18, Iss. 1, DOI 10.3390/s18010217.

[22] R. Vepa and F. Caliskan, "Application of observers to monitoring, failure detection a fault diagnosis in aircraft flight control," *Proc. Instn. Mech. Engrs., Part G: Journal of Aerospace Engineering,* vol. 209, 1995.

[23] A. Marcos, S. Ganguli, and G. Balas, "Application of H_∞ Fault Detection and Isolation to a Boeing 747-100/200 Aircraft," University of Minnesota, Department of Aerospace Eng. and Mechanics, 2005, DOI: 10.2514/6.2002-4944.

[24] J. George, "Lateral Directional Approximations to Aircraft," Indian Institute of Science, Department of Aerospace Engineering, 2005.

[25] R. Pratt, "Flight Control Systems: Practical Issues in Design and Implementation," *Control Engineering Practise,* 2001, vol. 9, Iss. 10, DOI 10.1006/S0967-0661(01)00072-7, 2001.

[26] L. Tian, "A study of nonlinear flight control system designs," Iowa State University, Department of Aerospace Engineering, 1999.

[27] B. Etkin and L. D. Reid, "Dynamics of Flight, Stability and Control," McGrawHill, Third Edition, 1996.

[28] M. G. R. Kumar and T. V. R. Murthy, "Fault Detection of Aircraft Plant Using Kalman Filter," *International Science Press IJCT*., vol. 8, no. 3, pp. 923–931, 2015.

[29] E. I. E. Madbouly I. A. Hameed and M. I. Abdo, "Reconfigurable Adaptive Fuzzy Fault-hiding Control for Greenhouse Climate Control System," *International Journal of Automation and Control.*, vol. 11, no. 2, pp. 164–187, 2017.

[30] J. Z. Sasiadek and P. Hartana, "Sensor Data Fusion Using Kalman Filter," *Information Fusion Proceedings of the Third International Conference,* 2000, vol.2, DOI: 10.1109/IFIC.2000.859866.

[31] V. R. Gajic, “Linear Observers Design and Implementation,” 2014, DOI: 978-1-4799-5233-5.

[32] F. Tadeo and M. A. Rami, “Observation with Bounds of Biological Systems, A Linear Programming Approach,” *In Proceedings of the Third International Conference on Bio-inspired Systems and Signal Processing,* 2010, pp. 230-235, DOI: 10.5220/0002717602300235.

[33] C. R. Robinson, “Decentralised Data Fusion Using Agents,” The University of York, Department of Electronics, 2008.

[34] G. Campa, Airlib version 1.11.0.0, The Aircraft Library. https://www.mathworks.com/matlabcentral/fileexchange/3019-airlib. Accessed: 2018-06-01.

[35] P. A. Samara, G. N. Fouskitakis, J. S. Sakellariou, and S. D. Fassois, “A Statistical Method for the Detection of Sensor Abrupt Faults in Aircraft Control Systems,” *IEEE Transactions on Control Systems Technology*, vol. 16, pp. 789–798, 2008.

[36] A. Gelb, “Applied Optimal Estimation,” Eleventh Edition, 1974.

APPENDIX A

AIRCRAFT STATES PLOTS

The States of Boeing 747

This chapter introduces the behavior and rate of changes for some of the other Boeing 747 states apart from the lateral states ($\beta, r, q, \emptyset$) that are mainly analyzed in the study for the simulation cases, respectively. The simulation period for Case II. is arranged to 20 seconds to get the trim observation. As can be seen in the figures below, in both Kalman filter and Luenberger observer methodologies, all of the states converge to trim values. However, particularly for yaw angle and altitude outputs of the aircraft with respect to time, it can be observed that Kalman filter has shown approximately 6 s faster response in trim than Luenberger observer. The aircraft sustains the steady state flight with excellent regularity, showing some transitional dynamics, however, this attitude is expected as an outcome of the nonlinearity nature in the aircraft. When it occurs while tracking a plot, an amplification is allowed to display that they are slight, hence they do not lead any problem.

Results of Kalman-based Approach:

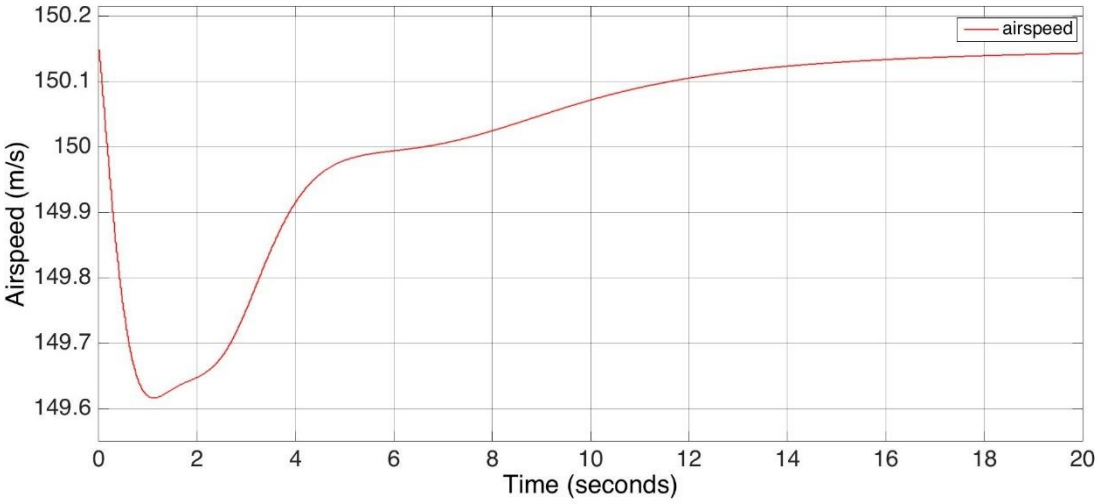

Figure A.1 Airspeed vs. Time

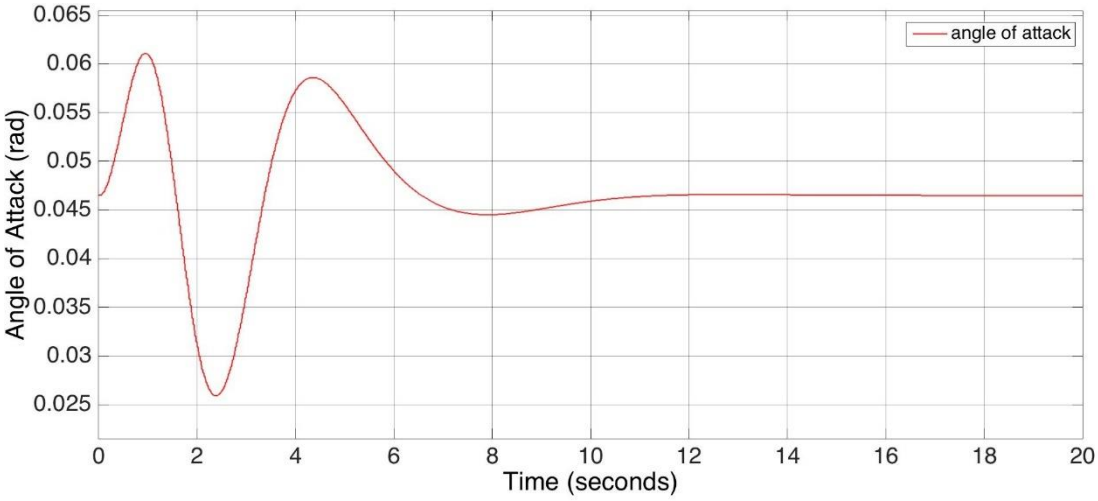

Figure A.2 Angle of Attack vs. Time

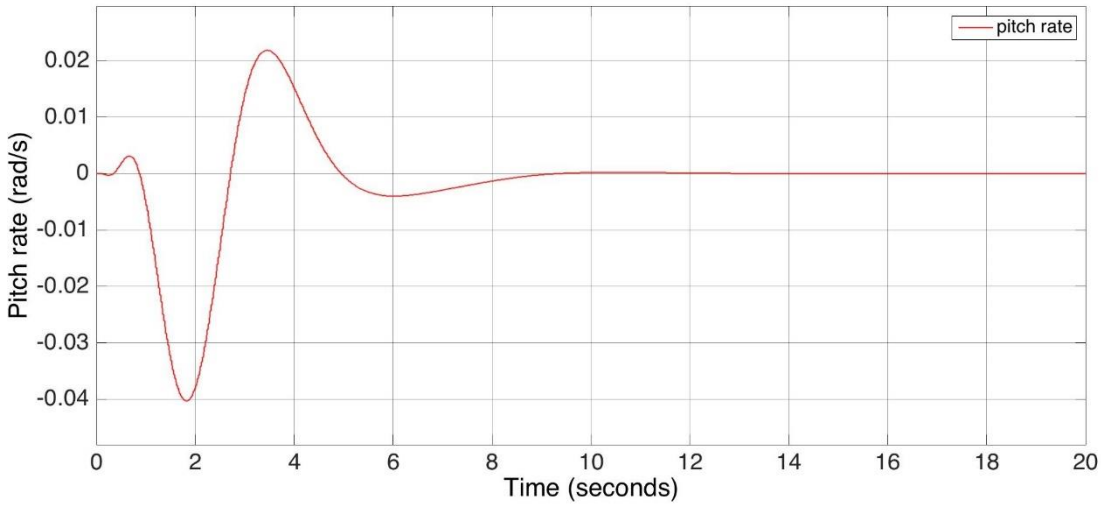

Figure A.3 Pitch Rate vs. Time

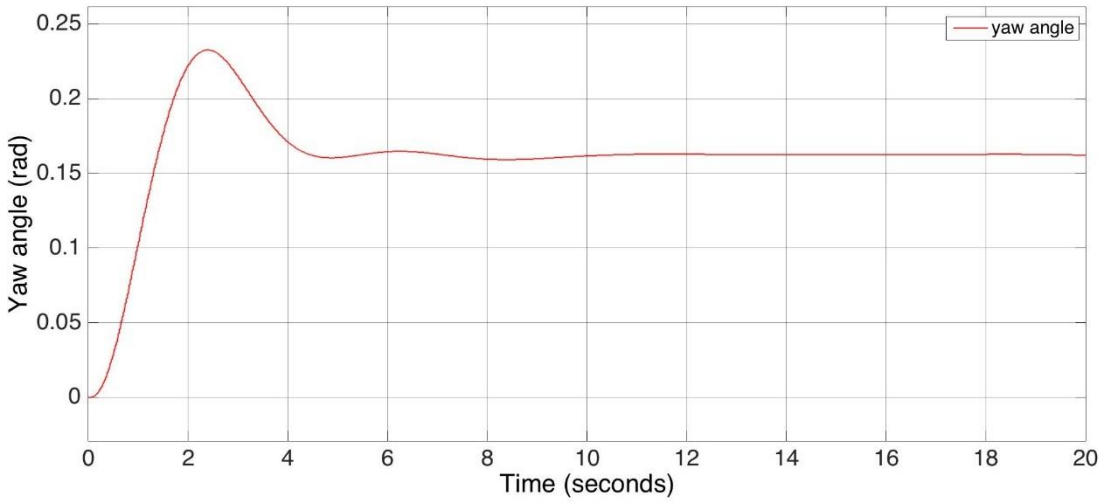

Figure A.4 Yaw Angle vs. Time

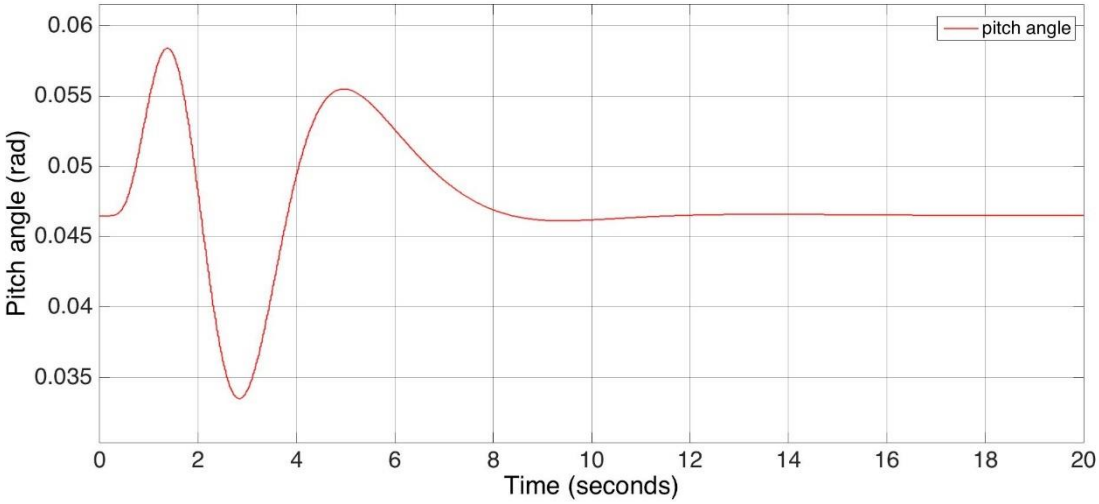

Figure A.5 Pitch Angle vs. Time

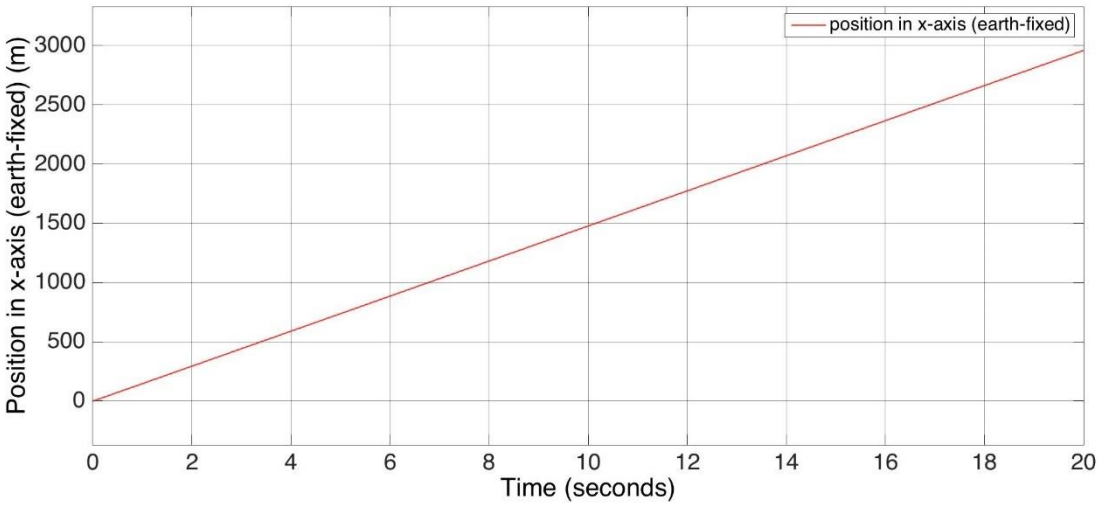

Figure A.6 Aircraft Position in X-Axis vs.Time

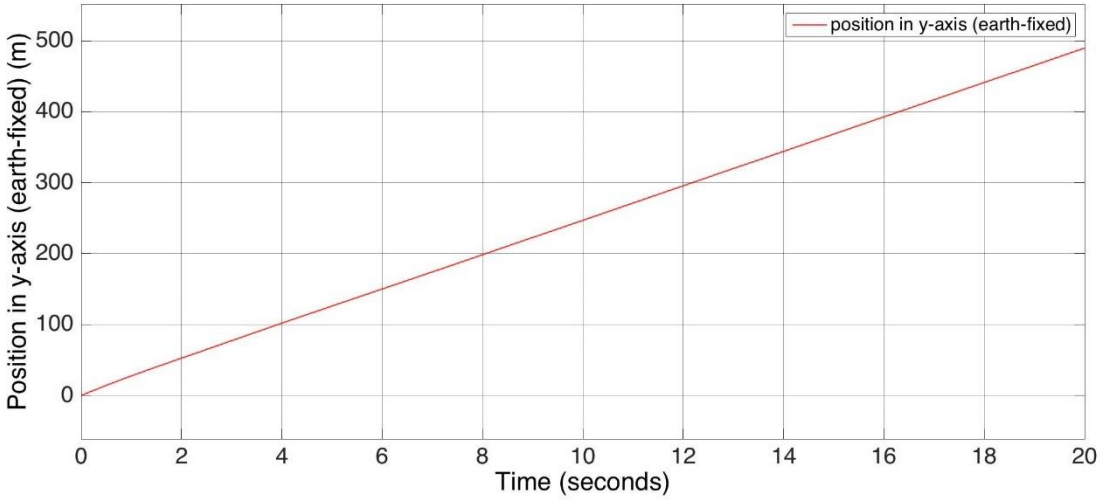

Figure A.7 Aircraft Position in Y-Axis vs. Time

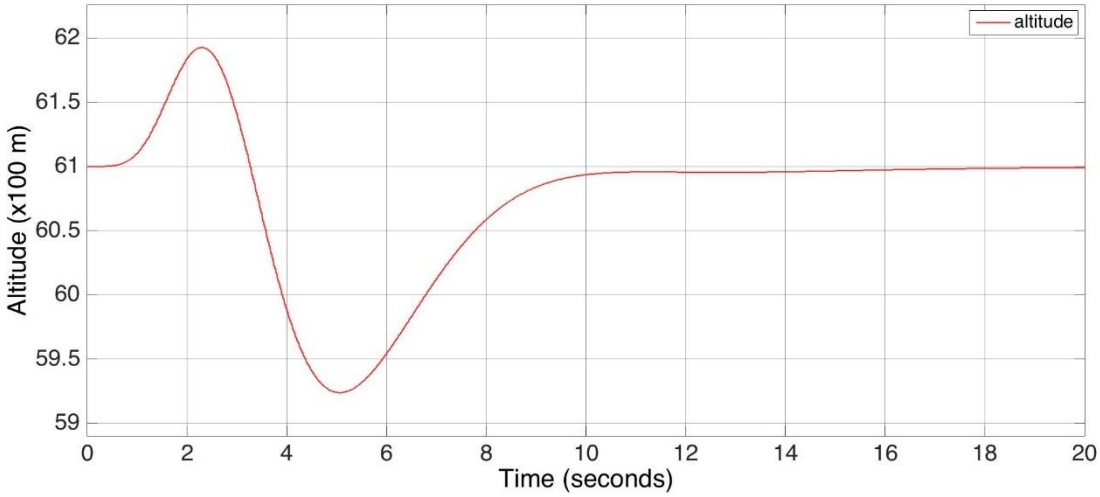

Figure A.8 Altitude vs. Time

Results of Luenberger-based Approach:

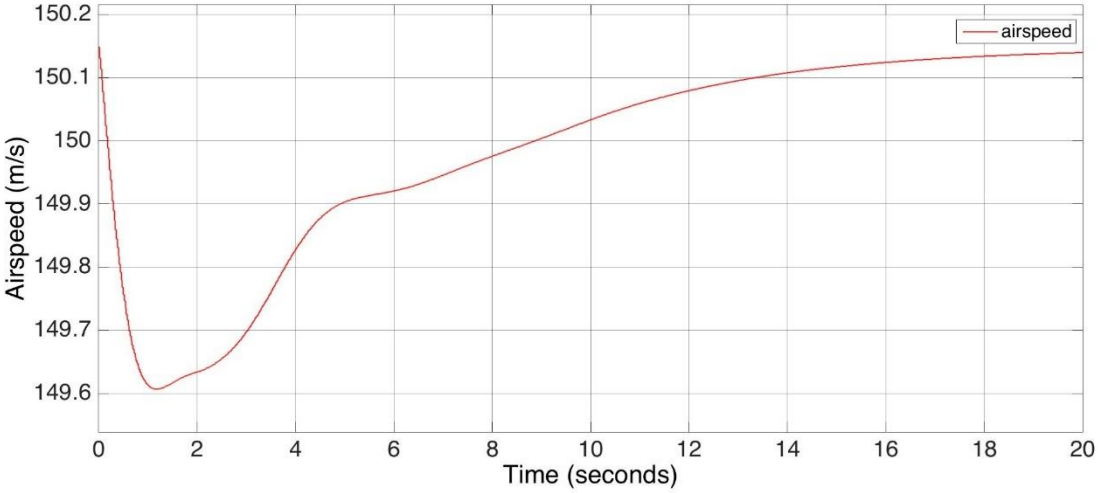

Figure A.9 Airspeed vs. Time

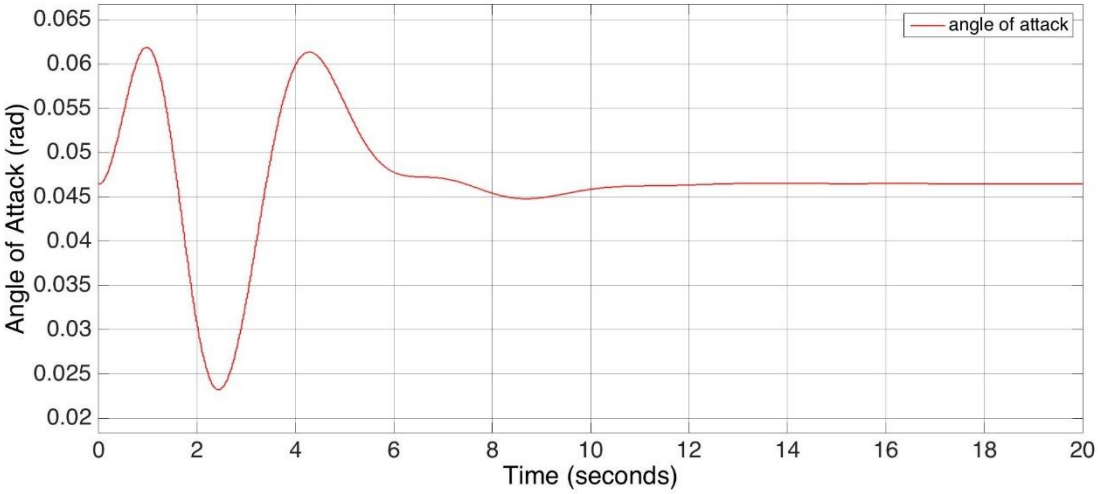

Figure A.10 Angle of Attack vs. Time

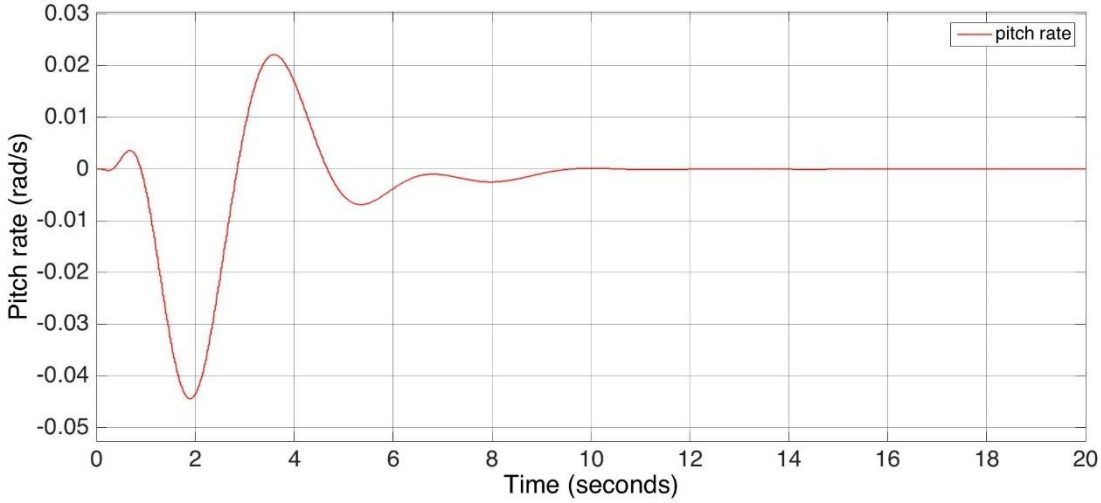

Figure A.11 Pitch Rate vs. Time

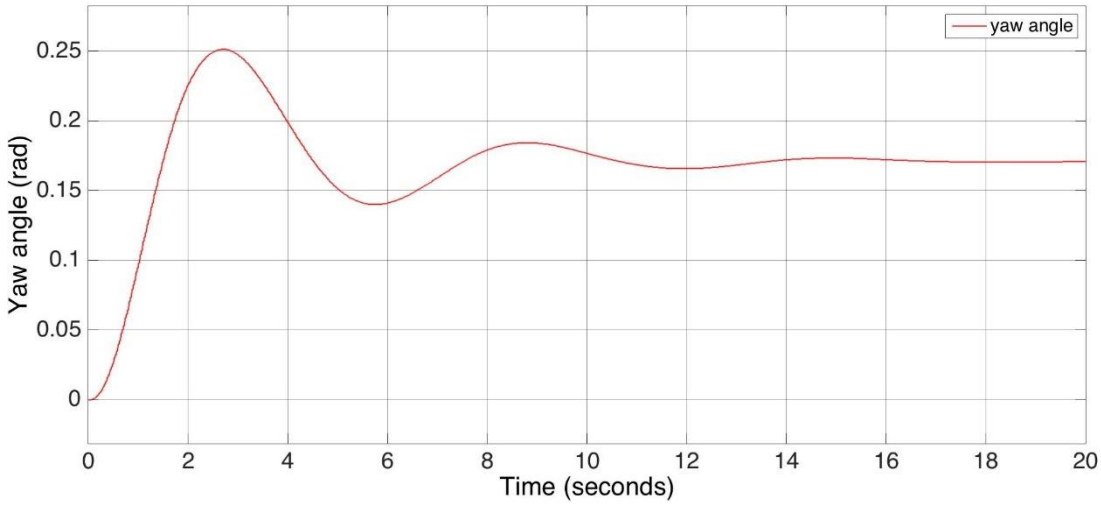

Figure A.12 Yaw Angle vs. Time

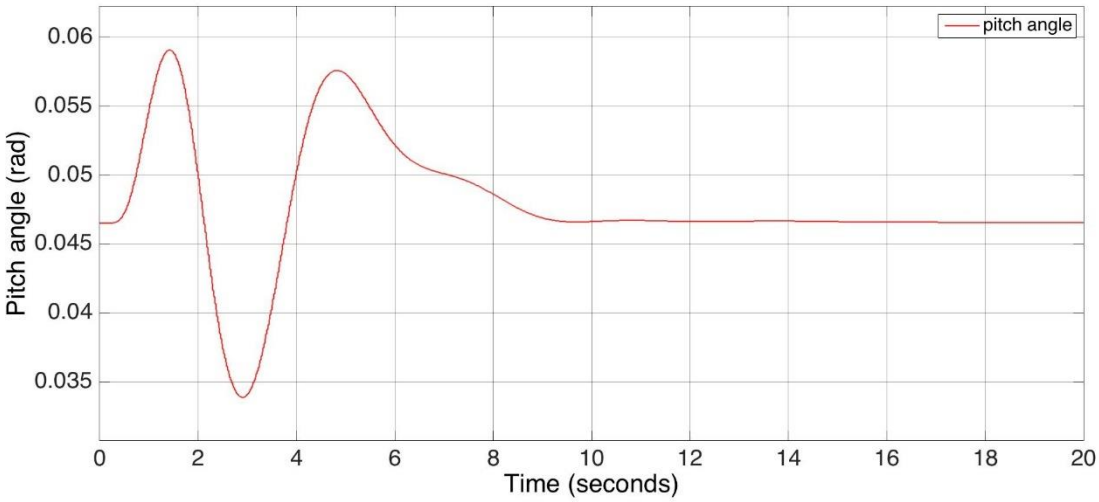

Figure A.13 Pitch Angle vs. Time

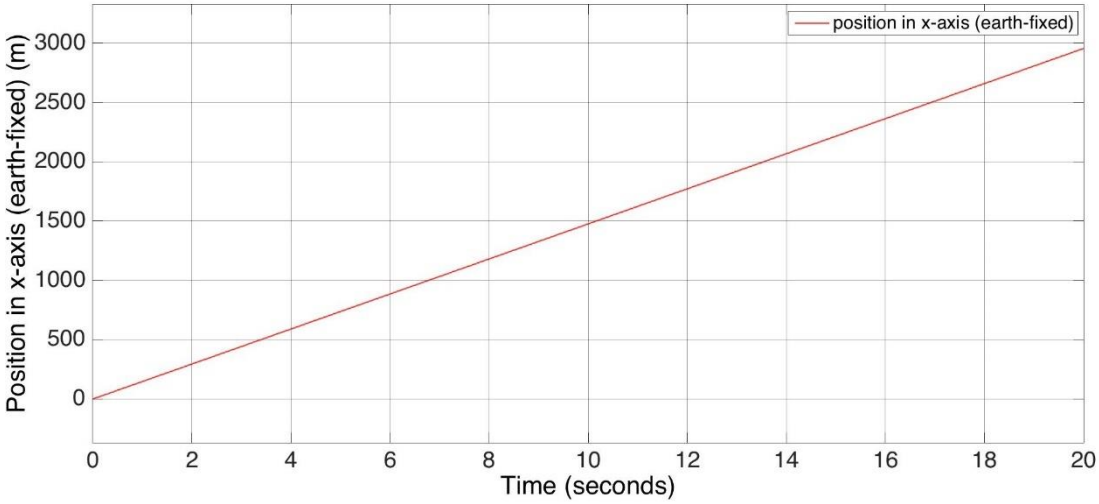

Figure A.14 Aircraft Position in X-Axis vs.Time

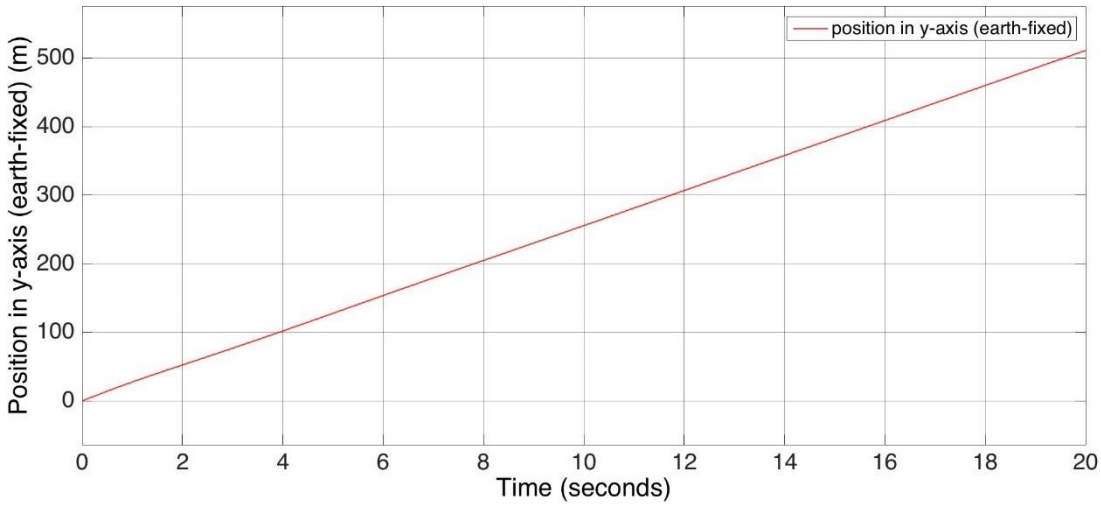

Figure A.15 Aircraft Position in Y-Axis vs. Time

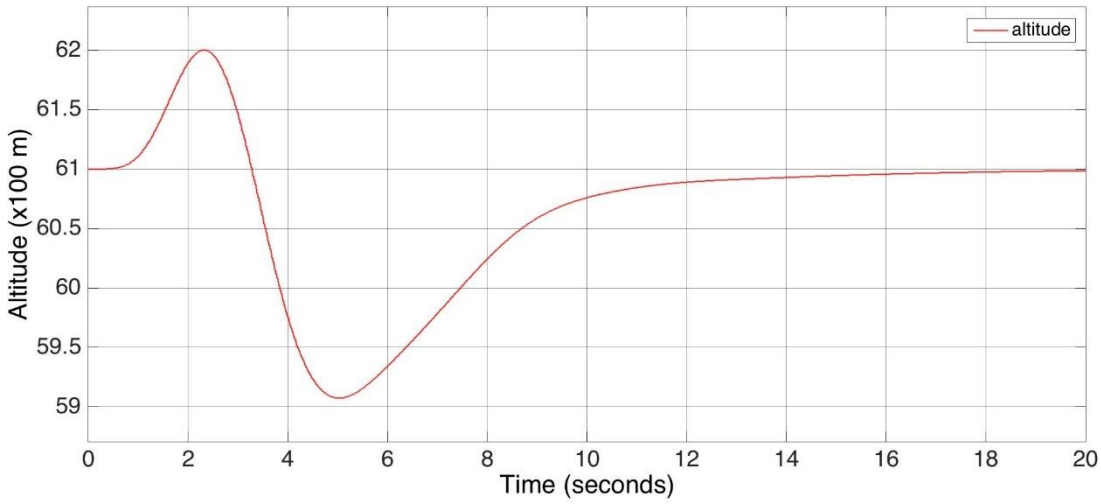

Figure A.16 Altitude vs. Time